

UNIVERSITÀ DEGLI STUDI DI PADOVA

DIPARTIMENTO DI INGEGNERIA INDUSTRIALE DII

Corso di Laurea Magistrale in Ingegneria Energetica

**Studying and analysis of cooling towers using the
Kloppers-Popper model in the MATLAB
environment**

Relatore

Prof.ssa: Anna Stoppato

Correlatore

Prof.: Predrag Raskovic

Candidato:

Simone Fabrizio 2022741

ANNO ACCADEMICO 2022/2023

Nomenclature

A	Area, m ²	Pr	Prandtl number, m ² s ⁻¹
a	Boolean variables	Q	Heat transfer rate, W
c_p	Specific heat at constant pressure, J kg ⁻¹ K ⁻¹	q	heat transfer rate ratio, W m ⁻²
D	mass diffusivity, m ² s ⁻¹	Sc	Smidth number, m ² s ⁻¹
DTW, dT	Temperature difference of each interval, °C or K	T	Temperature, °C or K
h	Heat transfer coefficient, W m ⁻² K ⁻¹	w	Air mass-fraction humidity, $\frac{\text{kg of water vapor}}{\text{kg of dry air}}$
i	Enthalpy, J kg ⁻¹	z	Binary variables
j, k, l	Runge-Kutta coefficient,		
K	thermal conductivity, W m ⁻¹ K ⁻¹		
Le_f	Lewis factor		
m	Flow rate, kg s ⁻¹		
Me_m	Merkel number (Merkel approach)		
Me_p	Merkel number (Poppe approach)		
p	Pressure, Pa		
		Greek Letters	
		α	thermal diffusivity
		β	volume interface
		Subscripts	
		a,dry,db	Dry air
		amb	ambient
		d	Mass
		fgvo	Reference temperature
		ma	Air-water mixture
		n	Number of matlab cycle - height of the tower
		sa	Saturated air
		ss	Supersaturated air
		sw	Saturation air
		v	Vapor
		w	Water
		wb	Wet bulb

Contents

1	Introduction	1
1.1	The Danube river	1
1.2	General information	1
1.3	Danube basin subdivision	2
1.4	Thermal pollution in Serbian Danube basin	3
1.4.1	Kostolac Power plant and why they need a cooling tower	6
1.5	Purpose of this thesis	8
1.6	Structure of this thesis	9
1.6.1	Abastract of Chapter 1	9
1.6.2	Abastract of Chapter 2	9
1.6.3	Abastract of Chapter 3	9
1.6.4	Abastract of Chapter 4	10
1.6.5	Abastract of Chapter 5	10
2	Cooling tower	11
2.1	Introduction to cooling tower	11
2.2	Types of Towers	13
2.2.1	Atmospheric cooling towers	13
2.2.2	2. Mechanical draft towers	14
2.2.3	3. Hybrid draft towers	15
2.2.4	1. Characterization by airflow:	15
2.2.5	2. Characterization by construction:	16
2.2.6	3. Characterization by shape:	16
2.2.7	4. Characterization by the method of heat transfer:	17
2.3	Cooling tower componets	18

2.3.1	Water basin	19
2.3.2	Tower framework	20
2.3.3	Water distribution system	21
2.3.4	Fan deck	22
2.3.5	Fan cylinders	23
2.3.6	Mechanical equipment support	24
2.3.7	Fill	24
2.3.8	Drift eliminators	25
2.3.9	Casing	26
2.3.10	Louvers	26
2.4	Natural draft cooling tower	28
2.5	How to design a cooling tower	31
2.5.1	Operative line	33
2.5.2	Equilibrium line	34
3	Mono-dimensional Cooling tower model	37
3.1	Heat and mass transfert	37
3.1.1	Conduction	38
3.1.2	Convection	39
3.2	Psychrometric chart	39
3.3	Lewis number	41
3.4	Poppe approach	42
3.4.1	Merkel theory	43
3.4.2	Poppe and Rogener theory	44
4	Developing MATLAB model	53
4.1	Runge-Kutta 4th Order Method (RK4)	53
4.1.1	RK4 Algorithm	54
4.1.2	Theoretical Background	54
4.2	Application of RK4 in Poppe model	55
4.3	Analysis of a natural draft wet-cooling tower with Poppe's approach	56
4.3.1	Inlet condition	57
4.3.2	Initial approximation of variables	60
4.3.3	Application of Runge-Kutta method to determine the working status of the cooling tower	63

Contents	ix
4.3.4 f,g,h and fss,gss,hss	70
4.3.5 Water Flow Rate	70
5 Conclusion	73
5.1 Model Envelope and Data Analysis	74
5.1.1 Result Comments	80
5.2 Conclusion	82
References	83
Appendix A - Matlab script collection	89
Appendix B - Plot collection	103

List of Figures

1.1	Danube Basin [1]	1
1.2	Danube subdivision [1]	3
1.3	Kostolac PPL [2]	6
1.4	Danube water temperature before PPL [3]	8
1.5	Average wind temperature [4]	8
2.1	Simple cooling tower cycle [5]	12
2.2	Natural draft tower	14
2.3	Fan draft tower	15
2.4	Example of cross/counterflow towers	16
2.5	Example of multiple cooling towers	17
2.6	Example of shape of cooling tower	18
2.7	Water basin of a tower [6]	20
2.8	Tower framework [6]	21
2.9	Spray zone of a tower [6]	22
2.10	Fan section of mechanical tower [6]	23
2.11	Fill and Drift system [6]	26
2.12	Tower with louvers [6]	27
2.13	Natural draft tower scratch	28
2.14	Internal view of spray zone natural draft tower [6]	30
2.15	Scratch of tower	32
2.16	Control volume	33
2.17	Eq. and op. line	35
3.1	Simple psychrometric chart [7]	40
3.2	Process involving in a psychrometric chart [8]	41

3.3	Control volume of counterflow fill [9]	44
3.4	Air side control volume [9]	45
3.5	Control volume on the fill [9]	49
4.1	Logical algorithm of MATLAB script	63
4.2	Logical algorithm of MATLAB script	69
5.1	Weather data results	75
5.2	Simulation in the Psychrometric chart	79
5.3	Water temperature for every month	80

Chapter 1

Introduction

1.1 The Danube river

1.2 General information

The Danube [3] is a river that originates in Germany, at the confluence of the Brigach and Breg tributaries near Donaueschingen in the Black Forest. However, the source of the Danube is generally considered to be a spring at the castle of Donaueschingen. At 2778 km in length and draining an area of 817 000 km², the river has an average annual water volume of 6550 m³/s, which flows into the Black Sea.



Fig. 1.1: Danube Basin [1]

The Danube River Basin is the second largest in Europe, the river flows through the territories of ten countries: Germany, Austria, Slovakia, Hungary, Croatia, Serbia, Bulgaria, Romania, Moldova, and Ukraine. Its hydrographic basin also en-

compasses parts of nine other nations: Italy, Poland, Switzerland, the Czech Republic, Slovenia, Bosnia and Herzegovina, Montenegro, North Macedonia, and Albania.

The Danube flows into the Black Sea through a delta that is the second-largest natural wetland in Europe. The basin supports a diverse aquatic ecosystem with numerous important natural areas, such as wetlands and floodplains. Its value extends beyond the environment, as it supports the supply of drinking water, agriculture, industry, fishing, tourism and recreational activities, energy production, navigation, and the final disposal of wastewater. To support these activities, many dams, embankments, navigation canals, and other hydraulic structures have been constructed throughout the region. However, the use of water resources for human purposes, including municipal, industrial, and agricultural activities, has caused changes in hydrological systems and resulted in problems with the quality and quantity of water, leading to significant environmental damage and a decline in quality of life.

1.3 Danube basin subdivision

The Danube basin can be divided into three parts [1]:

1. The upper Danube basin

stretches from its sources in the Black Forest Mountains to the Devín Gate, east of Vienna, where it meets the foothills of the Alps, the Little Carpathians, and the Leitha Mountains. The area includes to the north the Swabian and Franconian Jura, parts of the Oberpfälzer, Bavarian and Bohemian Forests, the Austrian Mühl- and Waldviertel, and the Bohemian-Moravian Highlands. South of the Danube is the Swabian-Bavarian-Austrian Pre-Alps and large parts of the Alps up to the watershed in the crystalline Central Alps. watershed in the crystalline Central Alps.

2. The Middle Danube Basin

covers a wide area from the Devín Gate to the impressive Danube Gorge near the Iron Gate, dividing the Southern Carpathians to the north and

the Balkan Mountains to the south. The middle Danube basin is bordered by the Carpathians to the north and east, the Carnic and Karavanke Alps, the Julian Alps, and the Dinaric Mountains to the west and south. This circle of mountains embraces the Pannonian plains and the Transylvanian highlands.

3. The Lower Danube Basin

includes the Romanian-Bulgarian Danube sub-basin downstream of the Cazane Gorge and the Siret and Prut sub-basins. It is bounded by the Carpathians to the north, the Bessarabian Plateau to the east, and the Dobrogea and Balkan Mountains to the south.

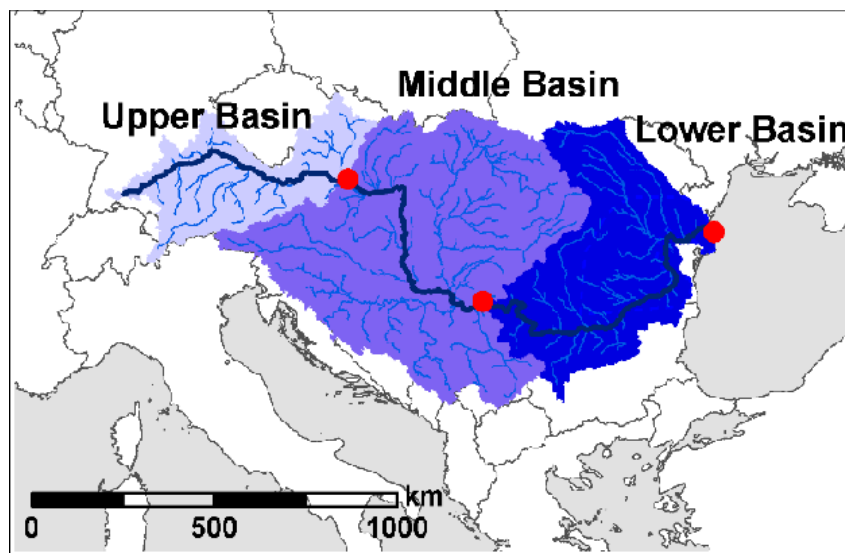


Fig. 1.2: Danube subdivision [1]

1.4 Thermal pollution in Serbian Danube basin

Thermal power plants (TPP) [10], particularly those fueled by coal, are recognized as significant contributors to air and water pollution. The primary environmental concern stems from the emission of harmful gases during combustion. Mitigating this issue has been a major focus, emphasizing the reduction of SO₂, NO_x, and CO₂ emissions. Regarding water pollution from power plants, attention has largely centered on the intake of toxic substances dissolved in wastewater that find their way into natural waterways, arising from TPP processes, slag, and ash

disposal. The development of air pollution control systems for fossil fuel combustion in recent decades has inadvertently led to the generation of new wastewater containing toxic substances discharged into natural waterways. Consequently, in late 2015, the US Environmental Protection Agency (EPA) introduced new regulations to safeguard water from toxic substances like arsenic, mercury, selenium, etc., which result from desulfurization, fly and bottom ash handling, and coal gasification, among others. While Milutinovic et al. discussed various environmental indicators for different scenarios in Serbia, thermal pollution of rivers was not considered in that research.

However, thermal pollution caused by the release of warm wastewater into natural water habitats is one of the most significant factors contributing to the degradation of natural ecosystems. This issue affects both TPP and nuclear plants. Proper operation of these plants, operating in the Rankine cycle, necessitates an adequate heat sink, leading to the extensive use of cooling water for steam condensation from low-pressure turbines. There are two primary cooling systems employed in steam power plants – closed (re-circulation) and open (once-through) systems. Closed cooling systems with wet cooling towers require a smaller amount of fresh water, which is mainly used to compensate for evaporation losses. In this setup, waste heat is dissipated to the atmosphere through evaporation and convection, leading to localized warming and humidification around the power plant. Dry and hybrid cooling towers are also used in closed-cycle systems, albeit with limited capacity.

In power plants employing the once-through cooling system, cold water is drawn directly from rivers, lakes, or the sea to condense the steam in the plant's condenser. The heated water is then discharged back into the downstream natural water source, elevating its temperature and disrupting the natural temperature and ecosystem balance. Thermal pollution is defined precisely as the alteration of natural water temperatures (rivers, lakes, oceans) due to human activities. It is essential to bear in mind that power plants using once-through cooling exhibit higher energy efficiency, up to 5%, compared to plants with closed-cycle cooling, owing to lower cooling water temperatures. As a result, in locations where feasible, large thermal power capacities are constructed near major rivers to provide both the necessary cooling water and improved energy efficiency for electricity generation. Nevertheless, due to the large quantities of waste heat released into

natural watercourses, new technological solutions are under scrutiny to achieve these objectives while conserving water resources.

As reported [11], the United States, China, and France are the primary producers of electricity from TPP, collectively contributing 26%, 16%, and 12% of overall thermal effluent into rivers, respectively. The proportion of once-through cooling systems in these countries stands at 17%, 8%, and 25%, respectively. In the US, one measure to protect surface waters from thermal pollution is the imposition of a limit on wastewater temperature to 32°C. In the EU, water temperatures downstream from discharge points are limited to a maximum of 3°C above natural temperatures. China is also taking steps to restrict water withdrawals and paying more attention to protecting rivers from thermal pollution in continental regions. The thermal regime of a river plays a crucial role in preserving its ecosystem and is intrinsically linked to safeguarding against thermal pollution. Predicting an increase in water temperature involves three groups of models – deterministic, stochastic, and regression models – encompassing atmospheric, topographical, and human impacts on the river's temperature regime. Waste heat from industrial and power plants, in addition to irrigation and deforestation in coastal areas, is a significant driver of changes in the thermal regime, impacting the survival of certain temperature-sensitive aquatic organisms.

Maintaining dissolved oxygen variability in water is of utmost importance for the quality of life in aquatic ecosystems. Elevated temperatures lead to reduced oxygen solubility while simultaneously increasing metabolic rates, influencing sediment oxygen demand, nitrification, photosynthesis, and respiration. On the other hand, in conditions of pronounced global warming and frequent droughts, the demand for cooling water in TPP restricts electricity production, particularly during summers. Consequently, certain plants must curtail their operations due to insufficient cooling water flow.

1.4.1 Kostolac Power plant and why they need a cooling tower

In Serbia, the total installed electricity generation capacity stands at 8359 MW [12]. The majority of this capacity, around 70%, is attributed to electricity generation from lignite TPP. An additional 353 MW comes from combined heat and power plants fueled by natural gas and liquid fuels, while 2835 MW is generated by hydropower plants. Out of the 18 TPP units, 13 employ a once-through cooling system. The highest concentration of capacities can be found along the banks of the Sava River in TPP Nikola Tesla A and B, where 8 units contribute to a total output of 2880 MW. On the Danube riverbanks, there are 4 operational units in TPP Kostolac A and Kostolac B, with capacities of 110 MW, 210 MW, and 2 units at 348.5 MW each. Additionally, there is an ongoing construction of a new 350 MW TPP unit named Kostolac B3 on the same site.



Fig. 1.3: Kostolac PPL [2]

Extensive research has been conducted on the pollution of the Danube River. International organizations like the International Commission for the Protection of the Danube River (ICPDR) [3] and the International Association of Water Supply Companies in the Danube River Catchment Area (IAWD) are actively involved in monitoring the water quality of the Danube. The Danube River Protection Convention was signed in Sofia, Bulgaria, in 1994, aiming to establish a legal framework for transboundary water management in the Danube River Basin. Serbia ratified the Danube River Protection Convention and became a full member of the ICPDR [3] in 2003. However, thermal pollution receives comparatively less attention in these documents compared to the discharge of toxic substances from wastewater.

1.4.1.1 Kostolac Power plant

TPP Kostolac (Fig. 1.3), managed by Elektroprivreda Srbije [13], is a coal-fired thermal power plant complex located on the right bank of the Danube River in

Kostolac, Požarevac. It ranks as Serbia's second-largest power plant, with TPP Nikola Tesla being the largest. By October 2020, the complex was operating four functional units, contributing approximately 10% of Serbia's electric power system capacity and nearly 11% of EPS's total electric power production.

The focus of the case study here centers around the 350 MW unit TPP Kostolac B1. The power plant utilizes water from the Danube for condenser cooling purposes. The process involves directing cold water from the Danube to the pump station through a cold water channel. After cooling the condenser, the heated water is discharged back into the Danube, utilizing a deepened riverbed of the river Mlava as the effluent channel.

The Danube's average annual water flow rate is approximately $5500 \text{ m}^3/\text{s}$, with low hydrology sensitivity. Although the impact of the effluent cooling water from TPP Kostolac B on thermal pollution is expected to be minimal, the Danube's course is vulnerable to various influences from numerous energy and industrial facilities. Thus, it is crucial to assess and minimize thermal pollution at specific locations. Studies by other authors [11] have shown an increase of $1 \text{ }^\circ\text{C}$ in the mean annual temperature along the Danube through Austria in the last decade, while indications suggest that the rise in water temperature began in Croatia in 1988.

The Republic Hydrometeorological Service of Serbia [14] gathers data from 15 reporting surface water stations along the Danube in Serbia. For the case of Kostolac B, the relevant reporting water station is located near the city of Smederevo, situated 10 km upstream from TPP Kostolac. Fig. 1.4 illustrates the average trend of Danube river temperatures over all the years of operation of the hydrological station at this location, meanwhile Fig: 1.5 illustrates the average trend of air temperature for the nearest wind station situated in the city of Požarevac. Approximately 25 km downstream from the power plant would be the water station of Veliko Gradište, but unfortunately, the data on Danube temperatures at that location is unavailable.

To make informed assessments, we will rely on the ICPDR [3] norms and studies conducted on other power plants along the Danube. Based on this, we will consider a maximum allowable temperature delta ranging from 1 to $3 \text{ }^\circ\text{C}$.

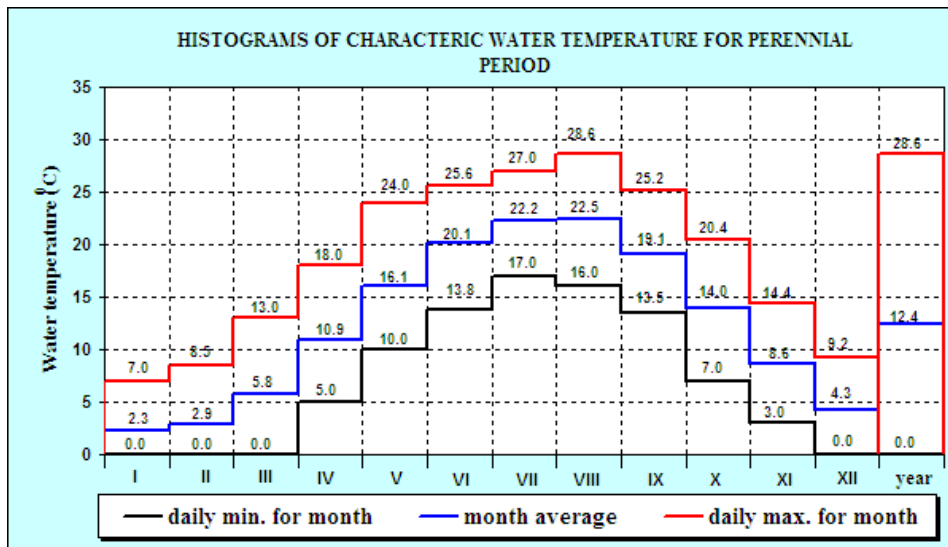


Fig. 1.4: Danube water temperature before PPL [3]

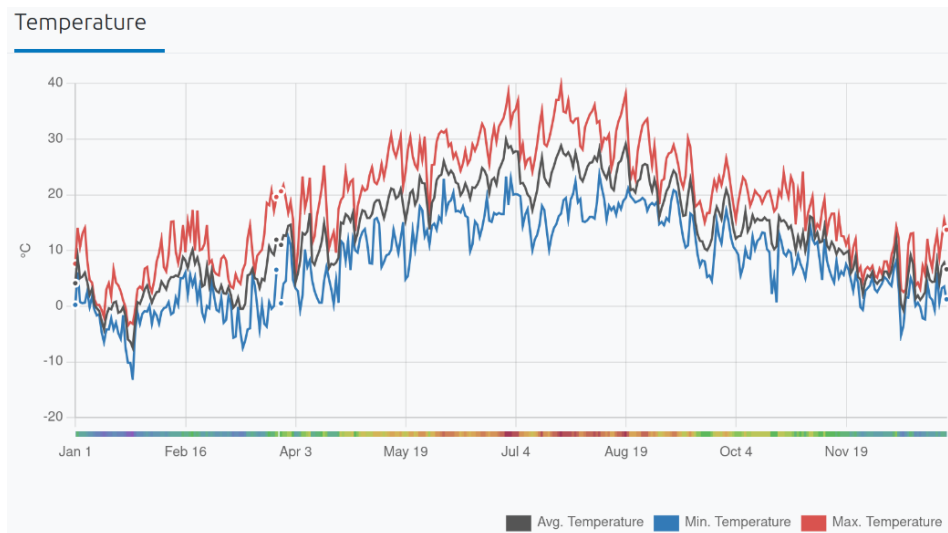


Fig. 1.5: Average wind temperature [4]

1.5 Purpose of this thesis

The purpose of this thesis will be to develop an algorithm using MATLAB to provide forecasts for the trend of air and water temperatures for reactor B of the Kostolac power plant. The main objective is to prevent thermal pollution of the Danube by lowering the water's outlet temperature, enabling the power plant to operate even during the hottest days, and better manage periods of full load operation.

1.6 Structure of this thesis

1.6.1 Abstract of Chapter 1

Thermal pollution in the Serbian Danube basin, mainly caused by thermal power plants like Kostolac, poses a significant environmental challenge. This study aims to develop a MATLAB algorithm for forecasting air and water temperature trends around the Kostolac Power Plant to prevent thermal pollution. By using historical data and adhering to ICPDR [3] guidelines, proactive measures can be implemented to ensure sustainable electricity generation while safeguarding the Danube's ecosystem. The proposed approach may have broader applications in mitigating thermal pollution near natural water sources worldwide.

1.6.2 Abstract of Chapter 2

Chapter 2 provides an extensive introduction to cooling towers, emphasizing their critical role in dissipating heat in power generation. Different types of cooling towers are introduced, including mechanical draft towers (forced draft and induced draft) and natural draft towers. The chapter explains the working principles of these towers and their advantages and limitations. It also provides an overview of other classification criteria for cooling towers, such as airflow, construction method, shape, and heat transfer method.

1.6.3 Abstract of Chapter 3

Unlike the previous chapter (section: 2.5), creating a one-dimensional model of a natural draft evaporative cooling tower requires considering additional parameters. In this chapter, we will explore how, using the theories formulated by Poppe and Kroger, along with a numerical method for solving differential equations known as Runge-Kutta, we can develop a MATLAB script that accurately describes the functioning of an evaporative cooling tower.

1.6.4 Abstract of Chapter 4

In this chapter, we present the development of a MATLAB model for the Runge-Kutta 4th Order (RK4) method, a numerical integration scheme widely used in solving initial value problems. The RK4 method is detailed, with a focus on its application to problems involving ordinary differential equations. The chapter outlines the logical process of creating the script, emphasizing the import of essential input data. These inputs include the inlet water temperature, dry bulb air temperature, wet bulb air temperature, and relative humidity. These parameters are pivotal in the subsequent calculations and simulations conducted within the script.

1.6.5 Abstract of Chapter 5

This chapter introduces a MATLAB model designed for the analysis of an evaporative cooling tower's performance. The model aims to predict water temperature trends, water usage, and heat dissipation. It operates as a one-dimensional static model and can serve as a foundation for a dynamic Simulink model, allowing for more detailed simulations with dynamic flows. The chapter concludes with plans to share the code and findings on GitHub, providing a valuable resource for further research and development.

Chapter 2

Cooling tower

2.1 Introduction to cooling tower

In every power generation or refrigeration cycle, the dissipation of heat is a crucial requirement. This holds for various systems such as chemical and process plant cycles, internal combustion engines, computers, and electronic systems. Traditionally, industrial plants have relied on bodies of water as the primary heat sink. The simplest and most cost-effective cooling method involved redirecting water from rivers, dams, or oceans to a plant's heat exchanger and returning it, heated, to its source. However, in industrialized countries, there are often limitations on the allowable temperature rise of the cooling water, which restricts the use of natural water for once-through cooling.

The selection of cooling sources for large industrial plants has become increasingly complex due to various factors:

- Decreasing availability of cooling water and suitable plant locations;
- Rapidly rising water costs, surpassing inflation rates in most industrialized countries;
- Noise restrictions and other environmental considerations;
- Increasing legislation and regulations

As a result of restrictions on thermal discharges into natural bodies of water, most new power plants or large industries requiring cooling are compelled to employ closed-cycle cooling systems. Cooling towers, particularly evaporative or wet cooling systems, are generally the most cost-effective choice for closed-cycle cooling, provided an adequate supply of suitable water is available at a reasonable

cost to meet the makeup water requirements of these systems. Regrettably, as highlighted by Burger, many cooling towers in the past have failed to meet design specifications, partially due to outdated design methods.

Air-cooled heat exchangers are commonly utilized in industries such as electronics, automotive, air conditioning, and refrigeration, as well as chemical and process plants, where cooling fluids at temperatures of approximately 60 °C or higher need to be cooled. Air-cooled or dry-cooling systems are often justified in industries or power plants where cooling water is either unavailable or prohibitively expensive. Depending on the specific application, a combination of dry/wet or wet/dry cooling systems may present the optimal choice, as suggested by Bartz and Mitchell. An appropriately designed and well-functioning cooling system can have a significant positive impact on plant performance and profitability.

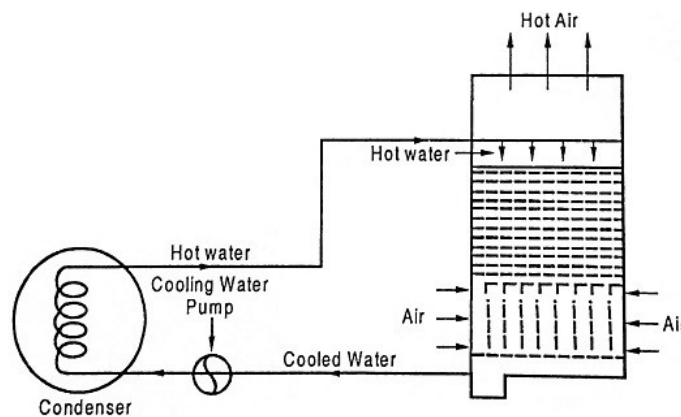


Fig. 2.1: Simple cooling tower cycle [5]

A cooling tower is a device that employs a combination of heat and mass transfer to cool water. The water to be cooled is distributed within the tower through methods such as spray nozzles, splash bars, or film fill, ensuring a large surface area of water is exposed to atmospheric air. Air movement is facilitated by fans (mechanical draft), natural draft, or the induction effect caused by water sprays. A portion of the water evaporates due to the air's lower moisture content compared to saturation at the water's temperature.

As evaporation requires energy to convert water from liquid to vapor, the water is cooled. *fig 2.1* illustrates a typical cooling circuit in a power plant. The turbine exhaust steam condenses in a surface condenser, transferring heat to the cooling

water circulating through the condenser tubes. The hot water leaving the condenser is directed to the cooling tower distribution basin and flows downward through the fill or packing. This process breaks up the water into small droplets or spreads it in a thin film, maximizing the contact area between the water and the cooling air. Finally, the water is drawn through the fill by the axial flow fan. After being cooled through a combination of evaporation and convective heat transfer, the water is continuously pumped back through the condenser.

Approximately 1–3% of the circulating water is lost due to evaporation. Over the years, a combination of theoretical and experimental studies, along with extensive practical experience, has led to improved design and operation of cooling systems. Unfortunately, despite these advancements, the full potential of these systems is not always realized due to inadequate maintenance and a lack of operating experience, as stated by Willa.

2.2 Types of Towers

Cooling towers are a critical component in many industrial processes [15], used to remove heat from water used in cooling systems. There are various types of cooling towers, each with their own strengths and weaknesses. To make an informed decision on which type of cooling tower to use, it is important to understand the different types available and their respective advantages and limitations.

2.2.1 Atmospheric cooling towers

These towers rely on natural airflow without the use of mechanical fans. A small atmospheric tower, as shown in *fig. 2.2a*, utilizes aspiration from a pressure-spray water distribution system. However, they are typically only suitable for very small sizes and are highly affected by adverse wind conditions. Due to their limited effectiveness in maintaining precise cold water temperatures, they are rarely recommended or used. On the other hand, hyperbolic natural draft towers (*fig. 2.2b*) are large, dependable, and predictable in their thermal performance. They utilize the density differential between heated air inside the stack and cooler ambient air outside to generate airflow. Although more expensive than other types, hyperbolic

towers are commonly employed in electric power generation and synfuels industries, where large heat loads exist and the absence of fan power can be recouped over time.

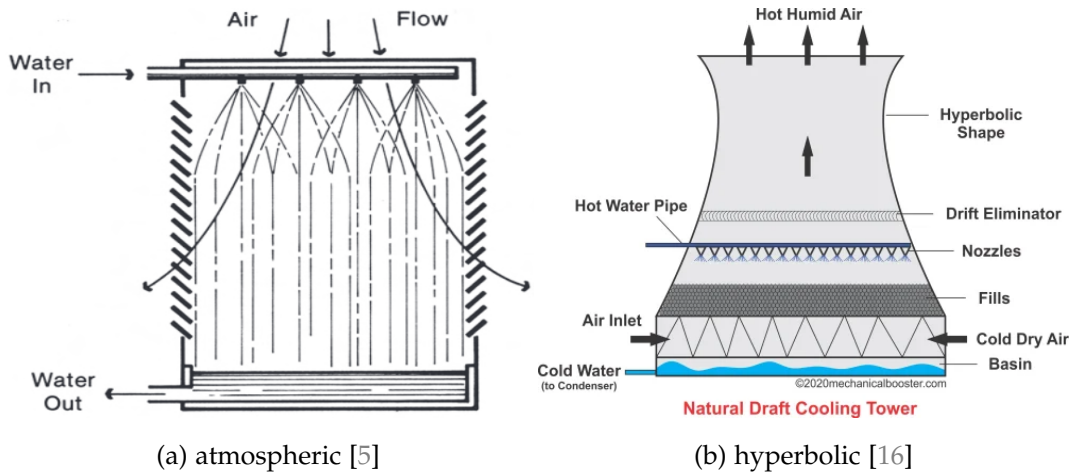


Fig. 2.2: Natural draft tower

2.2.2 2. Mechanical draft towers

These towers utilize one or multiple fans to create a controlled airflow. They offer greater stability in thermal performance compared to atmospheric towers, as they are less affected by psychrometric variables. Fans provide the flexibility to adjust airflow based on changing atmospheric and load conditions. Mechanical draft towers are categorized as forced draft or induced draft. Forced draft towers have high air entrance velocities and low exit velocities, making them prone to recirculation and less performance stable than induced draft towers. Forced draft towers often use centrifugal blowers and can be installed indoors or within specially designed enclosures to minimize recirculation. Induced draft towers have higher air discharge velocities and offer better protection against icing due to the location of the fan in the warm air stream. Induced draft towers are widely accepted and range in size from 3.5 m³/h to 160 m³/h.

2.2.3 3. Hybrid draft towers

These towers appear similar to natural draft towers with short stacks but are equipped with mechanical draft fans to enhance airflow. They are also known as fan-assisted natural draft towers and are designed to minimize horsepower requirements while maintaining a reasonable stack cost impact. The fans may only need to operate during high ambient and peak load periods. Fan-assisted natural draft towers with elevated discharge can be preferred in areas where low-level discharge plumes are not acceptable.

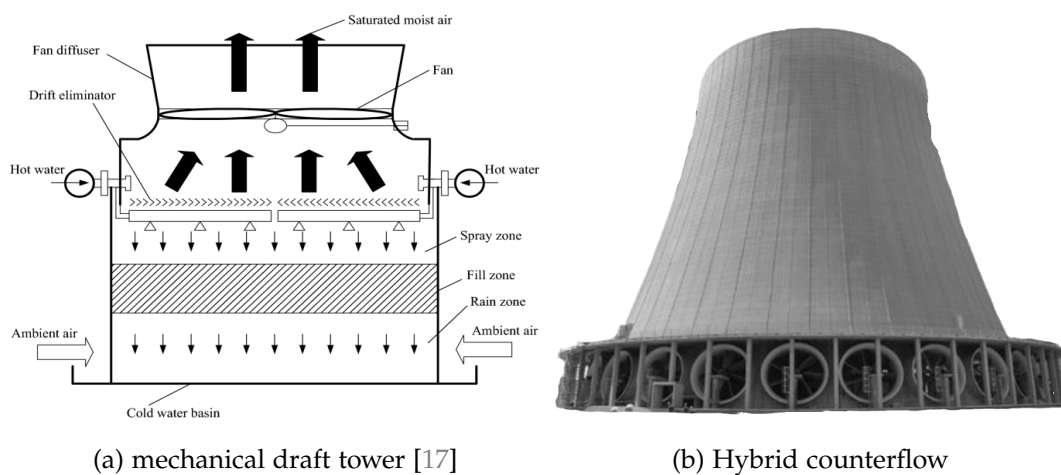


Fig. 2.3: Fan draft tower

Cooling towers can also be classified by other parameters such as airflow, construction, shape, and method of heat transfer.

2.2.4 1. Characterization by airflow:

Cooling towers can be characterized by the relative flow relationship between air and water within the tower. Counterflow towers (*Fig. 2.4a*) have upward airflow through the fill, opposite to the downward fall of water. While some smaller counterflow towers require more pump head and fan power, larger counterflow towers with low-pressure distribution systems and ample air management spaces can equalize or reverse this situation. Counterflow towers also restrict water exposure to sunlight, inhibiting algae growth.

Crossflow towers (*Fig. 2.4b*) have horizontal airflow across the downward fall of water. Water is delivered to hot water inlet basins and distributed to the fill by gravity. Crossflow towers allow easy maintenance due to the visibility and accessibility of the gravity distribution system. They can be further classified based on the number of fill banks and air inlets served by each fan, such as double-flow or single-flow towers.

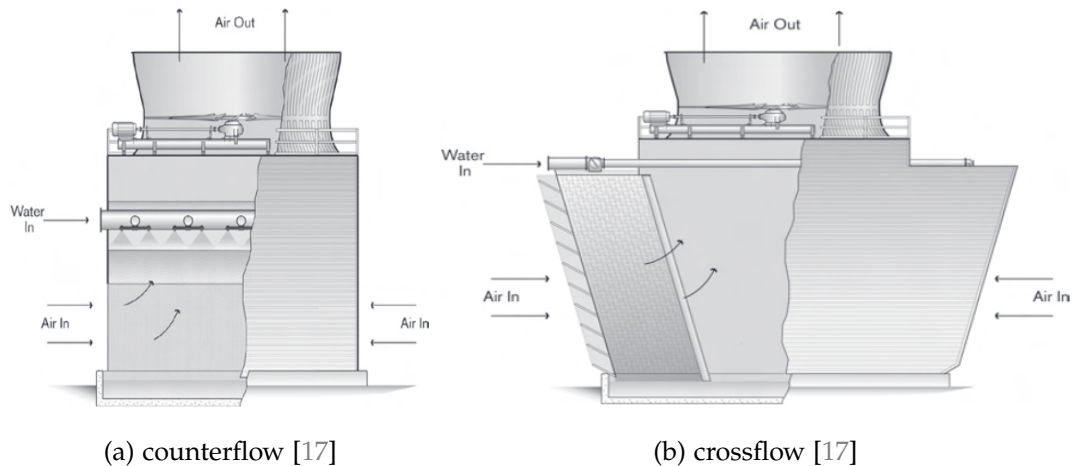


Fig. 2.4: Example of cross/counterflow towers

2.2.5 2. Characterization by construction:

Cooling towers can be field-erected or factory-assembled. Field-erected towers are primarily constructed on-site, while factory-assembled towers undergo almost complete assembly at the manufacturing facility and are transported to the site for final joining.

2.2.6 3. Characterization by shape:

Cooling towers can be categorized by their shape. Rectilinear towers are built in a cellular fashion, increasing linearly in length and the number of cells to achieve the desired thermal performance. Round Mechanical Draft (RMD) towers have a round plan configuration with fans clustered around the center point. Multi-faceted towers, like the Octagonal Mechanical Draft (OMD) tower, fall into the round tower classification. These towers can handle high heat loads with less site

area impact compared to multiple rectilinear towers and are less susceptible to recirculation.

2.2.7 4. Characterization by the method of heat transfer:

The previously mentioned towers are evaporative-type towers, where primary cooling occurs through evaporation. Dry towers, on the other hand, utilize dry surface coil sections for heat transfer without direct contact or evaporation between air and water. Plume abatement and water conservation towers employ dry surface coil sections to address specific problems or meet specific requirements. Here are some tower examples:

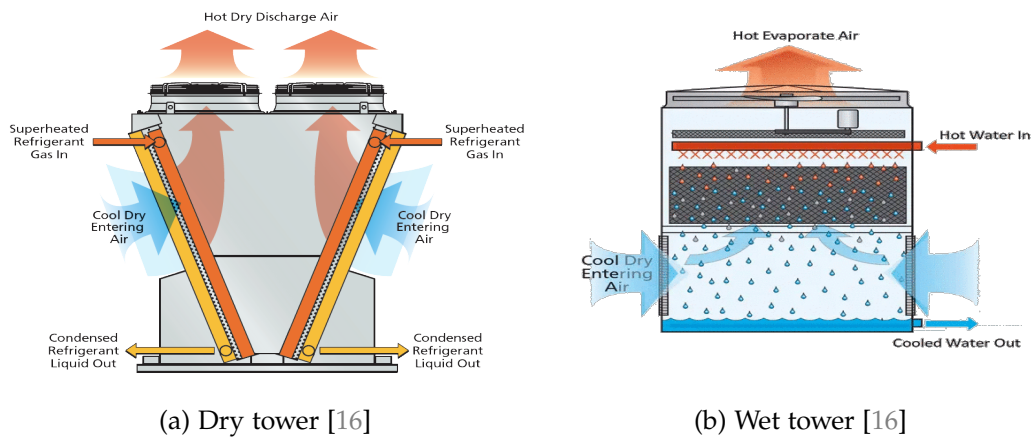
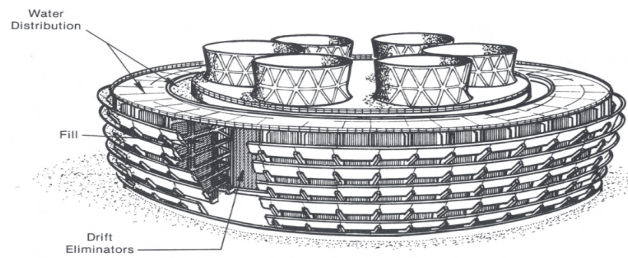
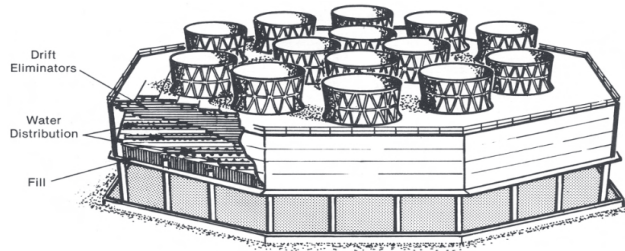


Fig. 2.5: Example of multiple cooling towers



(a) Rounded tower [15]



(b) Octagonal tower [15]

Fig. 2.6: Example of shape of cooling tower

2.3 Cooling tower componets

The structure of a cooling tower must be able to support the weight of the tower components, circulating water, snow and ice, and any internal fouling. Additionally, it must be able to withstand short-term loads caused by wind, maintenance, and seismic activity. The cooling tower must be able to maintain its integrity in various external atmospheric conditions and despite constant internal water exposure. It must also be able to withstand wide-ranging temperatures and the corrosive effects of high humidity and constant oxygenation [17].

However, the unique challenge of cooling towers is that the structure must also provide minimal obstruction to the free flow of air and water. This, combined with the constant vibratory forces from mechanical equipment operation, requires unique structural considerations in the design of cooling towers.

While basic design concepts are based on commonly accepted design codes, cooling tower manufacturers may need to modify these codes to account for unforeseen effects. The key components to consider in the design of cooling towers include the cold water basin, framework, water distribution system, fan deck, fan cylinders, mechanical equipment supports, fill, drift eliminators, casing, and louvers. The use of the best materials and improved techniques for integrating these

components is essential for creating a stable, reliable, and long-lasting cooling tower.

The components to be considered in this Section are the cold water basin, framework, water distribution system, fan deck, fan cylinders, mechanical equipment supports, fill, drift eliminators, casing, and louvers. The best materials for these components are continuously sought, along with improved techniques for integrating them into a stable, dependable, long-lasting unit.

2.3.1 Water basin

The cooling tower basin serves two primary functions: collecting the cold water after it has passed through the tower, and acting as the tower's primary foundation. It must also be accessible, cleanable, have adequate draining facilities, and be equipped with suitable screening to prevent entry of debris into the suction-side piping.

The type of basin used in a cooling tower installation depends on the location of the tower. Ground-level installations typically use concrete basins, while elevated or rooftop installations use basins provided by the cooling tower manufacturer, made from materials such as wood, steel, or plastic. These basins often come with drain and overflow fittings, make-up valves, sumps, screens, and provisions for anchorage. Concrete basins for wood or steel-framed, field-erected towers are usually designed and built by the purchaser, using dimensional and load information provided by the manufacturer. However, for concrete towers, the basins may be designed and built by the cooling tower manufacturer due to the integration of the basin into the overall tower structure and the extensive site-related concrete work required.

The basin support for a cooling tower installed over a wood or steel basin typically uses a grillage made of steel or concrete. The grillage must be able to support the total wet operating weight of the tower and associated piping, as well as any additional dead loads from stairways, catwalks, etc. It must also be able to withstand transient loads from wind, earthquake, and maintenance traffic.

The basin depth can vary depending on the type of basin. Wood, fiberglass, and steel basins are typically shallow and range from 35 cm to 50 cm deep. Concrete basins are typically deeper and can be adapted to the specific design criteria. The basin depth must be sufficient to provide sufficient hydraulic head for proper water flow into the sump(s) and to accept the transient water and potential back-flow at pump shutdown. Additionally, the basin may be made deep enough to hold a reserve in case of an interrupted make-up water supply or to stabilize water temperatures under highly variable weather conditions.

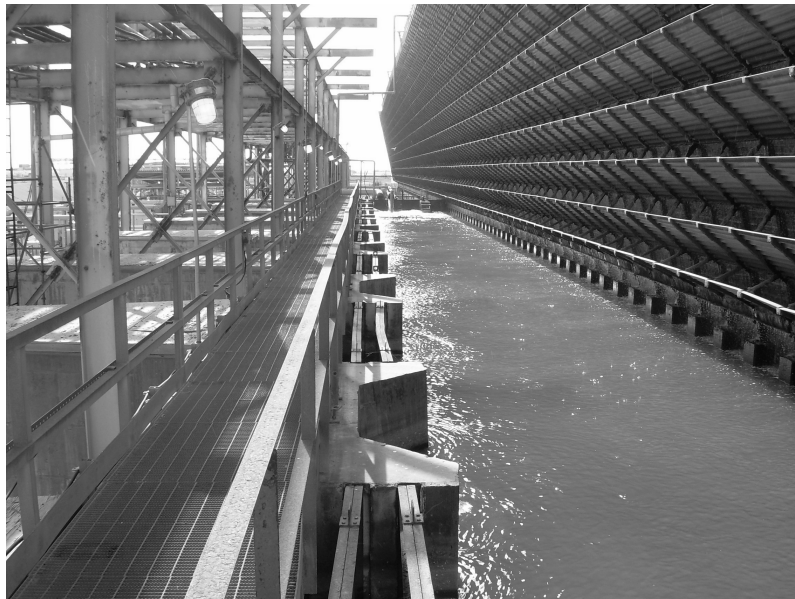


Fig. 2.7: Water basin of a tower [6]

2.3.2 Tower framework

It is a critical component in the construction of field-erected towers, and several materials can be used, including pultruded fiberglass, wood, concrete, and steel. The most commonly used material is pultruded fiberglass, but the choice of material may depend on local building codes or specific preferences. Steel is rarely used for field-erected towers, but it is more prevalent in factory-assembled towers, particularly those made of stainless steel, which is more resistant to corrosion. The standard wind load design for towers is 2 kPa, but higher values may be required in certain areas. If applicable, earthquake loads must comply with the zones de-

fined in the Uniform Building Code of the International Conference of Building Officials.

The design of the tower framework must also comply with the relevant codes and standards as the American Institute of Steel Construction manual (AISC) and the European standard EN 14705. The tower framework must also include diagonal bracing in the plane of the columns, which is usually of column size, and horizontal girts in the transverse and longitudinal directions to carry the fill modules and keep the unbraced column lengths to short vertical spans. The transverse and longitudinal girt lines should be at the same plane to achieve a determinant definition of lateral bracing of the columns against buckling. Concrete tower structural members may be a combination of precast and poured-in-place construction, and the design will vary according to the loads and tower configuration.



Fig. 2.8: Tower framework [6]

2.3.3 Water distribution system

The water distribution system within a cooling tower is typically the responsibility of the tower manufacturer, with site piping and associated components such as risers, valves, and controls being provided and installed by others. The magnitude and routing of the circulating water lines between the heat source and the tower location depend on factors such as the type of tower, topography, and site layout.

These lines may be buried to minimize issues such as thrust loading, thermal expansion, and freezing, or elevated to minimize installation and repair costs. In either case, the risers to the tower inlet must be externally supported, independent of the tower structure and piping.

There are two main types of water distribution systems: crossflow and counterflow. Crossflow towers allow for the use of a gravity-flow distribution system where the supply water is elevated to hot water distribution basins above the fill and flows over the fill through metering orifices located on the distribution basin floor. Counterflow towers typically require a pressure-type system of closed pipe and spray nozzles. Gravity systems are easy to inspect, clean, and maintain and are easily balanced, but they contribute little to overall heat transfer and tend to require a higher pump head in larger towers. Pressure spray systems are more susceptible to clogging and more difficult to balance, clean, maintain, and replace, but they contribute significantly to overall heat transfer and tend to have lower pump heads in larger towers.

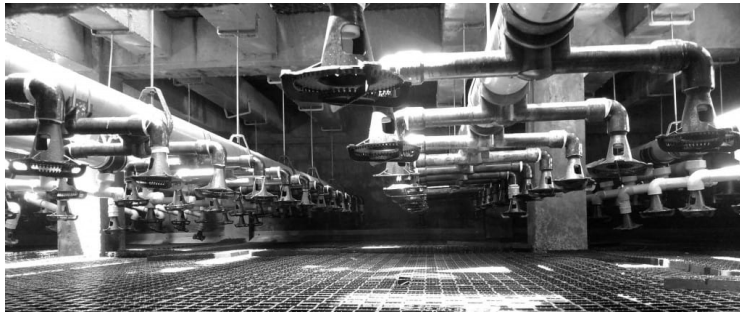


Fig. 2.9: Spray zone of a tower [6]

2.3.4 Fan deck

The fan deck plays a crucial role in the overall structural integrity of the cooling tower. It acts as a diaphragm, transmitting dead and live loads to the tower framing and providing a platform for the support of the fan cylinders. It also offers an accessway to the mechanical equipment and water distribution systems. The materials used for the fan deck must be compatible with the tower framework for the efficient and safe functioning of the tower. Common materials used for fan decks include tongue-and-groove fir plywood for wood towers, pultruded fiberglass re-

inforced plastic (FRP) for pultruded FRP towers, galvanized steel for steel towers, and prestressed double-tee sections for concrete towers. To ensure the safety of the tower, a uniform live loading design is implemented, typically 60 pounds per square foot on larger towers and 40 pounds per square foot on smaller towers. This ensures the stability and safety of the overall tower structure.

2.3.5 Fan cylinders

The design and construction of a fan cylinder is a crucial aspect of a cooling tower as it directly affects the flow of air through the tower. A well-designed fan cylinder incorporates several key features to ensure optimal performance. The inlet should be eased to promote smooth flow of air, the fan blade tip clearance should be minimal, the profile below and above the fan should be smooth, and the structural strength should be sufficient to maintain a stable plan and profile. The fan cylinder should also be of sufficient height to protect operating personnel or have a removable mesh guard that is structurally reinforced.

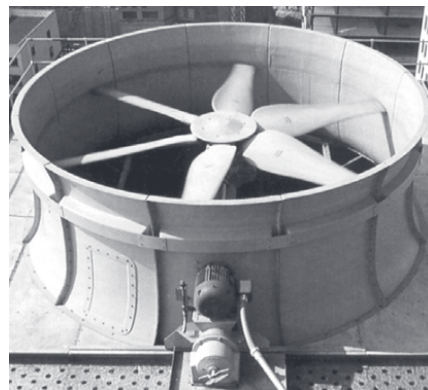


Fig. 2.10: Fan section of mechanical tower [6]

Fiber-reinforced plastic is the preferred material for fan cylinder construction due to its formability, strength, lightweight, stability, and resistance to water and weathering. Cylinders are formed over molds which accurately control contour and dimensions, resulting in a fan cylinder that approaches ideal air movement, coupled with minimum noise. Wood and steel can also be used for fan cylinder construction, but they usually result in lower fan efficiencies.

An extended-height fan cylinder, also known as a "fan stack," promotes the discharge of the saturated air stream at higher elevations, minimizing the effects of recirculation and interference. One type of fan stack is in the form of a flared diffuser that provides a gradual increase in cross-sectional area beyond the fan, resulting in a decrease in leaving air velocity. This effectively converts velocity pressure to static pressure, resulting in a significant increase in air delivery over

what could be accomplished with a straight cylinder at the same fan horsepower. These velocity-recovery cylinders are particularly useful for large industrial towers.

2.3.6 Mechanical equipment support

The framework of a cooling tower must be able to withstand the torsional forces encountered during the operation of large fans at high horsepower. To maintain proper alignment of the mechanical equipment, a means of ensuring a constant plane relationship throughout the motor-gear-reducer-fan drive train must be provided.

For smaller fan units, unitized steel weldments of structural cross-section are sufficient. However, the forces imposed by larger fans require the use of more sophisticated unitized supports. These typically consist of large, heavy-wall torque tubes welded to outriggers of structural steel. The material of choice for these unitized supports is carbon steel, which is hot-dip galvanized after fabrication. Stainless steel construction is also available, but it comes at a significant additional cost. The heavy construction and galvanization of carbon steel make stainless steel construction unnecessary in most cases.

2.3.7 Fill

The fill is one of the most important components of a cooling tower. Its ability to promote maximum contact surface and time between air and water determines the efficiency of the tower. There are two basic types of fill: splash type and film type. Splash-type fill breaks up the water by cascading it through offset levels of parallel splash bars. This type of fill is characterized by reduced air pressure losses and is not conducive to clogging, but is sensitive to inadequate support.

Film-type fill causes the water to spread into a thin film, flowing over large vertical areas to promote maximum exposure to the airflow. This type of fill is capable of providing more effective cooling capacity within the same amount of space but is extremely sensitive to poor water distribution, as well as the air blockage and turbulence that a poorly designed support system can perpetuate. The over-

all tower design must ensure uniform air and water flow throughout the entire fill area. Different types of fill are manufactured with different materials such as wood, plastics, stainless steel, or aluminum.

2.3.8 Drift eliminators

Drift eliminators are a by-product of the cooling tower that promotes the most intimate contact between water and air in the fill. Water droplets become entrained in the leaving air stream, and are collectively called "drift." These droplets should not be confused with pure water vapor or droplets formed by condensation of that vapor. Drift can potentially be a nuisance, as it can spot cars, windows, and buildings, and with the tower located upwind of power lines and substations, it can also be an operating hazard. Drift eliminators remove entrained water from the discharge air by causing it to make sudden changes in direction.

This results in a centrifugal force that separates water droplets from the air, depositing them on the eliminator surface, where they flow back into the tower. Designers try to avoid excess pressure losses while moving air through the eliminators, but a certain amount of pressure differential is beneficial as it promotes uniform airflow through the tower fill. Eliminators are classified by the number of directional changes or "passes," and may consist of two or more passes of spaced slats positioned in frames or be molded into a cellular configuration with labyrinth passages. Some towers that utilize film-type fill have drift eliminators molded integrally with the fill sheets.

Materials that are acceptable for fill are usually incorporated into eliminator design, with treated wood and various plastics, predominantly PVC, being the most widely used. In the 1970s, concern for the possible environmental impact of drift from cooling towers stimulated considerable research and development, leading to significant advances in drift eliminator technology.

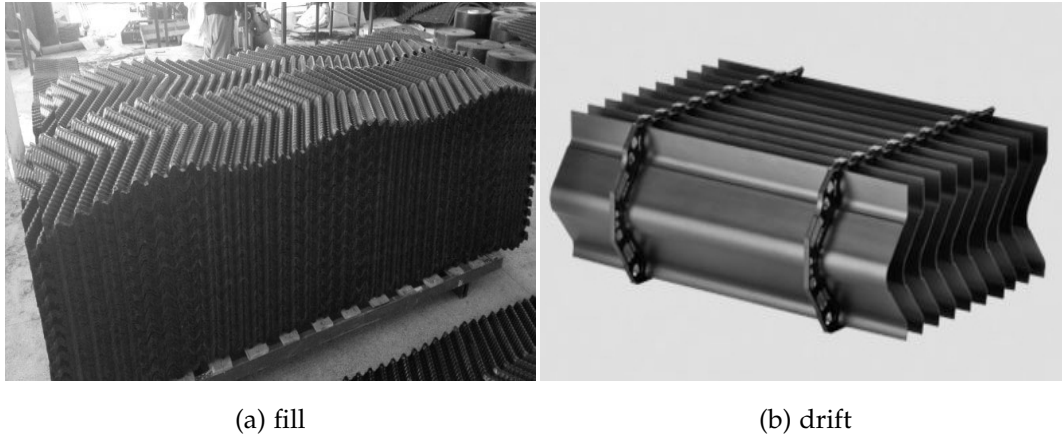


Fig. 2.11: Fill and Drift system [6]

2.3.9 Casing

The cooling tower casing plays a critical role in the operation of a cooling tower. It must be strong enough to contain water within the tower, provide an air plenum for the fan, and transmit wind loads to the tower framework. It must also be water-tight and corrosion resistant to prevent leaks and damage, and have fire retardant qualities to ensure safety. Additionally, the casing should be able to resist weathering and present a pleasing appearance. Currently, wood or steel-framed, field-erected towers are commonly cased with fire-retardant fiber-reinforced polyester corrugated panels that are overlapped and sealed to prevent leakage. Factory-assembled steel towers use galvanized steel panels, and concrete towers are cased with precast concrete panels. If desired, the casing can be extended to the height of the handrail for aesthetic purposes.

2.3.10 Louvers

Louvers are an important component of cooling towers as they help to retain circulating water within the tower and equalize airflow into the fill. Inlet louvers are standard on well-designed crossflow towers, while counterflow towers may only occasionally require them. Louvers must be able to support snow and ice loads and, when properly designed, can contribute to good operation in cold weather by retaining the increase in water flow near the air inlets, which is important for

ice control. However, closely spaced, steeply sloped louvers can impede free air-flow and contribute to icing problems. Increasing the width of the louvers can improve spacing and slope and improve water containment, but it also increases cost. Common materials used for louvers include corrugated fire-retardant fiber-reinforced polyester and treated Douglas Fir plywood for field-erected towers, galvanized steel for factory-assembled steel towers, and precast, prestressed concrete for concrete towers.

The design of louvers began in the early era of splash-type fill when their primary function was to control the large number of water droplets produced by the splashing action. With the advent of film-type fills, which have better water management characteristics, louver design was reassessed. As a result, highly visible louvers disappeared from certain cooling towers designed for operation only with film-type fill. However, splash-type fill is still widely used, especially in contaminated water service, and is expected to remain so for the foreseeable future. Furthermore, the use of film-fill towers without external louvers in certain operating conditions, such as excessively high water loadings, is ill-advised.



Fig. 2.12: Tower with louvers [6]

2.4 Natural draft cooling tower

Since we only studied the design of a natural draft cooling tower, we will exclude an in-depth analysis of a mechanical draft cooling tower.

Natural draft cooling towers [9] rely on the difference in density between the heated humid air inside the tower and the denser ambient air outside to create the necessary airflow through the fill. These towers can be configured as crossflow or counterflow arrangements (see Figs. 2.13a & 2.13b).

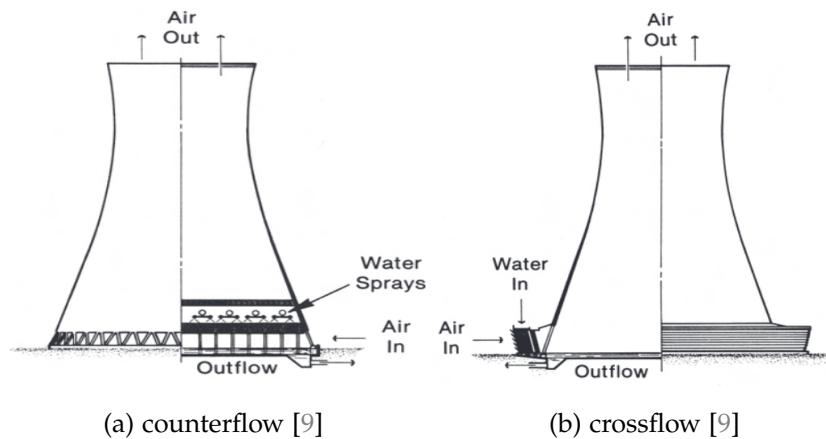


Fig. 2.13: Natural draft tower sketch

In crossflow towers, the air flows perpendicular to the downward falling water. The hot water is delivered through risers to distribution basins located above the fill, and gravity distributes it through low-pressure nozzles on the basin floor. Modern concrete cooling towers typically have a hyperbolic shape and can reach heights of up to 180 m. To reduce the tower's size, axial flow fans can be installed at the base. However, while this reduces the structural cost, it is offset by the capital cost of fan installation and operation. Fan-assisted natural draft cooling towers are considered in cases where alternative multibank mechanical draft units are deemed unacceptable due to excessive plume recirculation.

In modern fossil-fueled power plants equipped with wet-cooling systems, an average of 1.6–2.5 liters of cooling water is required per kWh(e) of net generation. For a 600 MWe coal-fired plant operating at a 70% annual capacity factor, the makeup water needed to replace cooling tower evaporation losses alone ranges between 5×10^6 m³ and 10×10^6 m³ annually. Drift, which refers to the carry-

over of water droplets by the air passing through the tower, also results in some water loss. In non-zero discharge plants using conventional wet-cooling towers, blowdown and drift losses combined typically account for 20–50% of evaporative losses, corresponding to 6–3 cycles of concentration of dissolved solids. A cycle of concentration represents the ratio of dissolved solids in the circulating water to that of the makeup water. While drift losses can be as low as 0.01% of the circulating water flow rate, blowdown encompasses all these losses. Consequently, the total makeup water requirements for the wet cooling system of the aforementioned 600 MWe coal-fired plant could exceed 11×10^6 m³ per year, with a waste stream averaging nearly 10,000 m³ per day for disposal, assuming low-quality makeup water is used. Figure 1.1.9 showcases several natural draft cooling towers at a power plant.

Nuclear power plants and geothermal power plants reject 45–50% more heat to the condenser cooling water per kWh(e) of net generation compared to fossil-fueled units. In geothermal power plants, the heat rejection per kWh(e) of net generation can be four or more times greater than that of fossil-fueled plants. Consequently, nuclear and geothermal power plants require greater makeup water and generate more blowdown. In contrast, combined cycle power plants, where only about one-third of the total electrical output is generated in the steam cycle, generally have lower makeup water and blowdown requirements than conventional fossil-fueled plants of similar size. If the water supply used for makeup is variable, a storage reservoir may be necessary to ensure an adequate supply at all times. However, evaporation and seepage losses from such a reservoir can contribute up to 20% to the overall makeup water requirements. In light of environmental considerations for limiting temperature rise in surface water and setting maximum temperature limits for returning cooling water, once-through helper-cooling towers have gained popularity. In this setup, river or surface water is first passed through a surface condenser to achieve the necessary cooling before being further cooled in a helper cooling tower and returned to its source. Depending on cooling water availability and environmental factors, plants with cooling towers can be operated in open circuits (without towers), closed circuits (relying on cooling towers), or open circuits where the cooling tower functions as a helper tower, as described by Chapelain.

Water costs have traditionally been a small component of the overall energy production costs. However, when considering the additional costs associated with using water for power plant cooling, such as pumping, water treatment, blowdown disposal and permit acquisition, water-related expenses become more significant. Moreover, restrictive legislation that prioritizes water use in a way unfavorable to utilities or chemical plants can have a more profound impact on the industry than rising water costs. Currently, there are various options available to reduce or eliminate makeup water requirements and wastewater in plant cooling systems. These include wet-cooling systems designed to operate with high cycles of concentration, different types of dry-cooling systems that do not consume water, and cooling tower systems that combine dry and wet-cooling technologies.



Fig. 2.14: Internal view of spray zone natural draft tower [6]

When conducting general studies to compare the economics of alternative heat rejection systems, it is crucial to consider all the potential advantages offered by water-conserving systems. For instance, dry-cooled or dry/wet-cooled plants do not necessarily have to be located at the same site as the base case wet-cooled plant used for comparison. The use of water-conserving systems allows for more flexibility in siting. Fuel cost savings resulting from situating a coal-fired plant near a mine where water availability may be limited for wet-cooling could outweigh the increased transmission costs. Employing a water-conserving heat-rejection system could enable the expansion of existing generating facilities at sites where there is insufficient water for wet-cooling, taking advantage of existing support and service facilities and rights-of-way. Even when an adequate water supply exists at a given site, the use of a water-conserving system can, in some cases, reduce in-

direct project costs and lead times by minimizing environmental studies, public hearings, and permit requirements.

In practice, other factors cannot be overlooked. These factors include changes in microclimate, equipment corrosion, emission of chemicals, reduced visibility, freezing of nearby surfaces, and potential health hazards like legionnaires' disease in poorly maintained systems, as noted by Crunden and Cuchens.

The impact of these factors on the comparative economics of alternative heat-rejection systems depends on the unique circumstances of each application. For the foreseeable future, wet-cooling towers are expected to remain the economical choice in most cases where an adequate supply of suitable makeup water is available at a reasonable cost. However, as water availability decreases, water costs rise, and more stringent environmental regulations and water use/accessibility guidelines are enforced, water-conserving heat-rejection systems will become increasingly practical and economically viable for power plants and other applications.

2.5 How to design a cooling tower

Current cooling tower technology [18] is based on the fact that the effects of evaporative and sensible heat transfer can be combined, within an acceptable margin of error, into one dependent on the enthalpy difference. This is the difference between the enthalpy of the film of air surrounding the water surface (assumed to be at water temperature) and the enthalpy of the general mass of air flowing through the tower. This enthalpy difference varies according to the point of measurement in the tower, but at all points, it provides the enthalpy potential or driving force for heat transfer.

The so-called combined transfer theory relies on certain approximations that are reasonable at normal cooling water temperatures especially when the characteristics of the packing have been determined according to the theory. However, the approximations become less valid with increasing water temperature and a more accurate analysis should be used in applications where the mean water temperature exceeds 35 °C.

As mentioned earlier, cooling towers are nothing more than air-water heat exchangers in which water condenses and changes phase as it cools. In this section

we will look at the theoretical sizing of an evaporation tower, taking into account the main parameters to be considered during an analysis. In the next chapter, we will analyze how to create a dynamic model of an evaporation tower, going on to create processes of iteration between parameters to also arrive at an optimization of the performance. Remembering that there are different types of cooling towers, we will give some examples of sizing for some specific configurations, bearing in mind that the general procedure does not change much from one configuration to another.

The basic idea, therefore, is to understand the dynamics that occur inside the cooling tower. To do this, the sketch in Figure 2.15 can be considered, which depicts a generic application of the tower. The concept is that this evaporative tower operates on a simple principle: hot water from a plant is sprayed inside the tower using the systems described earlier. The water then trickles down, while dry air flows in the opposite direction, upwards. As the air rises, it gradually absorbs heat from the water, becoming warmer and more humid. At the same time, the hot water cools down as it releases its heat of vaporization, creating a visible plume at the tower's outlet. Eventually, the cooled water is discharged from the bottom of the tower. In summary, the air receives heat from the hot water through the process of evaporation.

The variables considered for this sizing include, for both air and water, the flow rate, temperatures, specific heat, latent heat of evaporation, mass transfer coefficient, humidity, and enthalpy of the air.

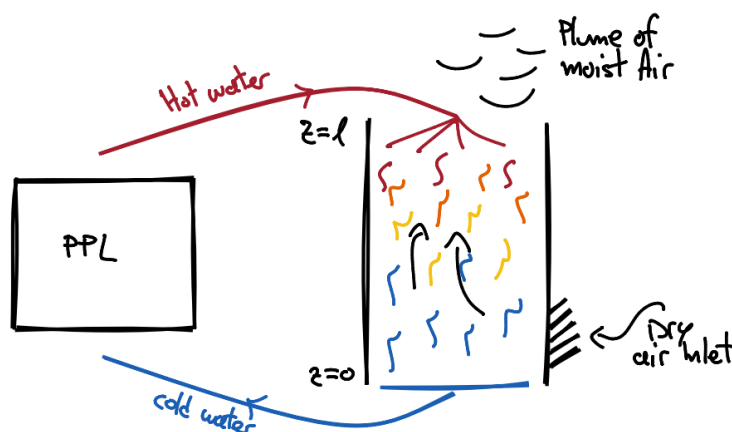


Fig. 2.15: Scratch of tower

For this equation, the assumption will be the following:

- Latent heat is transferred across the water-air interface by diffusion of water vapor.
- Sensible heat is also transferred by the temperature difference between the water and the air.
- The water to be cooled enters the top of the tower and the cooling air is either induced or forced through the tower from bottom to top for a counter-current tower.
- Adiabatic operation in the cooling tower.
- Dry air and water Flowrate are constant.
- No drift and leakage loss (water flow rate remains constant).
- The eventual location of the air fan has no effect.
- Interfacial areas are equal for heat and mass transfer.
- No influence of temperature on the transfer coefficients.
- Thermodynamic properties are constant across the cross-section of the tower.
- steady state conditions

2.5.1 Operative line

It is safe to say that the design and operation of cooling towers are based on the principles of mass and energy balances, which will be analyzed using a closed control volume (Fig.2.16), allowing us to obtain two fundamental curves for our tower: the operating curve and the equilibrium curve. Assuming that heat exchange occurs in countercurrent, with the bottom of the tower defined as the inlet ($n=0$), it can be seen a flow of cold air entering and a flow of cold water exiting. Conversely, at the exit of the control volume, it can be seen a flow of hot liquid enters and a flow of hot, moist air exits (n).

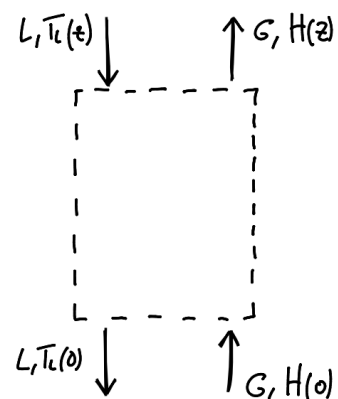


Fig. 2.16: Control volume

The balance of the accumulated energy in this control volume to obtain the first mass balance is written:

(Energy accumulated) = (heat into wet air) + (heat lost from water)

$$0 = m_a(i_{ma(0)} - i_{ma(n)}) + m_w \cdot c_{pw}(T_{w(n)} - T_{w(0)}) \quad (2.1)$$

$$i_{ma(n)} = i_{ma(0)} + \frac{m_w \cdot c_{pw}}{m_a} \cdot (T_{w(n)} - T_{w(0)}) \quad (2.2)$$

This now is going to provide an operating line that can be plotted in an enthalpy/temperature diagram. As it can be seen in Fig.2.17 the enthalpy of the gas phase is in the vertical axis and the temperature of the water steam is in the horizontal direction, $T_{w(0)}$ is the inlet water temperature meanwhile $T_{w(n)}$ is the outlet liquid temperature. $i_{ma(0)}$ is the initial point of the operative line and H_z is the last point of the operative line, which is a straight line.

2.5.2 Equilibrium line

To calculate the points necessary to constitute the equilibrium curve of the exchange, it needs to take into account that the enthalpy of the air depends both on its temperature but also on its degree of humidity. that can be written:

$$i_{masw} = c_{pma} \cdot T_a + \Delta i_v \cdot w \quad (2.3)$$

Where:

- $c_{pma} \cdot T_a$ Due to the heating of moist air
- $\Delta i_v \cdot w$ Due to the heat of evaporation of water, the greater the evaporation the greater the heat input given by it

Since the thermal conductivity of water is extremely greater than that of air, at the liquid-vapor interface, it can be defined that $w = w_{sw}(T_i) \simeq Y_{sw}(T_w)$, noting how the mole fraction of water in the air is strongly dependent on the temperature of the water itself.

Rewriting (2.3) as:

$$i_{masw} = c_{pma} \cdot T_a + \Delta i_v \cdot w_{sw}(T_w) \quad (2.4)$$

Going to plot our equilibrium curve we will notice how it is not a straight line but has a certain curvature as the temperature of the liquid T_w varies.

It can be noticed how in Fig. 2.17 there are two gaps between the two curves, which they will respectively call from the right $\Delta i_{ma(1)}$ and $\Delta i_{ma(2)}$ i.e. the driving force of the air in the inlet section of the water.

Driving force = Difference between the enthalpy that would exist if the airflow were in equilibrium with water and the actual enthalpy of the airflow.

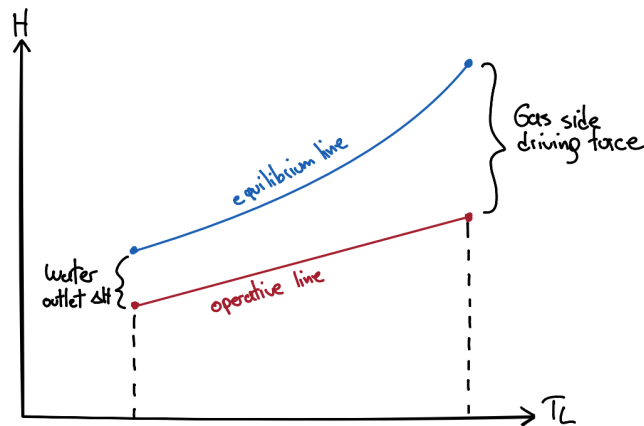


Fig. 2.17: Eq. and op. line

So the air is always in a condition of lower enthalpy than it should theoretically have. So heat always transfers from water to air precisely because the system tends to go to equilibrium and therefore tends to minimize the driving force.

It must be considered that there is a maximum value between the ratio of m_w/m_a flow rates (see equation (2.2)). Mainly this is the parameter where one can work the most to change the air outlet conditions, however, also consider that there is a maximum value between the ratio of m_w/m_a flow rates (see equation (2.2)). Mainly this is the parameter where one can work the most to change the air outlet conditions, however, varying this value too much can cause the operating curve to intersect the equilibrium curve, thus canceling out the driving force and making it impossible to cool the water after a certain temperature. This value too much can cause the operating curve to intersect the equilibrium curve, thus canceling out the driving force and making it impossible to cool the water after a certain temperature. Mass and energy balance can be written as:

Mass transfer rate :

$$\begin{aligned} (\text{WATER ACCUMULATE GAS SIDE}) &= (\text{WATER CONVECTION IN - OUT}) + \\ &(\text{NEW WATER FROM EVAPORATION}) \end{aligned} \quad (2.5)$$

heat transfer rate :

$$\begin{aligned} (\text{ENTHALPY ACCUMULATES ON THE GAS SIDE}) &= (\text{ENERGY CONVECTION IN-OUT}) + \\ &(\text{ENERGY ADDED BY HEAT TRANSFER FROM LIQUID TO GAS}) \end{aligned} \quad (2.6)$$

$$\begin{aligned} 0 &= m_a w \Big|_{n+dn} - m_a w \Big|_n + \beta \cdot \Delta n \cdot k_y \cdot (w_{sw} - w) \\ \lim_{\Delta w \rightarrow 0} &\rightarrow m_a \cdot \frac{dw}{dn} = -k_y \cdot a (w_{sw} - w) \end{aligned} \quad (2.5)$$

$$c_{pma} \cdot m_a \frac{dT_a}{dn} = -h \cdot \beta \cdot (T_w - T_a) \quad (2.6)$$

Having written these balance sheets, it is possible to proceed to obtain the equations that will help to find the design conditions of our evaporative tower. In particular, one will linearly combine the equations to obtain an enthalpy rate equation. Therefore, combining eq (2.5 - w contribution) with (2.6 - n contribution), one can obtain:

$$m_a \frac{d}{dn} (c_{pma} \cdot T_a + \Delta i_v Y) = h \cdot \beta \cdot (T_w - T_a) + k_y \cdot \beta \cdot \Delta i_v (w_{sw} - w) \quad (2.7)$$

$$m_a \frac{di}{dn} = h \cdot \beta \cdot (T_w - T_a) + k_y \cdot \beta \cdot \Delta i_v (w_{sw} - w) \quad (2.8)$$

Through the analogy of Chilton-Colburn, it can be written that:

$$\frac{k}{v} \cdot Sc^{\frac{2}{3}} = \frac{h}{v \cdot \rho \cdot c_{pv}} Pr^{\frac{2}{3}} = \frac{h}{v \cdot \rho \cdot C_p} Pr^{\frac{2}{3}} \quad (2.9)$$

Where:

1. $Sc \simeq Pr$ for the gas

$$2. k = \frac{k_y}{c_{tot}}$$

This allows us to write that $h \simeq k_y \cdot c_{pma}$ into (2.8), we obtain that:

$$m_a \frac{di}{dn} = k_y \cdot \beta [c_{pa}(T_w - T_a) + \Delta i_v (w_{sw} - w)] \quad (2.10)$$

$$m_a \frac{di}{dn} = i_{masw} - i_{ma} \quad (2.11)$$

In the end, the following equation can be used to find the minimum height required for the tower construction,

$$l = \int_0^l dn = \left[\frac{m}{k_y \beta} \right] \cdot \int_{i_{ma(0)}}^{i_{ma(l)}} \frac{di}{i_{masw} - i_{ma}} \quad (2.12)$$

Chapter 3

Mono-dimensional Cooling tower model

Before delving into the model and the MATLAB program I have constructed, I believe it is necessary to briefly explain how an evaporative cooling tower works in the psychrometric chart. This includes discussing the mass and energy exchanges and the influence of temperature and humidity inside the tower. These factors significantly affect the performance of the evaporative cooling tower, moving beyond a purely theoretical analysis as described earlier.

Analytical models or approaches that predict heat and mass transfer in cooling towers serve as the foundation for theoretical and experimental investigations into cooling tower performance. Understanding their limitations and applications is crucial. In this study, two different analytical models are employed: the Merkel and Poppe approaches. These models are utilized to evaluate heat and mass transfer processes in wet-cooling towers. Additionally, they help determine the transfer characteristics of cooling tower fill materials and subsequently assess cooling tower performance. The heat and mass transfer processes are visually represented using psychrometric charts.

3.1 Heat and mass transfert

The mechanism by which heat is transferred in physical equipment is quite complex; however, there appear to be two rather basic and distinct types of heat transfer processes [19]:

- **Conduction**

- Is the transfer by molecular motion of heat between one part of a body to another part of the same body or by one body and another in physical contact with it. In fluids, heat is conducted by nearly elastic collisions of the molecules or by an energy diffusion process.

- **Convection**

- Heat transfer involves the transfer of heat energy through the combined effects of conduction (thermal energy transfer within a solid) and fluid motion. It occurs when a fluid flows over a solid surface or when there is a temperature difference between a fluid and a solid in direct contact.

- **Radiation**

- Or more precisely thermal radiation, is a phenomenon identical to the emission of light and is significant across the entire range of wavelengths from zero to infinity. Frequently, the processes of conduction and radiation occur simultaneously, even within solid bodies.

However, in many engineering problems, the heat transferred by one of the modes is negligible compared with the other and can be assumed with good approximation to involve only one of the processes. Heat transferred between a flowing fluid and its bounding surface is often referred to as heat transfer by convection. The word convection applies to the fluid motion while the mechanisms of heat transfer anywhere in the fluid are only conduction and radiation. In a cooling tower, we can say that only conduction processes are involved (conduction and convection due to movement of the air).

3.1.1 Conduction

When a temperature gradient exists within a homogeneous substance, there is an energy transfer from the high-temperature region to the low-temperature region. Heat is transferred by conduction, and the heat transfer rate per unit area is proportional to the normal temperature gradient :

$$q = \frac{Q}{A} \propto \frac{dT}{dx} \quad (3.1)$$

Where the heat flux q , is the ratio of the heat transfer rate Q through the area A and $\frac{dT}{dx}$ is the temperature gradient in the direction of heat flow.

Introducing the thermal conductivity of a material k and considering the problem of one-dimensional steady-state conduction in a control volume having constant thermal conductivity and the same temperature gradient the following energy balance can be written:

$$Q = -kA \frac{dT}{dx} \quad (3.2)$$

$$Q_x = Q_{x+dx} \quad (3.3)$$

$$-kA \frac{dT}{dx} = -kA \frac{dT}{dx} + \frac{d}{dx} \left(-kA \frac{dT}{dx} \right) dx \quad (3.4)$$

$$\frac{d}{dx} \left(-kA \frac{dT}{dx} \right) dx = 0 \quad (3.5)$$

Considering two point x_1 where $T = T_1$ and x_2 where $T = T_2$, with $x_1 < x_2$ and $T_2 < T_1$ we can calculate the heat transfer rate :

$$Q = \frac{-kA(T_2 - T_1)}{x_2 - x_1} = \frac{T_1 - T_2}{\frac{x_1 - x_2}{kA}} \quad (3.6)$$

3.1.2 Convection

Convection is a process involving the mass movement of fluids. When a temperature difference produces a density difference resulting in mass movement, the process is called free or natural convection. When a pump or other similar device causes the mass motion to take place, the process is called forced convection.

The heat transfer between a fluid and solid surface when the fluid flows either by free or by forced convection is usually referred to as heat transfer by convection.

3.2 Psychrometric chart

Psychrometric charts are valuable tools widely used for analyzing heat and mass exchange involving moist air. These charts present the properties of air-water vapor mixtures graphically, aiding in the design and analysis of such processes. The state of the air at a given pressure is fully defined by two independent intensive properties.

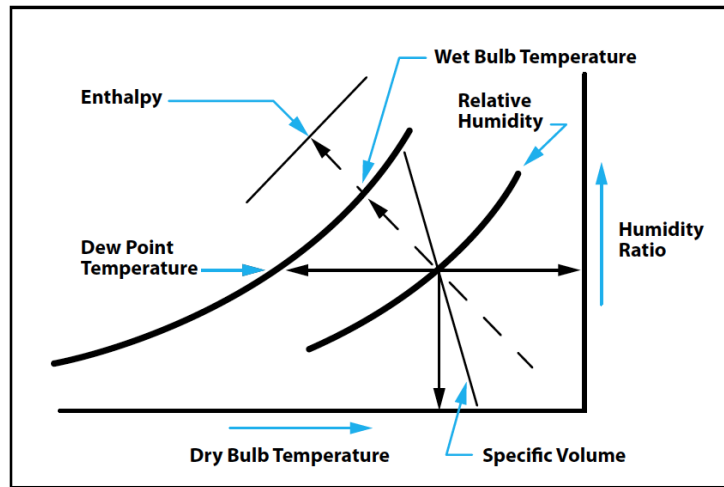


Fig. 3.1: Simple psychrometric chart [7]

The key features of a psychrometric chart are illustrated in Figure 3.1. The horizontal axis represents dry-bulb temperatures, while the vertical axis represents a specific humidity or humidity ratio. The left end of the chart features the saturation curve, where the relative humidity is 100%. All saturated air states lie on this curve. Other curves on the chart represent constant relative humidity, following a similar pattern. Enthalpy is represented by an inclined coordinate, wet-bulb temperature, and specific volume can also be included on a psychrometric chart.

Figure 3.2 illustrates different processes involving air-vapor mixtures on a psychrometric chart. When only heat transfer occurs without mass transfer, the humidity ratio remains constant as the moisture content of the air remains unchanged. Pure heating or cooling of the air takes place.

It is important to note that psychrometric charts describe air behavior in wet-cooling processes and are generally not applicable in the supersaturated region. However, psychrometric charts are extremely useful for analyzing and understanding the direction of enthalpy transfer in cooling towers. Enthalpy potential provides a qualitative indication of the direction of net heat flow in the fill region of cooling towers.

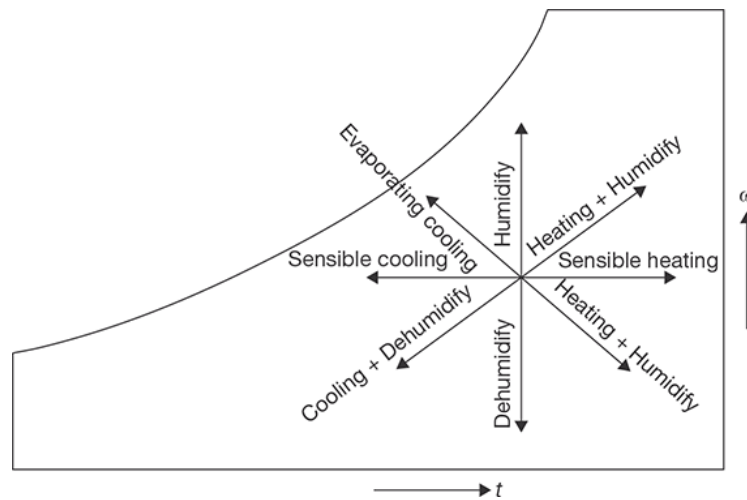


Fig. 3.2: Process involving in a psychrometric chart [8]

It should be clarified that a common misconception is that cooling towers cannot operate when the inlet air is saturated. However, even with saturated inlet air, there is still potential for sensible and latent heat transfer. The excess water vapor transferred to the free stream air will condense, contributing to the overall heat transfer process.

3.3 Lewis number

The Lewis number [20] is a dimensionless parameter used in fluid dynamics and heat transfer to characterize the relative importance of thermal diffusion to mass diffusion in a fluid mixture. It is named after Warren K. Lewis, an American chemical engineer. In thermodynamics, the Lewis number (Le) is defined as the ratio of thermal diffusivity to mass diffusivity. It is given by the equation:

$$Le_f = \frac{\alpha}{D} \quad (3.7)$$

Where:

- α is the thermal diffusivity of the mixture
- D is the mass diffusivity of the mixture.

Thermal diffusivity (α) represents how quickly heat can be conducted through a material, while the mass diffusivity (D) represents how quickly mass (such as the diffusion of one species of gas or liquid into another) can occur in the mixture.

The Lewis number provides information about the relative rates of heat and mass transfer. A Lewis number greater than one ($Le > 1$) indicates that heat transfer is more rapid than mass transfer, meaning thermal diffusion dominates. On the other hand, a Lewis number less than one ($Le < 1$) suggests that mass transfer is more rapid than heat transfer, indicating that mass diffusion is dominant.

In the context of a cooling tower, the Lewis number is a dimensionless parameter used to characterize the relative importance of thermal diffusion to mass diffusion during the cooling process. The Lewis number for a cooling tower is typically defined as the ratio of the thermal diffusivity of the air to the mass diffusivity of the water vapor in the tower.

$$Le_f = \frac{\alpha_{air}}{D_{water\ vapor}} \quad (3.8)$$

The value of the Lewis number in a cooling tower depends on the specific operating conditions, such as the air and water vapor properties, temperature, and flow rates. The exact value of the Lewis number can vary for different cooling tower designs and configurations.

Understanding the Lewis number in a cooling tower helps in analyzing the efficiency and performance of the cooling process, and it can be used in the design and optimization of cooling tower systems.

3.4 Poppe approach

Before discussing the Poppe model [21], it is important to explain the Merkel theory on which it is based. The Merkel theory was developed in the early 1920s and is widely used in the analysis of cooling tower performance.

The Merkel theory simplifies the analysis of heat and mass transfer in cooling towers by making several assumptions so the Merkel theory provides a simplified approach to calculate the heat and mass transfer in a cooling tower.

The Poppe model, developed by Poppe and Rogener in the early 1970s, builds upon the Merkel theory but removes some of its simplifying assumptions. This model provides a more accurate representation of cooling tower performance by considering additional factors, such as non-isothermal behavior and variable heat transfer coefficients along the tower height.

By incorporating the Poppe model into the analysis, the cooling tower performance can be better understood and more accurately predicted. The Poppe model takes into account the variations in temperature and heat transfer coefficients, leading to improved accuracy in assessing the overall performance of the cooling tower.

3.4.1 Merkel theory

In 1925, Merkel developed a theory for evaluating the performance of cooling towers. However, this work went largely unnoticed until 1941 when the paper was translated into English. Since then, the Merkel model has gained widespread application and is now recommended by international standards.

The Merkel theory [22] [23] simplifies the calculation of heat and mass transfer in wet-cooling towers by making several critical assumptions. However, due to these assumptions, the Merkel method does not accurately capture the physics of the heat and mass transfer process in the cooling tower fill.

The Merkel theory relies on the following critical simplifying assumptions:

- The Lewis factor, L_{ef} , is assumed to be equal to unity, which has a small impact but affects results at low ambient temperatures.
- The air exiting the tower is assumed to be saturated with water vapor and is characterized solely by its enthalpy. This assumption is negligible above an ambient temperature of 20°C but becomes significant at lower temperatures.
- The reduction in water flow rate due to evaporation is neglected in the energy balance. This simplification has a greater impact at elevated ambient temperatures.

Additionally, Merkel introduced a coefficient known as the Merkel number, which represents the mass transfer coefficient and area density of the fill in a wet-cooling tower. It is defined as the ratio of the actual mass transfer rate of water vapor from the water phase to the maximum possible mass transfer rate.

The actual mass transfer rate corresponds to the rate at which water vapor is transferred from the water phase to the gas phase in the cooling tower, while

the maximum mass transfer rate represents the theoretical limit of mass transfer achievable under ideal conditions.

The Merkel number takes into account various factors such as cooling tower design, packing material, water and air flow rates, and temperature differences between the water and air. It provides a measure of the cooling tower's effectiveness in transferring heat and moisture. The equation for calculating the Merkel number will be presented in the subsequent approach.

3.4.2 Poppe and Rogener theory

In this section, we will only present Poppe's approach [24] since, as mentioned earlier, it involves modifying certain parts of Merkel's theory, particularly in the calculation of specific heats, relying more on empirical rather than theoretical processes.

Let's consider the two control volumes shown in Figures 3.3 and 3.4. As described in Chapter 2, we can write the mass and energy balance equations for these volumes. For Fig. 3.3, let's start with its mass balance, which states that the differ-

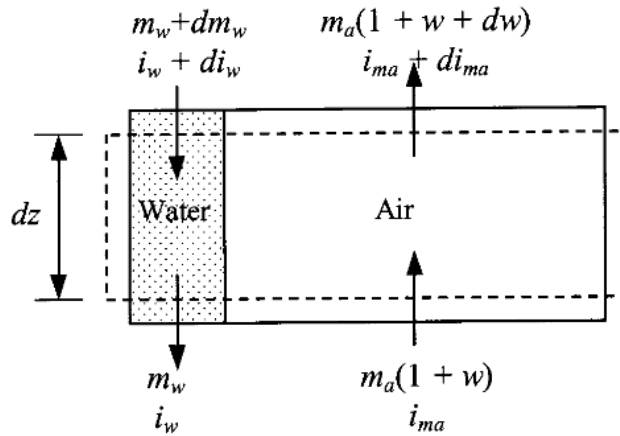


Fig. 3.3: Control volume of counterflow fill [9]

ence in water flow rate between the inlet and outlet of the control volume, under steady-state conditions, is equal to the dry air flow rate multiplied by the difference in humidity:

$$(m_w + dm_w) + m_a \cdot (1 + w) = m_w + m_a \cdot (1 + w + dw) \quad dm_w = m_a \cdot dw \quad (3.9)$$

Regarding the energy balance of the system, we can refer to the control volume shown in Fig. 3.3:

$$m_a di_{ma} - m_w di_w - i_w dm_w = 0 \quad (3.10)$$

Here, i_{ma} represents the enthalpy of the air-vapor mixture described in equation 3.20 as a subscript of this paragraph. Substituting equation 3.9 into 3.10, assuming that the specific heat within the control volume, for an infinitesimal height increment dz considered, is constant, we can find that:

$$m_a di_{ma} - m_w di_w - i_w \cdot m_a dw = 0 \quad (3.11a)$$

$$i_w = c_{p_w} \cdot T_w \quad (3.11b)$$

$$m_a di_{ma} - m_w \cdot c_{p_w} dT_w - c_{p_w} \cdot T_w \cdot m_a dw \quad (3.11c)$$

After rearranging the equations:

$$dT_w = \frac{m_a}{m_w} \cdot \left(\frac{1}{c_{p_w}} di_{ma} - T_w dw \right) \quad (3.12)$$

Consider the interface between the water and the air in Fig. 3.4. An energy balance

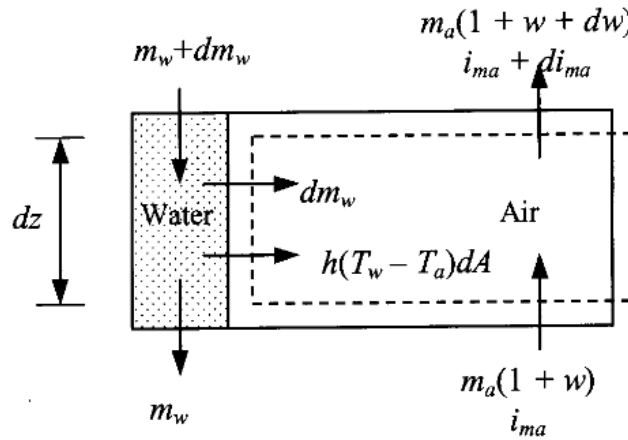


Fig. 3.4: Air side control volume [9]

at the interface yields:

$$dQ = dQ_m + dQ_c \quad (3.13)$$

where dQ_m is the enthalpy transfer due to the difference in vapor concentration between the saturated air at the interface and the mean stream air and dQ_c is the sensible heat transfer due to the temperature difference. The mass transfer at the interface is expressed by:

$$dm_w = h_d(w_{sw} - w)dA \quad (3.14)$$

The corresponding enthalpy transfer for the mass transfer in Eq. 3.14 is

$$dQ_m = i_v dm_w = i_v h_d (w_{sw} - w) dA \quad (3.15)$$

Where i_v is the enthalpy of water vapor at the bulk water temperature T_w :

$$i_v = i_{fgvo} + c_{pv} T_w \quad (3.16)$$

The convective heat transfer from Fig. 2 is given by :

$$dQ_c = h(T_w - T_a)dA \quad (3.17)$$

The temperature differential in Eq. 3.17 can be replaced by an enthalpy differential. The enthalpy of saturated air evaluated at the local bulk water temperature is given by:

$$i_{masw} = c_{pa} T_w + w_{sw} (i_{fgwo} + c_{pv} T_w) \quad (3.18)$$

$$i_{masw} = c_{pa} T_w + w i_v + (w_{sw} - w) i_v \quad (3.19)$$

Where Eq. 3.19 was founded by substituting Eq. 3.16 into 3.18.

The enthalpy of the air-water vapor mixture per unit mass of dry air is expressed by:

$$i_{ma} = c_{pa} T_a + w (i_{fgwo} + c_{pv} T_a) \quad (3.20)$$

Subtract Eq. 3.20 from 3.19. The resultant equation can be simplified if the small differences in specific heats, which are evaluated at different temperatures, are ignored:

$$T_w - T_a = \frac{(i_{masw} - i_{ma}) - (w_{sw} - w) i_v}{c_{pma}} \quad (3.21)$$

Where the equation describing c_{pma} is :

$$c_{pma} = c_{pa} - w c_{pv} \quad (3.22)$$

Substitute Eq. (3.21) into Eq. 3.17. Substitute the resultant equation and Eq. 3.15 into Eq. 3.13 to find after rearrangement:

$$dQ = h_d \cdot \left[\frac{h}{c_{pma} \cdot h_d} \cdot (i_{masw} - i_{ma}) + \left(1 - \frac{h}{c_{pma} \cdot h_d} \right) \cdot i_v (w_{sw} - w) \right] dA \quad (3.23)$$

Where $\frac{h}{c_{pma}} \cdot h_d$ is known as the Lewis factor Le_f and is an indication of the relative rates of heat and mass transfer in an evaporative process. Bosnjakovic developed an empirical relation for the Lewis factor Le_f for air–water vapor systems. The Lewis factor for unsaturated air :

$$Le_f = 0.865^{0.667} \cdot \left(\frac{w_{sw} + 0.622}{w + 0.622} - 1 \right) / \left[\ln \left(\frac{w_{sw} + 0.622}{w + 0.622} \right) \right] \quad (3.24)$$

The enthalpy transfer to the air stream from Eq. 3.23 is :

$$di_{ma} = \frac{1}{m_a} dQ = \frac{h_d dA}{m_a} \cdot \left[Le_f (i_{masw} - i_{ma} + (1 + Le_f) \cdot i_v (w_{sw} - w)) \right] \quad (3.25)$$

For a one-dimensional model of the cooling tower fill, where the available area for heat and mass transfer is the same at any horizontal section through the fill, the transfer area for a section dz is usually expressed as :

$$dA = a_{fi} \cdot A_{fr} dz \quad (3.26)$$

Where a_{fi} is the area density of the fill and A_{fr} is the corresponding frontal area of the face area. Substituting Eq. 3.26 into Eq. 3.25 :

$$\frac{di_{ma}}{dz} = \frac{h_d \cdot a_{fi} \cdot A_{fr}}{m_a} \cdot \left[Le_f (i_{masw} - i_{ma} + (1 + Le_f) \cdot i_v (w_{sw} - w)) \right] \quad (3.27)$$

From that point, the Merkel theory (3.4.1) to simplify the analysis of an evaporative process, the evaporative loss is assumed negligible, which means $dw = 0$ from Eq. 3.12, and that the Lewis factor is equal to unity. The governing Eq. 3.12 and 3.27 of the counterflow evaporative process simplify respectively to :

$$dT_w = \frac{m_a}{m_w} \cdot \left(\frac{1}{c_{pw}} \frac{di_{ma}}{dz} \right) \quad (3.28)$$

$$\frac{di_{ma}}{dz} = \frac{h_d \cdot a_{fi} \cdot A_{fr}}{m_a} \cdot (i_{masw} - i_{ma}) \quad (3.29)$$

Which describe respectively the change in the enthalpy of the air-water vapor mixture and the change in water temperature as the air travel distance changes. These Eq. can be combined to yield upon integration the Merkel number equation :

$$Me_m = \frac{h_d \cdot A}{m_w} = \frac{h_d \cdot a_{fi} \cdot A_{fr} \cdot L_{ft}}{m_w} = \frac{h_d \cdot a_{fi} \cdot A_{fr} \cdot L_{ft}}{G_w} = \int_{T_{wout}}^{T_{win}} \frac{c_{pw} dT_w}{(i_{masw} - i_{ma})} \quad (3.30)$$

where Me_m is the Merkel number according to the Merkel approach. It is not possible to calculate the state of the air leaving the fill according to this equation.

Merkel assumed that the air leaving the fill was saturated with water vapor. This assumption enables the air temperature leaving the fill to be calculated.

From that point, Poppe and Rogener did not make the simplifying assumptions Merkel made. They derived the governing equation through the fill by following a different strategy than Merkel. Whereas the governing Eq. 3.29 and 3.30 according to the Merkel theory describe the changes of the enthalpy of the air-water vapor mixture and water temperature to the change of air travel distance, Poppe and Rilgener describe the change of the humidity ratio and the enthalpy of the air-water vapor mixture to the change of water temperature.

So the Eq. 3.14 and 3.26 can be substituted in the Eq. 3.10 to find:

$$m_w di_w = h_d dA \left[i_{masw} - i_{ma} + (Le_f - 1) \cdot \right. \quad (3.31)$$

$$\left. [i_{masw} - i_{ma} - i_v(w_{sw} - w)] - c_{pw} T_w (w_{sw} - w) \right] \quad (3.32)$$

And Eq. 3.12 became :

$$\frac{dw}{dT_w} = \frac{di_{ma}}{T_w di_w} - \frac{m_w}{T_w \cdot m_a} \quad (3.33)$$

Substitute Eq. 3.25 and Eq. 3.32 into Eq. 3.33:

$$\frac{di_w}{dT_w} = c_{pw} \frac{m_w}{m_a} \left(\frac{(w_{sw} - w)}{i_{masw} - i_{ma} + (Le_f - 1) \cdot [i_{masw} - i_{ma} - i_v(w_{sw} - w)] - c_{pw} T_w (w_{sw} - w)} \right) \quad (3.34)$$

And substituting Eq. 3.48 into Eq. 3.33 the enthalpy can be rewritten as :

$$\frac{di_{ma}}{dT_w} = c_{pw} \frac{m_w}{m_a} \left(1 + \frac{c_{pw} T_w (w_{sw} - w)}{i_{masw} - i_{ma} + (Le_f - 1) \cdot [i_{masw} - i_{ma} - i_v(w_{sw} - w)] - c_{pw} T_w (w_{sw} - w)} \right) \quad (3.35)$$

The Merkel number, according to the Poppe model became :

$$Me_p = \int \frac{m_w}{m_a} \cdot \frac{dw/dT_w}{w_{sw} - w} dT_w \quad (3.36)$$

and in its differential form using Eq. 3.36 and Eq. 3.48 :

$$\frac{dMe_p}{dT_w} = \frac{c_{pw}}{i_{masw} - i_{ma} + (Le_f - 1) \cdot [i_{masw} - i_{ma} - i_v(w_{sw} - w)] - c_{pw} T_w (w_{sw} - w)} \quad (3.37)$$

The ratio of the mass flow rates, m_w , and the enthalpy i_{ma} changes as the air moves towards the top of the fill. The change in the mass flow rate is determined by considering the control volume of a portion of the fill illustrated in Fig. 3.5

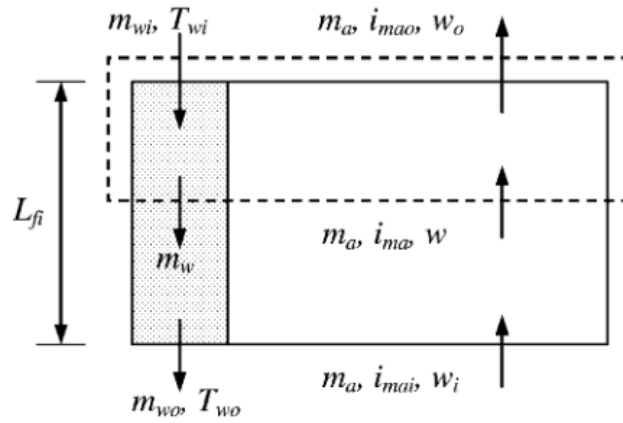


Fig. 3.5: Control volume on the fill [9]

The varying water mass flow rate can be determined from the known inlet water mass flow rate. From the control volume in Fig 3.5 a mass balance will yield :

$$m_{wi} = m_w + m_a(w_0 - w) \quad (3.38)$$

$$\frac{m_w}{m_a} = \frac{m_{wi}}{m_a} \left(1 - \frac{m_a}{m_{wi}}(w_0 - w) \right) \quad (3.39)$$

The preceding system of equations is only applicable to unsaturated air. In some cases, the air can become saturated before it leaves the fill. Because the water temperature is still higher than the temperature of the air, the potential for heat and mass transfer still exists. Under these conditions, the excess water vapor will condense as a mist

3.4.2.1 Case of Supersaturated air

The control volumes in Fig. 3.3 and 3.4 are also applicable for supersaturated air. Since the excess water vapor will condense as a mist, the enthalpy of supersaturated air is expressed by :

$$\dot{i}_{ss} = c_{pa}T_a + w_{sa}(\dot{i}_{fgw_0} + c_{pv}T_a) + (w_{sw} - c_{pw}T_a w_{sa}) \quad (3.40)$$

where w_{sa} is the humidity ratio of saturated air at temperature T_a . Assume that the heat and mass transfer coefficients for supersaturated and unsaturated air are the same. The driving potential for mass transfer is the humidity ratio difference between the saturated air at the air-water interface and the saturated free stream air, thus :

$$dm_w = h_d(w_{sw} - w_{sa})dA \quad (3.41)$$

The enthalpy driving potential for supersaturated air can be obtained by subtracting Eq. 3.40 from Eq. 3.19. By introducing :

$$c_{pv}T_w(w - w_{sa}) - c_{pv}T_w(w - w_{sw}) + c_{pw}T_w w_{sa} - c_{pw}T_w w_{sw} \quad (3.42)$$

which adds up to zero, In the resultant enthalpy differential, the temperature differential can be obtained by manipulation.

$$T_w - T_a = \frac{(i_{masw} - i_{ss}) - (w_{sw} - w_{sa})i_v + c_{pw}T_w(w - w_{sa})}{c_{pmas}} \quad (3.43)$$

where c_{pmas} is the specific heat of supersaturated air per unit mass and is defined as :

$$c_{pmas} = c_{pa} + w_{sa}c_{pv} + c_{pw}(w - w_{sa}) \quad (3.44)$$

Proceeding along the same lines as in the case of unsaturated air, but using the equations written above the new equation for the enthalpy, humidity ratio and Merkel number will be :

$$\frac{di_{ma}}{dT_w} = c_{pw} \frac{m_w}{m_a} \left(\frac{(w_{sw} - w_{sa})}{i_{masw} - i_{ss} + (Le_f - 1) \cdot \left[\begin{array}{l} i_{masw} - i_{ss} - (w_{sw} - w_{sa})i_v \\ + c_{pw}T_w(w - w_{sa}) \end{array} \right]} + c_{pw}T_w(w - w_{sw}) \right) \quad (3.45)$$

$$\frac{di_{ma}}{dT_w} = c_{pw} \frac{m_w}{m_a} \left(1 + \frac{c_{pw}T_w(w_{sw} - w_{sa})}{i_{masw} - i_{ss} + (Le_f - 1) \cdot \left[\begin{array}{l} i_{masw} - i_{ss} - (w_{sw} - w_{sa})i_v \\ + c_{pw}T_w(w - w_{sa}) \end{array} \right]} + c_{pw}T_w(w - w_{sw}) \right) \quad (3.46)$$

$$\frac{dMe_p}{dT_w} = \frac{c_{pw}}{i_{masw} - i_{ss} + (Le_f - 1) \cdot \left[\begin{array}{l} i_{masw} - i_{ss} - (w_{sw} - w_{sa})i_v \\ + c_{pw}T_w(w - w_{sa}) \end{array} \right]} + c_{pw}T_w(w - w_{sw}) \quad (3.47)$$

And reporting the analog for the non-supersaturated:

$$\frac{di_w}{dT_w} = c_{pw} \frac{m_w}{m_a} \left(\frac{(w_{sw} - w)}{i_{masw} - i_{ma} + (Le_f - 1) \cdot [i_{masw} - i_{ma} - i_v(w_{sw} - w)] - c_{pw} T_w (w_{sw} - w)} \right) \quad (3.48)$$

$$\frac{di_{ma}}{dT_w} = c_{pw} \frac{m_w}{m_a} \left(1 + \frac{c_{pw} T_w (w_{sw} - w)}{i_{masw} - i_{ma} + (Le_f - 1) \cdot [i_{masw} - i_{ma} - i_v(w_{sw} - w)] - c_{pw} T_w (w_{sw} - w)} \right) \quad (3.49)$$

$$\frac{dMe_p}{dT_w} = \frac{c_{pw}}{i_{masw} - i_{ma} + (Le_f - 1) \cdot [i_{masw} - i_{ma} - i_v(w_{sw} - w)] - c_{pw} T_w (w_{sw} - w)} \quad (3.50)$$

Chapter 4

Developing MATLAB model

4.1 Runge-Kutta 4th Order Method (RK4)

The fourth-order Runge-Kutta method [25], often abbreviated as RK4, is a popular numerical algorithm used to solve ordinary differential equations (ODEs). It is one of the most common numerical methods for numerically integrating differential equations and is used in a variety of fields, including physics, engineering, and computational sciences.

RK4 is an explicit method, which means it calculates the next value of the function (or functions) based on the previous values and the time step, without explicitly solving the differential equation. This method is known for its accuracy and is quite stable for many applications.

The Runge-Kutta 4th Order method is an explicit numerical integration scheme for solving initial value problems of the form:

$$\left[\frac{dy}{dt} = f(t, y), \quad y(t_0) = y_0 \right]$$

Here, t is the independent variable, $y(t)$ is the unknown function we want to solve for, $f(t, y)$ is a given function that represents the derivative of y concerning t , and y_0 is the initial value of y at the starting point t_0 .

The RK4 method approximates the solution $y(t)$ by taking four weighted steps based on the derivative $f(t, y)$ at different points. The algorithm is as follows:

4.1.1 RK4 Algorithm

Given the initial value problem as described above, the RK4 method proceeds as follows:

1. Set the initial values: $(t_0), (y_0)$.
2. Choose a step size h (a small positive number) to determine the interval between successive points: $(t_0, t_1 = t_0 + h, t_2 = t_1 + h, \dots)$
3. Iterate using the RK4 formula to approximate $y(t_n)$ at each time step (t_n) :

$$\begin{aligned} k_1 &= h \cdot f(t_n, y_n) \\ k_2 &= h \cdot f\left(t_n + \frac{h}{2}, y_n + \frac{k_1}{2}\right) \\ k_3 &= h \cdot f\left(t_n + \frac{h}{2}, y_n + \frac{k_2}{2}\right) \\ k_4 &= h \cdot f(t_n + h, y_n + k_3) \\ y_{n+1} &= y_n + \frac{1}{6}(k_1 + 2k_2 + 2k_3 + k_4) \end{aligned}$$

where (y_n) is the approximate solution at (t_n) , and (y_{n+1}) is the updated approximate solution at $(t_{n+1} = t_n + h)$.

4.1.2 Theoretical Background

The RK4 method is derived from Taylor series expansion and truncating higher-order terms. The local truncation error of the RK4 method is on the order of $O(h^5)$, making it a fourth-order accurate method. It means that for sufficiently small step sizes h , the RK4 method provides an accurate approximation of the true solution.

4.1.2.1 Theorem 1: Local Truncation Error (LTE) of RK4

If $y(t)$ is the exact solution of the initial value problem $\frac{dy}{dt} = f(t, y)$ with initial condition $y(t_0) = y_0$, and y_n is the value obtained by the RK4 method at $t_n = t_0 + nh$, then the local truncation error LTE_n at each step is $O(h^5)$.

4.1.2.2 Theorem 2: Global Error of RK4

If the RK4 method is applied with a fixed step size h over a finite interval $[t_0, T]$, then the global error E at time T is $O(h^4)$.

4.2 Application of RK4 in Poppe model

Building upon the theory discussed in section 3.4.2, this section will describe how the MATLAB code was constructed by modifying and using the Runge-Kutta method to solve the differential equations described in the previous chapter.

First, we will explain the process of solving the three differential equations 3.49, 3.36, 3.50, or 3.45, 3.46, 3.47, for air under supersaturation conditions. To simplify the code and the logical process, we have chosen to rewrite these equations as follows:

$$\frac{dw}{dT_w} = f(w, i_{ma}, T_w) \quad (4.1)$$

$$\frac{di_{ma}}{dT_w} = g(w, i_{ma}, T_w) \quad (4.2)$$

$$\frac{dMe_p}{dT_w} = h(w, i_{ma}, T_w) \quad (4.3)$$

and in case of supersaturation conditions:

$$\frac{dw}{dT_w} = f(w, i_{ss}, T_w) \quad (4.4)$$

$$\frac{di_{ma}}{dT_w} = g(w, i_{ss}, T_w) \quad (4.5)$$

$$\frac{dMe_p}{dT_w} = h(w, i_{ss}, T_w) \quad (4.6)$$

Next, we divide the fill into one or more intervals with the same water temperature difference across each interval. Additionally, we specify levels (an imaginary horizontal plane through the fill at the top and bottom and between two fill intervals). Initial values of the variables w , i_{ma} , and T_w are required at a specific level, let's say level n . Using the following equations, we can determine the values of the variables at level $(n + 1)$:

$$w_{(n+1)} = w_{(n)} + \frac{j_{(n+1,1)} + 2 \cdot j_{(n+1,2)} + 2 \cdot j_{(n+1,3)} + j_{(n+1,4)}}{6} \quad (4.7)$$

$$i_{ma(n+1)} = i_{ma(n)} + \frac{k_{(n+1,1)} + 2 \cdot k_{(n+1,2)} + 2 \cdot k_{(n+1,3)} + k_{(n+1,4)}}{6} \quad (4.8)$$

$$Me_{p(n+1)} = Me_{p(n)} + \frac{l_{(n+1,1)} + 2 \cdot l_{(n+1,2)} + 2 \cdot l_{(n+1,3)} + l_{(n+1,4)}}{6} \quad (4.9)$$

where :

$$j_{(n+1,1)} = \Delta T_w \cdot f(w_{(n)}, i_{ma(n)} T_{w(n)}) \quad (4.10)$$

$$k_{(n+1,1)} = \Delta T_w \cdot g(w_{(n)}, i_{ma(n)} T_{w(n)}) \quad (4.11)$$

$$l_{(n+1,1)} = \Delta T_w \cdot h(w_{(n)}, i_{ma(n)} T_{w(n)}) \quad (4.12)$$

$$j_{(n+1,2)} = \Delta T_w \cdot f\left(w_{(n)} + \frac{j_{(n+1,1)}}{2}, i_{ma(n)} + \frac{k_{(n+1,1)}}{2}, T_{w(n)} + \frac{\Delta T_w}{2}\right) \quad (4.13)$$

$$k_{(n+1,2)} = \Delta T_w \cdot g\left(w_{(n)} + \frac{j_{(n+1,1)}}{2}, i_{ma(n)} + \frac{k_{(n+1,1)}}{2}, T_{w(n)} + \frac{\Delta T_w}{2}\right) \quad (4.14)$$

$$l_{(n+1,2)} = \Delta T_w \cdot h\left(w_{(n)} + \frac{j_{(n+1,1)}}{2}, i_{ma(n)} + \frac{k_{(n+1,1)}}{2}, T_{w(n)} + \frac{\Delta T_w}{2}\right) \quad (4.15)$$

$$j_{(n+1,3)} = \Delta T_w \cdot f\left(w_{(n)} + \frac{j_{(n+1,2)}}{2}, i_{ma(n)} + \frac{k_{(n+1,2)}}{2}, T_{w(n)}\right) \quad (4.16)$$

$$k_{(n+1,3)} = \Delta T_w \cdot g\left(w_{(n)} + \frac{j_{(n+1,2)}}{2}, i_{ma(n)} + \frac{k_{(n+1,2)}}{2}, T_{w(n)}\right) \quad (4.17)$$

$$l_{(n+1,3)} = \Delta T_w \cdot h\left(w_{(n)} + \frac{j_{(n+1,2)}}{2}, i_{ma(n)} + \frac{k_{(n+1,2)}}{2}, T_{w(n)}\right) \quad (4.18)$$

$$j_{(n+1,4)} = \Delta T_w \cdot f\left(w_{(n)} + j_{(n+1,3)}, i_{ma(n)} + k_{(n+1,3)}, T_{w(n)} + \Delta T_w\right) \quad (4.19)$$

$$k_{(n+1,4)} = \Delta T_w \cdot g\left(w_{(n)} + j_{(n+1,3)}, i_{ma(n)} + k_{(n+1,3)}, T_{w(n)} + \Delta T_w\right) \quad (4.20)$$

$$l_{(n+1,4)} = \Delta T_w \cdot h\left(w_{(n)} + j_{(n+1,3)}, i_{ma(n)} + k_{(n+1,3)}, T_{w(n)} + \Delta T_w\right) \quad (4.21)$$

The next section will explain the complete construction of the script step by step.

4.3 Analysis of a natural draft wet-cooling tower with Poppe's approach

The model was written using MATLAB r2023a and subsequently validated using data obtained from (.. insert table and validation data).

Now, let's describe the logical process of creating the script. Some variables will change nomenclature compared to the reference written in the nomenclature at the end of Chapter 3. However, the units of measurement will remain the same.

4.3.1 Inlet condition

As the first step in creating the program, the available input data was imported. These input values serve as the basis for the calculations and simulations performed in the script. These input data include:

- Inlet water temperature
- Dry bulb air temperature
- Wet bulb air temperature
- Relative humidity

Subsequently, an estimation of the water flow rate required for the proper functioning of the evaporative tower was made based on the data provided for the Danube. All these values were included in a block called *d* to make the data independent and encapsulate them within a single variable.

This approach helps to organize and manage the input data efficiently, ensuring that they are easily accessible and modifiable as needed throughout the script. The use of the *d* block simplifies the code structure and enhances its readability.

```
%% Input data  
d = struct();           % Input data  
d.Tairin    = 11.05;   % °C  
d.Tairindry = 15.45;   % °C  
d.Pair      = 84100;   % Pa  
d.Twout     = 27.77;   % °C  
d.Twin      = 40;      % °C  
d.mw        = 12500;   % kg/s
```

Next, we set the number of cycles to be performed to solve the differential equations as $N = 50$. This value determines the precision and granularity of the calculations.

Then, we initialized the length of the vectors with zeros to speed up the computations and optimize memory usage. This step preallocates memory for the vectors and avoids frequent reallocation during the iterative process, enhancing the efficiency of the code.

Finally, we performed some unit conversions to ensure consistency in the calculations.

```

N = 5; % Number of steps of RK method

%% Inizialization of vectors
Tdb = zeros(1, N + 2);
Twb = zeros(1, N + 1);
Tw = zeros(1, N + 1);
w = zeros(1, N + 2);
ima = zeros(1, N + 2);
Mep = zeros(1, N + 1);

%% Computation of Air properties temperature
% Tdb = Dry bulb K
% Twb = Wet bulb K
% w = Humidity ratio kg/kg
% ima = Enthalpy of gas phase J/kg dry air

Tdb(1) = d.Tairindry +273.15;
Twb(1) = d.Tairin +273.15;

```

The calculation of initial variables started, particularly the enthalpy of the air entering the evaporative tower, its humidity, and pressure, using Eq. 3.20 and the following empirical formulas obtained from Kroger:

$$\begin{aligned}
 z = & 10.79586 \left(1 - \frac{273.15}{T_{wb}} \right) + 5.02808 \log_{10} \left(\frac{273.15}{T_{wb}} \right) \\
 & + 1.50474 \cdot 10^{-4} \left[1 - \left(10^{-8.29692 \cdot \left(\frac{T_{wb}}{273.15} \right)} - 1 \right) \right] \\
 & + 4.2873 \cdot 10^{-4} \left[10^{4.76955 \cdot \left(1 - \frac{273.15}{T_{wb}} \right)} - 1 \right] \\
 & + 2.786118312
 \end{aligned} \tag{4.22}$$

Where z is a parameter needed to calculate the water vapor's pressure evaluated at wet-bulb air temperature:

$$p_v = 10^z \tag{4.23}$$

Next, we proceed with calculating the specific heats required to determine the enthalpy of the incoming air, following the guideline given by Poppe's model. For this purpose, we utilize empirical formulas determined by Kroger. Since these formulas will be used multiple times throughout the script, we will write them once to provide a reference. We will specify the reference temperature T each time we use them.

$$w = \frac{2501.6 - 2.3263 * (T_{wb} - 273.15)}{2501.6 + 1.8577 * (T_{wb} - 273.15) - 4.184 * (T_{wb} - 273.15)} \cdot \frac{0.62509 * p_v}{p_{amb} - 1.005 * p_v} \quad (4.24)$$

$$- \frac{1.00416 * ((T_{db} - 273.15) - (T_{wb} - 273.15))}{2501.6 + 1.8577 * (T_{db} - 273.15) - 4.184 * (T_{wb} - 273.15)}$$

$$T = \frac{T_{db} + 273.15}{2} \quad (4.25)$$

$$c_{pa} = 1.045356 \cdot 10^3 - 3.161783 \cdot 10^{-1} \cdot T + 7.083814 \cdot 10^{-4} \cdot T^2 - 2.705209 \cdot 10^{-7} \cdot T^3 \quad (4.26)$$

$$c_{pv} = 1.3605 \cdot 10^3 + 2.31334 \cdot T - 2.46784 \cdot 10^{-10} \cdot T^5 + 5.91332 \cdot 10^{-13} \cdot T^6 \quad (4.27)$$

$$i_{fgwo} = 3.4831814 \cdot 10^6 - 5.8627703 \cdot 10^3 \cdot 273.15 + 12.139568 \cdot 273.15^2 - 1.40290431 \cdot 10^{-2} \cdot 273.15^3 \quad (4.28)$$

$$i_{ma} = c_{pa} \cdot (T_{db} - 273.15) + w \cdot (i_{fgwo} + c_{pv} \cdot (T_{db} - 273.15)) \quad (4.29)$$

Eq. 4.25 represents the reference temperature used for calculating the specific heats, where T_{db} is the dry bulb temperature. Eq. 4.29 represents our first value of the enthalpy of the incoming air. The following code block summarizes what has been discussed so far:

```
% Computation of pressure of water vapor evaluated at Twb
z(1) = 10.79586 * (1-273.15/Twb(1)) + 5.02808 * log10(273.15/Twb(1)) ...
+1.50474e-4 * (1 - (10 ^ (-8.29692 * (Twb(1) / 273.15)) - 1)) ...
+4.2873e-4 * (10 ^ (4.76955 * (1 - 273.15 / Twb(1)))) - 1) ...
+ 2.786118312;

pv_wb = 10^z(1);

%Merkel Number
Mep(1) = 1.55;
```

```

% Computation of humidity ratio for saturated air
w(1) = ((2501.6-2.3263 * (Twb(1)-273.15)) / ...
(2501.6 + 1.8577 * (Twb(1)-273.15) - 4.184*(Twb(1)-273.15)))* ...
((0.62509 * pv_wb) / (d.Pair - 1.005 * pv_wb)) - ...
((1.00416 * ((Tdb(1)-273.15) - (Twb(1)-273.15))) / ...
(2501.6+1.8577 * (Tdb(1)-273.15) - 4.184*(Twb(1)-273.15)));

% Value to put in database for computation of mass flow rate in f,g,h
d.wo = w(1);

%% Computation of enthalpy and specific heat capacity

% Temperature used as reference for the computation
T = (Tdb(1) + 273.15) / 2;
% Specific heat of dry air [J/kgK]
cpa = 1.045356e3 - 3.161783e-1*T +7.083814e-4*T^2 - 2.705209e-7*T^3;

% Specific heat of saturated water vapor [J/kgK]
cpv = 1.3605e3 + 2.31334*T -2.46784e-10*T ^ 5 + 5.91332e-13*T^6;

%Latent heat of water evaluated at 0°C
d.ifgwo = 3.4831814e6 - 5.8627703e3*273.15 + 12.139568*273.15^2 ...
- 1.40290431e-2*273.15^3;

% Enthalpy of air-water vapor mixture [J/kg dry air K]
ima(1) = cpa * (Tdb(1)-273.15) + w(1) * (d.ifgwo+cpv * (Tdb(1)-273.15));

```

4.3.2 Initial approximation of variables

As described in Fig. 2.2b and Fig. 2.16, we can envision the cooling tower as a countercurrent heat exchanger, where air enters from the base of the tower while water is sprayed from the top. Since we consider the base of the tower as the reference point $z = 0$, we are not aware of the temperature of the water exiting the tower (the inlet of our system). The same applies to the air exit values. Therefore, we need to proceed with an estimation.

Five cooling tower design variables are chosen and solved through an iterative procedure. These variables are:

- m_{air} = Air vapor mass flow rate;
- T_{db} = Dry bulb air temperature;
- T_w = Water temperature;
- w = Humidity ratio
- $p_{v(wb)}$ = Pressure of water vapor;

Initial approximations for the variables must be supplied for the first iteration of the cooling tower analysis. A preliminary estimate can be made based on empirical results and simple physical models. The initial approximations of the water outlet temperature, $T_{w(1)}$, and the outlet air temperature, $T_{db(end)}$, are determined from empirical relations found in the literature. The initial approximation for the mass flow rate is found from a simple heat balance of the cooling tower. The air outlet humidity is determined by assuming that the air is saturated at the air outlet of the fill. An empirical formula to determine the approximate water outlet temperature is according to Johnson and Priester:

So for the temperature, the equation will be :

$$T_{w(out)} = \frac{T_{w(in)} + 2T_{wb(in)} + T_{db(in)}}{4} \quad (4.30)$$

$$T_{db(out)} = \frac{T_{w(in)} - T_{w(out)}}{2} \quad (4.31)$$

For the specific heat, pressure, and enthalpy, the formulas described previously were used, such as Eq. 4.26, 4.27, 4.22, 4.23, and 4.25 with $T = \frac{T_{db(out)} + 273.15}{2}$

The initial approximated air mass flow rate can be obtained by a simple heat balance for the cooling tower:

$$m_{air}(i_{ma(out)} - i_{ma(in)}) = m_w c_{pw}(T_{w(in)} - T_{w(out)}) \quad (4.32)$$

$$m_{av} = m_{dry} = \frac{2 \cdot m_{air}}{2 + w_{in} + w_{end}} \quad (4.33)$$

Here is the respective MATLAB script

```

%% Initial approximation of variables

% Outlet water temperature approximation based on Poppe Models [K]
Tw(1) = ((d.Twin + 273.15) + 2 * Twb(1) + Tdb(1)) / 4;
% Outlet air temperature approximation based on Poppe Models [K]
Tdb(end) = ((d.Twin + 273.15 + Tw(1)) / 2);
% Temperature used as reference for the end value of computation
TEND = (d.Twin + 273.15 + Tw(1)) / 2;

% Specific heat of water [J/kgK] evaluated at (Twin+Twout)/2
cpw(1) = 8.15599e3 - 2.80627 * 10 * TEND + 5.11283e-2 * ...
        TEND ^ 2 - 2.17582e-13 * TEND ^ 6;

z(2) = 10.79586 * (1-273.15/Tdb(end)) + 5.02808 * log10(273.15/Tdb(end))
+ 1.50474e-4 * (10^(-8.29692 * (Tdb(end)/273.15) - 1)) ...
+ 4.2873e-4 * (10^(4.76955 * (1-273.15/Tdb(end)))) - 1) ...
+ 2.786118312;

pv_wb(2) = 10^z(2);
w(end) = (0.6250 * pv_wb(2)) / (d.Pair - 1.005 * pv_wb(2));
d.wend = w(end);
T2 = (Tdb(end) + 273.15) / 2;

cpa(2) = 1.045356e3 - 3.161783e-1*T2 + 7.083814e-4*T2^2 - 2.705209e-7*T2^3;
cpv(2) = 1.3605e3 + 2.31334*T2 - 2.46784e-10*T2^5 + 5.91332e-13*T2^6;
ima(end) = cpa(2) * (Tdb(end)-273.15) + w(end)*(d.ifgwo+cpv(2)* ...
        (Tdb(end)-273.15));
% Vapor mass flow rate [kg/s]
mair = (d.mw(1)*cpw(1)*((d.Twin+273.15)-Tw(1))) ...
        /(ima(end)-ima(1));

% Dry air mass flow rate [kg dry/s]
d.madry = (2 * mair) / (2 + d.wo + d.wend);

```


4.3.3 Application of Runge-Kutta method to determine the working status of the cooling tower

To prepare for solving the system of differential equations, as a first step, we set the incremental temperature difference for each step to:

$$DTW = \frac{T_{w(in)} - T_{w(out)}}{N} \tag{4.34}$$

where $N =$ is the number of steps. Subsequently, we established a reference $DELTA$ to determine the system's sensitivity in calculating the air supersaturation condition. The following block diagram outlines the algorithm used for solving the system:

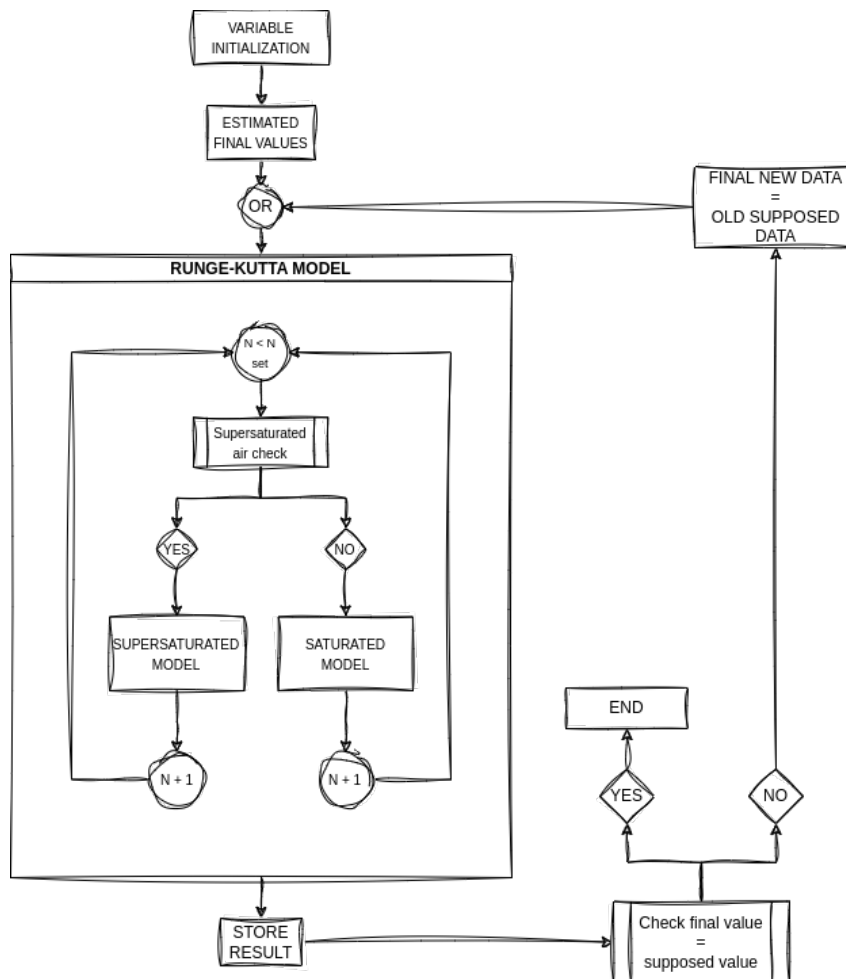


Fig. 4.1: Logical algorithm of MATLAB script

```

DTW = ((d.Twin + 273.15) - Tw(1)) / N;
DELTA = 0.005;
d.a = false;

% Runge-Kutta 4th order to resolve the ODEs system of Cooling-Tower
for n=1:N
if d.a==false
j(n+1,1)=DTW*f(w(n),ima(n),Tw(n),d);
k(n+1,1)=DTW*g(w(n),ima(n),Tw(n),d);
l(n+1,1)=DTW*h(w(n),ima(n),Tw(n),d);

j(n+1,2)=DTW*f(w(n)+(j(n+1,1))/2,ima(n)+(k(n+1,1))/2,Tw(n)+DTW/2,d);
k(n+1,2)=DTW*g(w(n)+(j(n+1,1))/2,ima(n)+(k(n+1,1))/2,Tw(n)+DTW/2,d);
l(n+1,2)=DTW*h(w(n)+(j(n+1,1))/2,ima(n)+(k(n+1,1))/2,Tw(n)+DTW/2,d);

j(n+1,3)=DTW*f(w(n)+(j(n+1,2))/2,ima(n)+(k(n+1,2))/2,Tw(n)+DTW/2,d);
k(n+1,3)=DTW*g(w(n)+(j(n+1,2))/2,ima(n)+(k(n+1,2))/2,Tw(n)+DTW/2,d);
l(n+1,3)=DTW*h(w(n)+(j(n+1,2))/2,ima(n)+(k(n+1,2))/2,Tw(n)+DTW/2,d);

j(n+1,4)=DTW*f(w(n)+j(n+1,3),ima(n)+k(n+1,3),Tw(n)+DTW,d);
k(n+1,4)=DTW*g(w(n)+j(n+1,3),ima(n)+k(n+1,3),Tw(n)+DTW,d);
l(n+1,4)=DTW*h(w(n)+j(n+1,3),ima(n)+k(n+1,3),Tw(n)+DTW,d);

w(n+1)=w(n)+(j(n+1,1)+2*j(n+1,2)+2*j(n+1,3)+j(n+1,4))/6;
ima(n+1)=ima(n)+(k(n+1,1)+2*k(n+1,2)+2*k(n+1,3)+k(n+1,4))/6;
Mep(n+1)=Mep(n)+(l(n+1,1)+2*l(n+1,2)+2*l(n+1,3)+l(n+1,4))/6;

% Calculate air temperature [K]
Tw(n+1)=Tw(n)+DTW;
Tdb(n+1)=dry(w(n+1),Tw(n+1),ima(n+1),d);
[~,Twb(n+1),~,~,~]=psychro(Tdb(n+1),:,:,ima(n+1));
[~,~,~,~,~,iss(n+1)]=checkss(w(n+1),Tdb(n+1),d);
imact=checkima(w(n+1),Tdb(n+1),d);
ERRima=abs((imact-iss(n+1))/(imact+iss(n+1)));
end

if n>1&&Twb(n)>Tdb(n)&&d.a==false&&ERRima>DELTA

[~,~,~,~,~,iss(n)]=checkss(w(n),Tdb(n),d);
X=['Aria sovrassatura, ciclo n=',num2str(n)];

```

```

disp(X);
d.a=true;

j(n+1,1)=DTW*fss(w(n),iss(n),Tw(n),Tdb(n),d);
k(n+1,1)=DTW*gss(w(n),iss(n),Tw(n),Tdb(n),d);
l(n+1,1)=DTW*hss(w(n),iss(n),Tw(n),Tdb(n),d);

j(n+1,2)=DTW*fss(w(n)+(j(n+1,1))/2,iss(n)+(k(n+1,1))/2,Tw(n)+DTW/2,Tdb(n),d);
k(n+1,2)=DTW*gss(w(n)+(j(n+1,1))/2,iss(n)+(k(n+1,1))/2,Tw(n)+DTW/2,Tdb(n),d);
l(n+1,2)=DTW*hss(w(n)+(j(n+1,1))/2,iss(n)+(k(n+1,1))/2,Tw(n)+DTW/2,Tdb(n),d);

j(n+1,3)=DTW*fss(w(n)+(j(n+1,2))/2,iss(n)+(k(n+1,2))/2,Tw(n)+DTW/2,Tdb(n),d);
k(n+1,3)=DTW*gss(w(n)+(j(n+1,2))/2,iss(n)+(k(n+1,2))/2,Tw(n)+DTW/2,Tdb(n),d);
l(n+1,3)=DTW*hss(w(n)+(j(n+1,2))/2,iss(n)+(k(n+1,2))/2,Tw(n)+DTW/2,Tdb(n),d);

j(n+1,4)=DTW*fss(w(n)+j(n+1,3),iss(n)+k(n+1,3),Tw(n)+DTW,Tdb(n),d);
k(n+1,4)=DTW*gss(w(n)+j(n+1,3),iss(n)+k(n+1,3),Tw(n)+DTW,Tdb(n),d);
l(n+1,4)=DTW*hss(w(n)+j(n+1,3),iss(n)+k(n+1,3),Tw(n)+DTW,Tdb(n),d);

w(n+1)=w(n)+(j(n+1,1)+2*j(n+1,2)+2*j(n+1,3)+j(n+1,4))/6;
ima(n+1)=iss(n)+(k(n+1,1)+2*k(n+1,2)+2*k(n+1,3)+k(n+1,4))/6;
Mep(n+1)=Mep(n)+(l(n+1,1)+2*l(n+1,2)+2*l(n+1,3)+l(n+1,4))/6;

% Calculate air temperature [K]
Tw(n+1)=Tw(n)+DTW;
Tdb(n+1)=dry(w(n+1),Tw(n+1),ima(n+1),d);
Twb(n+1)=Tdb(n+1)

else if d.a==true;

j(n+1,1)=DTW*fss(w(n),ima(n),Tw(n),Twb(n),d);
k(n+1,1)=DTW*gss(w(n),ima(n),Tw(n),Twb(n),d);
l(n+1,1)=DTW*hss(w(n),ima(n),Tw(n),Twb(n),d);

j(n+1,2)=DTW*fss(w(n)+(j(n+1,1))/2,ima(n)+(k(n+1,1))/2,Tw(n)+DTW/2,Twb(n),d);
k(n+1,2)=DTW*gss(w(n)+(j(n+1,1))/2,ima(n)+(k(n+1,1))/2,Tw(n)+DTW/2,Twb(n),d);
l(n+1,2)=DTW*hss(w(n)+(j(n+1,1))/2,ima(n)+(k(n+1,1))/2,Tw(n)+DTW/2,Twb(n),d);

j(n+1,3)=DTW*fss(w(n)+(j(n+1,2))/2,ima(n)+(k(n+1,2))/2,Tw(n)+DTW/2,Twb(n),d);
k(n+1,3)=DTW*gss(w(n)+(j(n+1,2))/2,ima(n)+(k(n+1,2))/2,Tw(n)+DTW/2,Twb(n),d);
l(n+1,3)=DTW*hss(w(n)+(j(n+1,2))/2,ima(n)+(k(n+1,2))/2,Tw(n)+DTW/2,Twb(n),d);

```

```

j(n+1,4)=DTW*fss(w(n)+j(n+1,3),ima(n)+k(n+1,3),Tw(n)+DTW,Twb(n),d);
k(n+1,4)=DTW*gss(w(n)+j(n+1,3),ima(n)+k(n+1,3),Tw(n)+DTW,Twb(n),d);
l(n+1,4)=DTW*hss(w(n)+j(n+1,3),ima(n)+k(n+1,3),Tw(n)+DTW,Twb(n),d);

w(n+1)=w(n)+(j(n+1,1)+2*j(n+1,2)+2*j(n+1,3)+j(n+1,4))/6;
ima(n+1)=ima(n)+(k(n+1,1)+2*k(n+1,2)+2*k(n+1,3)+k(n+1,4))/6;
Mep(n+1)=Mep(n)+(l(n+1,1)+2*l(n+1,2)+2*l(n+1,3)+l(n+1,4))/6;

% Calculate air temperature [K]
Tw(n+1)=Tw(n)+DTW;
Tdb(n+1)=dry(w(n+1),Tw(n+1),ima(n+1),d);
Twb(n+1)=Tdb(n+1);

end
end
%Water/Air ratio flow rate
d.mw(n+1)=d.mw(n)+d.madry*(w(n+1)-w(n));

end

ERRima= abs((ima(end) - ima(end -1)) / (ima(end) + ima(end -1)))

```

4.3.3.1 For loop Analysis

To prepare for solving the system of differential equations, let's delve into the workings of the for loop in the MATLAB program. For clarity, we'll utilize logical diagrams to enhance the comprehension of the code.

In our context, we've configured the number of iterations N to 5. This divides the tower's spray zone height into equal sections. Both temperature and other parameters vary linearly within each section. Initially, the system calculates parameters j , k and l as per equations from (4.10) to (4.21). Subsequently, values for humidity, enthalpy, and the Merkel number are calculated with equations from (4.7) to (4.9).

Next, values for the upcoming step are computed for variables:

- Water temperature $\rightarrow T_{w(n+1)} = DTW + T_{w(n)}$

- Dry-bulb and wet-bulb air temperatures (with **dry** script, check appendix for the complete reference)

$$\rightarrow T_{db} = T_w - (((i_{masw} - i_{ma}) - (w_{sw} - w) * i_v) / c_{pma})$$

Subsequently, a verification block is executed for the acquired parameters, involving three scripts:

- **psychro**
 - This script calculates air properties using a psychrometric chart, It was developed by [ref] and it is used, particularly, to calculate the wet bulb temperature given the dry one and enthalpy or humidity ratio
- **checkss**
 - Developed by me, this script calculates enthalpy when the air experiences vapor oversaturation. The complete code is available in the appendix (..), with its functionality explained later.
- **checkima**
 - Also developed by me, similar to **iss**, it computes air enthalpy under unsaturated conditions, using the just-calculated air temperature instead of water temperature as a reference. Further details can be found in the appendix.

Assuming we're in the second cycle ($n = 2$), the script calculates parameters for the section's end, conceptually representing the input for the next level ($n + 1$). Dry-bulb and wet-bulb air temperatures are compared. If the wet-bulb temperature exceeds the dry-bulb temperature and the calculated enthalpy error from **checkss** surpasses a threshold named **DELTA**, the newly performed calculation is overwritten using equations tailored for air in supersaturation conditions. A dual supersaturation check is employed to mitigate temperature oscillations due to script inaccuracies and approximations. The equations used for this program block are provided below.

4.3.3.2 Checkss and sovrsaturated air script

The MATLAB function **checkss** is designed to calculate air enthalpy in supersaturation conditions. It takes inputs of humidity, dry-bulb temperature, pressure, and the reference enthalpy under standard air conditions (eq. ...). Its outputs are:

1. Supersaturation pressure
2. Specific heat of dry air
3. Specific heat of air-vapor mixture
4. Specific heat of water at wet-bulb air temperature
5. Supersaturated air enthalpy

Formulas in 4.24 are used to calculate a new parameter called w_{sa} , the rate of air humidity supersaturation at its dry-bulb temperature. Modified formulas are as follows:

$$w_{sa} = \frac{2501.6 - 2.3263 \cdot (T_{db} - 273.15)}{2501.6 + 1.8577 \cdot (T_{db} - 273.15) - 4.184 \cdot (T_{db} - 273.15)} \cdot \frac{0.62509 \cdot p_{vwb}}{p_{amb} - 1.005 \cdot p_{vwb}} \quad (4.35)$$

Here, z and p_{wp} are calculated according to equations (4.22), (4.23), with T referenced as $T = T_{db}$.

If the air is indeed in a state of supersaturation, the program, as previously mentioned, overwrites the freshly calculated data with new equations for permanent air supersaturation conditions. j, k, l are computed similarly, substituting i_{ma} calculated earlier with i_{ss} . For the differential equation resolution, Eq. (3.48), (3.49), and (3.50) are used, which led to the rewriting of functions 4.4, 4.5 and 4.6 adjusting them to the new equations. Wet-bulb temperature is set equal to dry-bulb temperature from this point onwards.

Within the script, you'll notice a variable named $d.a$. It serves as a boolean switch, as once the air is supersaturated, it's assumed that it cannot reduce its humidity again. This variable enables us to exclude all calculations performed before the new cycle, setting its value to true and moving to equations for calculations in a condition of permanent air supersaturation.

The equations for calculating parameters, once the system is in a state of supersaturation, don't differ significantly from those used previously. Only one modifi-

cation is made to the functions f_{ss} , g_{ss} , and h_{ss} , thanks to variable a (recall that d indicates it's allocated in a general matrix shared among all scripts). The logical algorithm diagram below explains its functioning; for code details, please refer to the appendix.

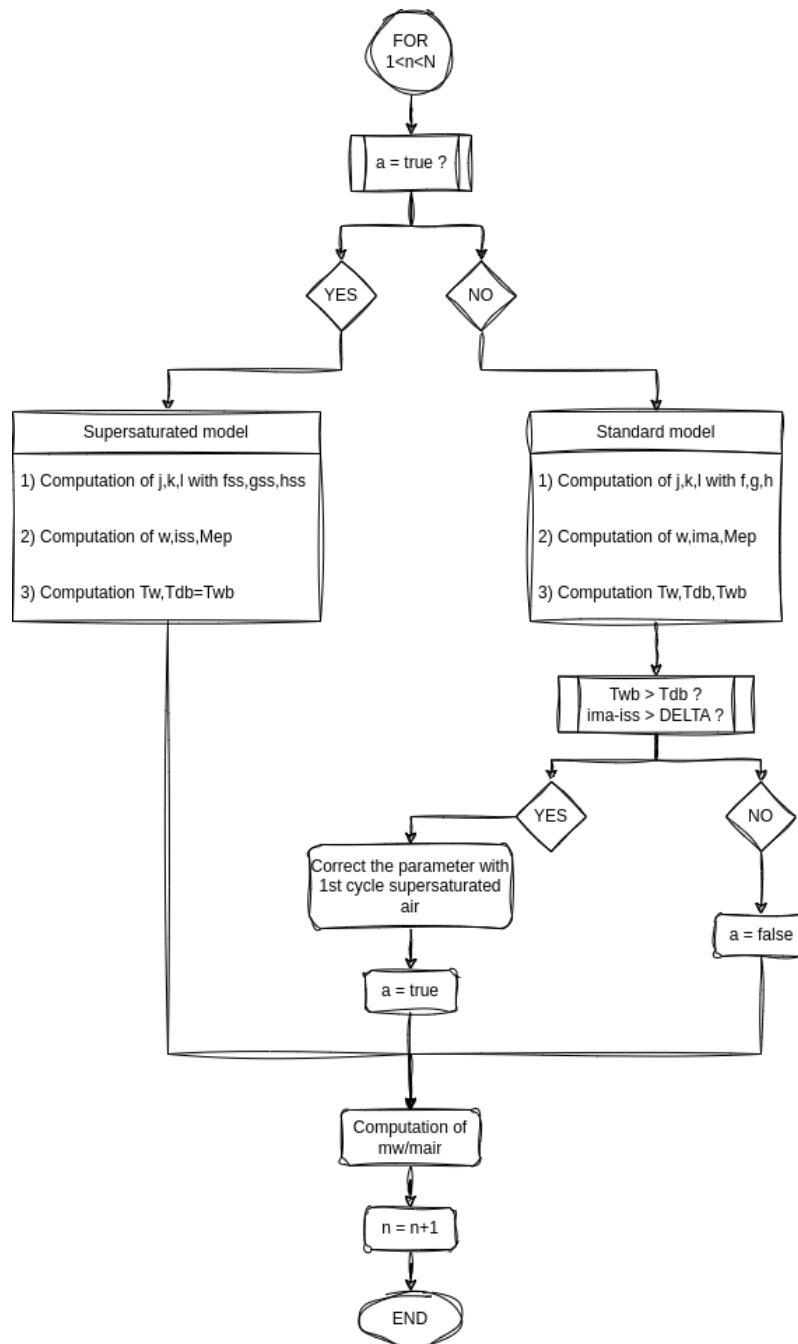


Fig. 4.2: Logical algorithm of MATLAB script

4.3.4 f, g, h and f_{ss}, g_{ss}, h_{ss}

These functions were created to facilitate the script's execution. They reference the six differential equations described in Chapter 3 but take humidity, enthalpy, and water temperature values dynamically as inputs as the runge-kutta method asks. Inside these functions, equations are provided to calculate:

- z
- Saturation pressure of water
- Saturation humidity ratio
- Water vapor enthalpy
- Moist air saturation enthalpy
- $mw/mair$
- Le_f
- The respective differential equation

For the f_{ss} , g_{ss} and h_{ss} functions, additional supersaturation-related parameters are included:

- w_{sa}
- iss

Parameters for normal cycle functions are calculated with a reference temperature derived from water temperature, as it is not yet saturated. It is assumed that the air's saturation temperature equals the current water temperature. For supersaturated cycles, parameters are calculated using the air temperature, which is already saturated.

4.3.5 Water Flow Rate

At the conclusion of the cycle, the water flow rate is finally calculated to determine the ratio between water flow and dry airflow, which is essential for solving the differential equations:

$$m_{w(n+1)} = m_{w(n)} + m_{air(dry)} \cdot (w_{(n+1)} - w_n) \quad (4.36)$$

$$\frac{m_w}{m_a} = \frac{m_w}{m_{air(dry)}} \cdot \left(1 - \frac{m_{air(dry)}}{m_w} \cdot (w_{out} - w_{in}) \right) \quad (4.37)$$

Here, w_{out} refers to the humidity value at the outlet (at state $n + 1$ within the **for** loop), which will change for matrices j , k and l .

For models in a non-oversaturated state, the calculation of reference temperatures (T) has been carried out using the water temperature. This choice stems from considering the maximum temperature at which the air could become 100% saturated with water vapor. Subsequently, these reference temperatures have been recalculated using the "checkima" function to ensure their validity. Once the air becomes oversaturated, the reference temperature shifts to the air temperature itself.

References in this chapter have been tailored to the script rather than the previously discussed Poppe theory. You will find all terms with adjusted references in the glossary.

Chapter 5

Conclusion

The developed program aims to facilitate the design process of an evaporative cooling tower by providing a reasonably accurate representation of water temperature trends, water usage and dissipated heat during the evaporation process. Operating as a one-dimensional model, it takes static inputs rather than relying on databases or other dynamic sources. This script can subsequently serve as the foundation for implementing a Simulink model, utilizing its functions to create a more comprehensive analytical and control model. This extended model would operate with dynamic flows rather than static values.

Adopting a zone-centered modeling approach offers additional advantages. Notably, it permits a detailed examination of edge cases. For instance, under scenarios where the ambient air is exceptionally dry, latent cooling could constitute more than 100% of the total cooling effect. This unusual situation arises when the incoming air temperature exceeds that of the outgoing water, leading to a counterintuitive heat flow from the air to the water. Furthermore, the zone-based model developed here allows for estimating the point within the fill media where air first becomes saturated (in our case, at level 3). This information, in turn, aids prospective designers in determining various geometric dimensions of the cooling tower.

The fill media height plays a pivotal role in cooling tower design. Inadequate fill height could result in insufficient cooling, while excessive height might lead to increased visible plume length, entailing additional capital and operational costs. Another significant advantage of a zone-focused model is the robust estimation of evaporated water volume from each zone within the cooling tower. Understanding

this metric is crucial for determining the replenishment water quantity necessary to maintain an adequate cooling level within the industrial plant.

5.1 Model Envelope and Data Analysis

Once I completed the development of the main algorithm, I decided to analyze the hypothetical operating conditions of the evaporative tower every month. I assumed a constant and appropriate water flow originating from the power plant's condenser to ensure the minimal discharge of water into the Danube basin, thus protecting the water resources.

To do this, I utilized the open-source archive, Open-Meteo, and downloaded a database of climatic conditions (temperature, humidity, and pressure) on an hourly basis for the past 10 years from the location of Požarevac, the nearest city with available climatic data to the power plant.

Upon obtaining this dataset, I created a Python program to calculate the monthly average of temperature, humidity, and pressure data over 10 years. I then exported these obtained averages to the MATLAB script mentioned earlier, which was adapted to be executed for various operating conditions (please refer to the Appendix A for the full code). Fig. 5.1 and Tab. 5.1 present this data, see Appendix B for the graphs:

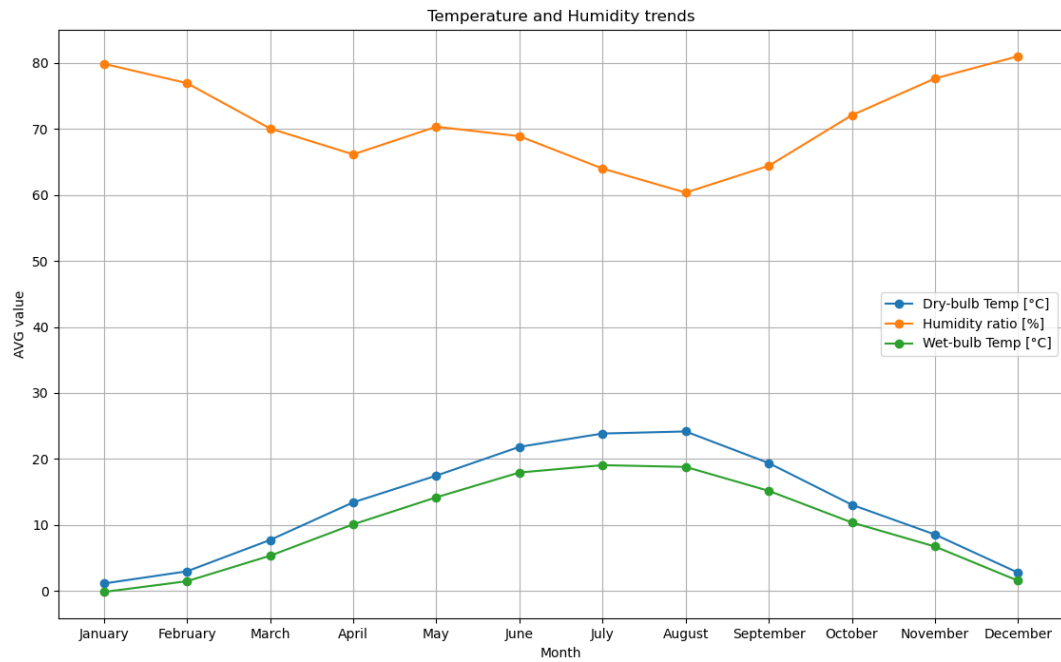


Fig. 5.1: Weather data results

Month	Dry-bulb Temp [°C]	Wet-bulb Temp [°C]	Humidity ratio [%]	Pressure [hPa]
January	1.10	-0.18	79.89	1008.02
February	2.95	1.45	76.96	1007.50
March	7.70	5.31	70.08	1006.71
April	13.40	10.07	66.16	1004.71
May	17.45	14.17	70.35	1003.44
June	21.82	17.93	68.91	1004.21
July	23.84	19.04	64.01	1003.83
August	24.15	18.78	60.36	1005.53
September	19.36	15.15	64.42	1006.75
October	13.04	10.35	72.10	1009.39
November	8.53	6.71	77.66	1008.40
December	2.74	1.52	81.04	1011.68
AVG	13.01	10.02	71.00	1006.68

Table 5.1: Weather data results

Here the result of the simulations:

Tdb	Twb	Tw	ima	w	Mep
1.00	0.00	12.75	9502.58	0.0034	1.55
11.82	13.74	20.20	36581.74	0.0098	3.47
18.83	18.83	27.65	53221.34	0.0098	4.65
24.33	24.33	35.10	72578.45	0.0098	5.41
28.83	28.83	42.55	91916.69	0.0098	5.86
32.62	32.62	50.00	111240.69	0.0098	6.12

Table 5.2: Gennuary data

Tdb	Twb	Tw	ima	w	Mep
3.00	1.00	13.75	11240.39	0.0033	1.55
13.21	14.55	21.00	39367.88	0.0103	3.43
19.98	19.98	28.25	56980.03	0.0103	4.61
25.32	25.32	35.50	76570.68	0.0103	5.36
29.70	29.70	42.75	96142.94	0.0103	5.81
33.40	33.40	50.00	115701.50	0.0103	6.08

Table 5.3: February data

Tdb	Twb	Tw	ima	w	Mep
8.00	5.00	17.00	18680.61	0.0042	1.55
16.99	17.63	23.60	49054.73	0.0126	3.28
23.09	23.09	30.20	68127.63	0.0126	4.39
27.97	27.97	36.80	88235.44	0.0126	5.10
32.01	32.01	43.40	108326.50	0.0126	5.53
35.46	35.46	50.00	128405.76	0.0126	5.79

Table 5.4: March data

Tdb	Twb	Tw	ima	w	Mep
13.00	10.00	20.75	29395.94	0.0065	1.55
20.96	21.32	26.60	61652.18	0.0160	3.10
26.35	26.35	32.45	81502.82	0.0160	4.09
30.73	30.73	38.30	101993.65	0.0160	4.75
34.41	34.41	44.15	122469.29	0.0160	5.15
37.58	37.58	50.00	142935.70	0.0160	5.40

Table 5.5: April data

Tdb	Twb	Tw	ima	w	Mep
17.00	14.00	23.75	39418.56	0.0088	1.55
24.08	24.24	29.00	73033.66	0.0192	2.95
28.93	28.93	34.25	93519.54	0.0192	3.86
32.92	32.92	39.50	114196.68	0.0192	4.47
36.31	36.31	44.75	134858.91	0.0192	4.86
103.31	103.31	50.00	155514.75	0.0192	5.10

Table 5.6: May data

Tdb	Twb	Tw	ima	w	Mep
22.00	18.00	27.00	51067.34	0.0114	1.55
27.65	27.35	31.60	86724.95	0.0231	2.78
33.64	34.03	36.20	122610.49	0.0346	4.64
37.05	37.05	40.80	142173.51	0.0346	5.55
39.94	39.94	45.40	163283.83	0.0346	6.04
42.50	42.50	50.00	184388.17	0.0346	6.33

Table 5.7: June data

Tdb	Twb	Tw	ima	w	Mep
24.00	19.00	28.00	54275.08	0.0118	1.55
28.88	28.29	32.40	91123.21	0.0243	2.72
34.57	34.80	36.80	127736.20	0.0362	4.56
37.88	37.88	41.20	148195.32	0.0362	5.52
40.69	40.69	45.60	169476.96	0.0362	6.03
43.18	43.18	50.00	190754.89	0.0362	6.32

Table 5.8: July data

Tdb	Twb	Tw	ima	w	Mep
24.00	19.00	28.00	54275.08	0.0118	1.55
28.88	28.29	32.40	91123.21	0.0243	2.72
34.57	34.80	36.80	127736.20	0.0362	4.56
37.88	37.88	41.20	148195.32	0.0362	5.52
40.69	40.69	45.60	169476.96	0.0362	6.03
43.18	43.18	50.00	190754.89	0.0362	6.32

Table 5.9: August data

Tdb	Twb	Tw	ima	w	Mep
19.00	15.00	24.75	42162.07	0.0091	1.55
25.34	25.15	29.80	76973.31	0.0202	2.89
31.83	32.34	34.85	112254.84	0.0313	4.83
35.50	35.50	39.90	131419.25	0.0313	5.74
38.59	38.59	44.95	152532.90	0.0313	6.24
41.30	41.30	50.00	173638.82	0.0313	6.52

Table 5.10: September data

Tdb	Twb	Tw	ima	w	Mep
13.00	10.00	20.75	29395.94	0.0065	1.55
20.96	21.32	26.60	61652.18	0.0160	3.10
26.35	26.35	32.45	81502.82	0.0160	4.09
30.73	30.73	38.30	101993.65	0.0160	4.75
34.41	34.41	44.15	122469.29	0.0160	5.15
37.58	37.58	50.00	142935.70	0.0160	5.40

Table 5.11: October data

Tdb	Twb	Tw	ima	w	Mep
9.00	7.00	18.25	22752.77	0.0054	1.55
18.06	19.01	24.60	53120.49	0.0138	3.22
23.94	23.94	30.95	71464.60	0.0138	4.26
28.66	28.66	37.30	91581.55	0.0138	4.93
32.60	32.60	43.65	111682.37	0.0138	5.35
35.96	35.96	50.00	131771.88	0.0138	5.60

Table 5.12: November data

Tdb	Twb	Tw	ima	w	Mep
3.00	2.00	14.25	13011.12	0.0040	1.55
13.47	15.22	21.40	40812.33	0.0108	3.41
20.17	20.17	28.55	57639.08	0.0108	4.54
25.46	25.46	35.70	77181.71	0.0108	5.27
29.80	29.80	42.85	96706.26	0.0108	5.70
33.47	33.47	50.00	116217.28	0.0108	5.96

Table 5.13: December data

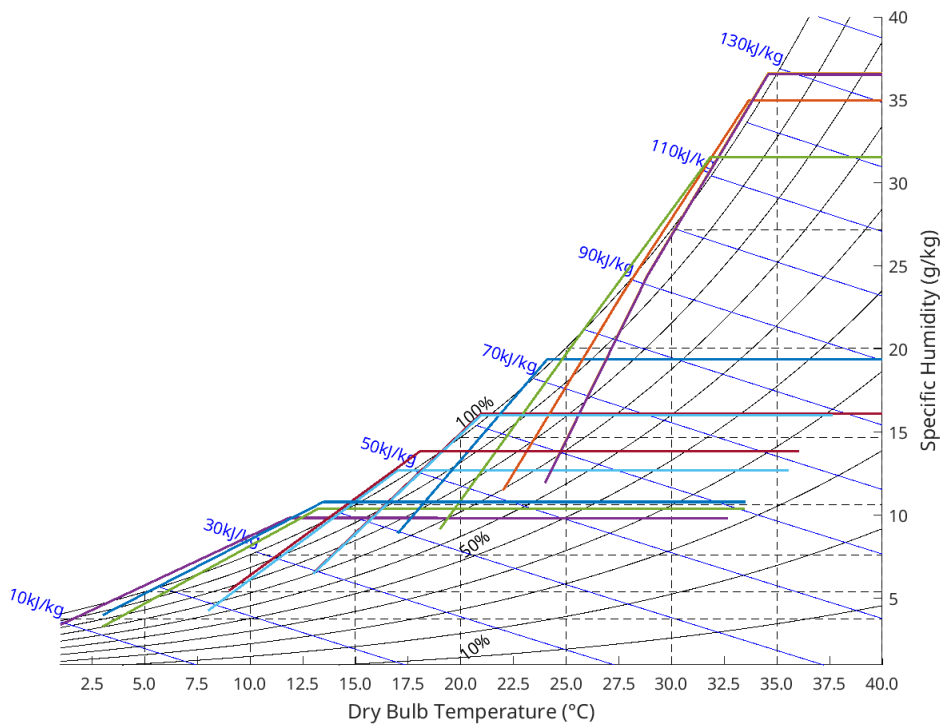


Fig. 5.2: Simulation in the Psychrometric chart

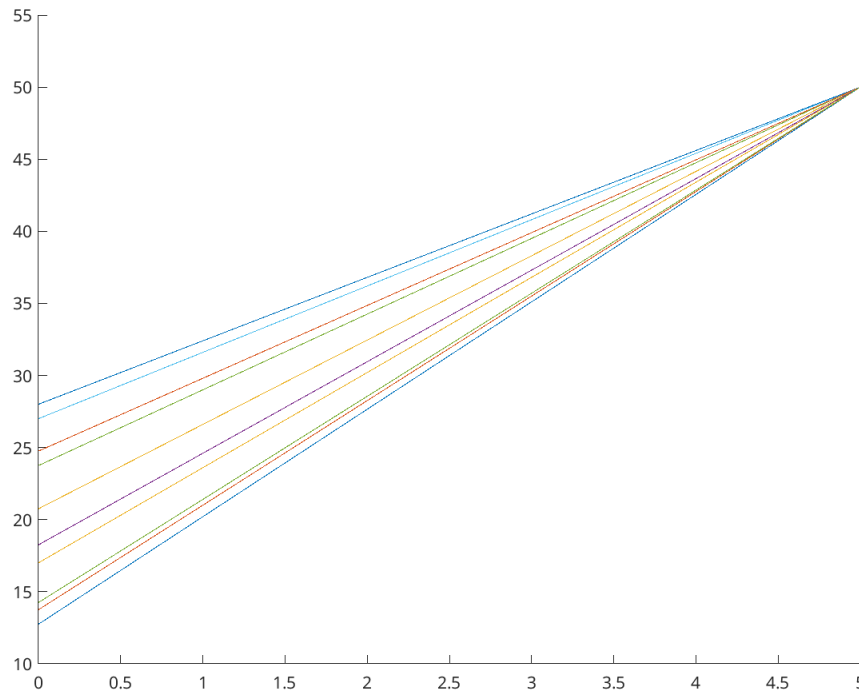


Fig. 5.3: Water temperature for every month

5.1.1 Result Comments

The analysis was conducted to gain insight into the trend of water temperatures at the outlet of the evaporative tower, aiming to minimize thermal pollution in the Danube River. The tables and graphs presented reveal a notable shift in the water temperature at the tower's discharge, ranging from approximately 12°C in January to about 28°C in July and August. It's essential to remember that the water discharge temperature depends on the incoming air and water temperatures, which, for our simulation, were held constant at 50°C.

Observing Graph 5.2, we notice that when the values of air temperature and humidity exceed the saturation curve on the psychrometric chart, the transformation continues with constant specific humidity. This leads to a cessation of water evaporation, which was a deliberate design choice to manage issues related to air oversaturation, in the absence of dynamic control systems like partialization of air and water flow. Once saturation is reached, I also decided to maintain the

wet bulb temperature equal to the dry bulb temperature of the air since neither the Poppe model nor the psychrometric chart can effectively handle conditions beyond saturation.

In May, there was an anomaly in the script, resulting in an extremely off-scale final value. Consequently, this particular data point will be excluded from consideration.

It's noteworthy that nearly all simulations reach the saturation point around the 2/3 iteration. This is likely due to the substantial water flow entering the evaporative tower. However, this outcome was expected and, in a sense, it tests the functionality of the evaporative tower under extreme conditions.

Furthermore, it's evident that during the winter months, the water outlet temperatures are extremely low. Referring to Fig 1.4, we can observe that for the first three months, the average Danube temperatures range between 2°C and 6°C. Considering the study of thermal pollution previously made [11], which without a cooling tower in the hottest month of the year, with a discharge flow rate of 29.5 m s⁻³ which is 29300 kg s⁻¹ so more than double our water flow rate; the temperature average temperature of the Danube change from 18°C to 27°C with exhaust temperature of water around about 60°C to 70°C. So it's clear that by introducing a cooling tower we can operate well below the initial 3°C limit set at the beginning of this study. It can be deduced that by operating with a dynamic model and control systems, such as PID controllers for temperature and flow rates, and by accessing a more comprehensive database, we could optimize the temperature conditions to enhance the tower's production efficiency and reduce operational costs.

5.2 Conclusion

In conclusion, I would like to share some personal reflections on the work completed:

- This project was initiated in collaboration with the University of Nis to address the issue of thermal pollution from Serbian power plants in the Danube and Sava rivers. I consider this project to be in an "alpha" state, serving as a tool to gain an understanding of how an evaporative tower operates while allowing for a broad range of output data variations. However, due to limited obtainable data, the program provides a general overview of the problem.
- I am eager to implement this "static" model in Simulink or other modeling programs, delving into the realm of electronic controls for the partialization of air and water flows based on specific needs. Additionally, I will consider all the variables that were omitted, such as the nonlinear behavior of temperatures when air and water come into contact with the fins after the spray zone, as well as other systems described in Chapter 2.
- I will publish all the code and research findings on GitHub, in a public repository, so that my work can serve as a starting point or source of inspiration for others: <https://github.com/Akamarai/Cooling-tower-Master-thesis>.

References

1. Environmental danube report. Electric Power Industry of Serbia. [Online]. Available: <https://www.eps.rs/eng/Documents/PE%20EPE%20Report%20on%20Environmental%20State%202020.pdf>
2. Pictures. [Online]. Available: <https://www.planplus.rs/en/kostolac-b-thermal-power-plant/36656>
3. Icpdr danube report. International Commission for the Protection of the Danube River. [Online]. Available: <https://www.icpdr.org/main/sites/default/files/Danube-River-Basin-Management-Plan-2021.pdf>
4. Open-meteo archive. [Online]. Available: <https://open-meteo.com/>
5. Pictures. [Online]. Available: <https://www.eeeguide.com/what-is-a-cooling-tower/>
6. Open-meteo archive. [Online]. Available: <https://it.freepik.com/search?format=search&query=cooling%20tower>
7. Pictures. [Online]. Available: <https://blog.parker.com/site/usa/en-US/details-home-page/hvacr-tech-tip-a-psychrometrics-reminder-for-the-hvacr-technician-us>
8. Pictures. [Online]. Available: <https://hvac-eng.com/psychrometric-processes/>
9. D. Kroger, *Air-cooled Heat Exchangers And Cooling Towers: Thermal-flower Performance Evaluation And Design*, Vol. 2. Pennwell Corp, 2004. [Online]. Available: <libgen.li/file.php?md5=289968151bdff0d0d8fbfe94b3857f51>
10. (2023, February) Energy sector information rs. Ministry of Energy, Mining and Infrastructure of the Republic of Serbia. [Online]. Available: <https://www.mem.sr.gov.rs/en/energy-sector/>
11. M. Lakovic, M. Banjac, J. Bogdanovic-Jovanovic, M. Jovceviski, and Z. Milovanovic, "Risk of thermal pollution of the danube passing through serbia due to thermal power plants," *Thermal Science*, vol. 22, pp. 1323–1336, 01 2018.
12. Serbian power plant information. Elektroenergetika. [Online]. Available: <https://www.elektroenergetika.info/te-sr.htm>
13. Power plant kostolac. Balkan Green Energy News. [Online]. Available: <https://balkangreenenergynews.com/eps-considering-shutdown-of-coal-power-plant-kostolac-a/>
14. Republic hydrometeorological service of serbia. [Online]. Available: https://www.hidmet.gov.rs/index_eng.php
15. I. John C. Hensley Marley SPX Cooling Technologies, *Cooling Tower Fundamentals*, 2nd ed., 1985. [Online]. Available: <libgen.li/file.php?md5=5ed547277bd4138bc6d175a7451a08b4>

16. Pictures. [Online]. Available: <https://www.evapco.eu/dry-cooling-101>
17. D. G. Kroger, *Air-Cooled Heat Exchangers and Cooling Towers: Thermal-Flow Performance Evaluation and Design, Vol. 1.* Pennwell Books, 2004. [Online]. Available: libgen.li/file.php?md5=a775eb3cc64995008bc10b8c1bc820ae
18. Cooling tower lesson - students notes. University of California - Santa Barbara. [Online]. Available: <https://sites.chemengr.ucsb.edu/~ceweb/courses/che120c/index.html?syllabus.html&1>
19. A. Ghajar and Y. Cengel, *Heat and Mass Transfer - Fundamentals and Applications, 6th Edition, McGraw-Hill Education, New York, NY, 2020.*, 04 2021.
20. B. E. Rapp, "Chapter 9 - fluids," in *Microfluidics: Modelling, Mechanics and Mathematics*, ser. Micro and Nano Technologies, B. E. Rapp, Ed. Oxford: Elsevier, 2017, pp. 243–263. [Online]. Available: <https://www.sciencedirect.com/science/article/pii/B9781455731411500095>
21. M. Llano-Restrepo and R. Monsalve-Reyes, "Modeling and simulation of counterflow wet-cooling towers and the accurate calculation and correlation of mass transfer coefficients for thermal performance prediction," *International Journal of Refrigeration*, vol. 74, pp. 47–72, 2017. [Online]. Available: <https://www.sciencedirect.com/science/article/pii/S0140700716303474>
22. R. Abdo, Y. Rodrigues, V. Silva, L. Cabezas-Gómez, and S. Hanriot, "The difference between merkel and poppe models and its influence on the prediction of wet-cooling towers," 11 2013.
23. J. C. Kloppers and D. G. Kröger, "Cooling Tower Performance Evaluation: Merkel, Poppe, and e-NTU Methods of Analysis," *Journal of Engineering for Gas Turbines and Power*, vol. 127, no. 1, pp. 1–7, 02 2005. [Online]. Available: <https://doi.org/10.1115/1.1787504>
24. J. Kloppers and D. Kröger, "A critical investigation into the heat and mass transfer analysis of counterflow wet-cooling towers," *International Journal of Heat and Mass Transfer*, vol. 48, no. 3, pp. 765–777, 2005. [Online]. Available: <https://www.sciencedirect.com/science/article/pii/S0017931004004041>
25. E. Hairer, C. Lubich, and M. Roche, *The numerical solution of differential-algebraic systems by Runge-Kutta methods.* Springer, 2006, vol. 1409.
26. L. Shiqi, L. Qiankun, and S. Jinchun, "A comprehensive synthesis approach of re-circulating cooling water system based on stage-wise structure and poppe method," *Alexandria Engineering Journal*, vol. 61, no. 10, pp. 7733–7748, 2022. [Online]. Available: <https://www.sciencedirect.com/science/article/pii/S1110016822000242>
27. P. Navarro, J. Ruiz, M. Hernández, A. Kaiser, and M. Lucas, "Critical evaluation of the thermal performance analysis of a new cooling tower prototype,"

- Applied Thermal Engineering*, vol. 213, p. 118719, 2022. [Online]. Available: <https://www.sciencedirect.com/science/article/pii/S1359431122006639>
28. Systematic control approach to improve the energy efficiency of an industrial cooling tower. MathWorks. [Online]. Available: <https://www.mathworks.com/content/dam/mathworks/mathworks-dot-com/images/events/matlabexpo/in/2018/a-systematic-control-approach-to-improve-the-energy-efficiency-of-an-industrial-cooling-tower.pdf>

Appendix A

Appendix A - Matlab script collection

Main matlab script

```
function [Tdb, Twb, Tw, ima, w, Mep, water, d] = modellosupersaturo(Tairindry, Tairin,Pair, N, d)
%% Inizialization of vectors
water=d.mw;
Tdb = zeros(1, N + 2);
Twb = zeros(1, N + 1);
Tw = zeros(1, N + 1);
w = zeros(1, N + 2);
ima = zeros(1, N + 2);
Mep = zeros(1, N + 1);
d.P = Pair;
%% Computation of Air properties temperature
% Tdb = Dry bulb K
% Twb = Wet bulb K
% w = Humidity ratio kg/kg
% ima = Enthalpy of gas phase J/kg dry air

Tdb(1) = Tairindry +273.15;
Twb(1) = Tairin +273.15;

% Computation of pressure of water vapor evaluated at Twb
z(1) = 10.79586 * (1 - 273.15 / Twb(1)) + 5.02808 * log10(273.15 / Twb(1)) ...
+1.50474e-4 * (1 - (10 ^ (-8.29692 * (Twb(1) / 273.15)) - 1)) ...
+4.2873e-4 * (10 ^ (4.76955 * (1 - 273.15 / Twb(1))) - 1) ...
+ 2.786118312;

pv_wb = 10 ^ z(1);

%%Merkel Number
Mep(1) = 1.55;

% Alternative to calculate pv
% pv_wb_alt = IAPWS_IF97('psat_T', Tdb(1)) * 10^-6;

% Computation of humidity ratio for saturated air
w(1) = ((2501.6 - 2.3263 * (Twb(1) - 273.15)) / (2501.6 + 1.8577 * (Twb(1) - 273.15) - 4.184 * (Twb(1) - 273.15))) * ...
```

```

((0.62509 * pv_wb) / (d.P - 1.005 * pv_wb)) - ...
((1.00416 * ((Tdb(1) - 273.15) - (Twb(1) - 273.15))) / (2501.6 + 1.8577 * (Tdb(1) - 273.15) - 4.184 * (Twb(1) - 273.15)));

d.wo = w(1); % Value to put in database for computation of mass flow rate in f,g,h

%% Computation of enthalpy and specific heat capacity

T = (Tdb(1) + 273.15) / 2; % Temperature used as reference for the computation

% Specific heat of dry air [J/kgK]
cpa = 1.045356e3 -3.161783e-1 * T +7.083814e-4 * T ^ 2 -2.705209e-7 * T ^ 3;

% Specific heat of saturated water vapor [J/kgK]
cpv = 1.3605e3 + 2.31334 * T -2.46784e-10 * T ^ 5 +5.91332e-13 * T ^ 6;

% Latent heat of water evaluated at 0°C
d.ifgwo = 3.4831814e6 -5.8627703e3 * 273.15 + 12.139568 * 273.15 ^ 2 -1.40290431e-2 * 273.15 ^ 3;

% Enthalpy of air-water vapor mixture [J/kg dry air K]
ima(1) = cpa * (Tdb(1) - 273.15) + w(1) * (d.ifgwo + cpv * (Tdb(1) - 273.15));
%% Initial approximation of variables
Tw(1) = ((d.Twin + 273.15) + 2 * Twb(1) + Tdb(1)) / 4; % Outlet water temperature approximation based on Poppe Models [K]
Tdb(end) = ((d.Twin + 273.15 + Tw(1)) / 2); % Outlet air temperature approximation based on Poppe Models [K]
TEND = (d.Twin + 273.15 + Tw(1)) / 2; % Temperature used as reference for the end value of computation

% Specific heat of water [J/kgK] evaluated a (Twin+Twout)/2
cpw(1) = 8.15599e3 - 2.80627 * 10 * TEND +5.11283e-2 * TEND ^ 2 -2.17582e-13 * TEND ^ 6;

z(2) = 10.79586 * (1 - 273.15 / Tdb(end)) + 5.02808 * log10(273.15 / Tdb(end)) ...
+1.50474e-4 * (10 ^ (-8.29692 * (Tdb(end) / 273.15) - 1)) ...
+4.2873e-4 * (10 ^ (4.76955 * (1 - 273.15 / Tdb(end))) - 1) ...
+ 2.786118312;

pv_wb(2) = 10 ^ z(2);
w(end) = (0.6250 * pv_wb(2)) / (d.P - 1.005 * pv_wb(2));
d.wend = w(end);
T2 = (Tdb(end) + 273.15) / 2;

cpa(2) = 1.045356e3 -3.161783e-1 * T2 +7.083814e-4 * T2 ^ 2 -2.705209e-7 * T2 ^ 3;
cpv(2) = 1.3605e3 + 2.31334 * T2 -2.46784e-10 * T2 ^ 5 +5.91332e-13 * T2 ^ 6;
ima(end) = cpa(2) * (Tdb(end) - 273.15) + w(end) * (d.ifgwo + cpv(2) * (Tdb(end) - 273.15));
% Vapor mass flow rate [kg/s]
mair = (d.mw * cpw(1) * ((d.Twin + 273.15) - Tw(1))) / (ima(end) - ima(1));

% Dry air mass flow rate [kg dry/s]
d.madry = (2 * mair) / (2 + d.wo + d.wend);

%% Application of Runge-Kutta method to determine the working status of the cooling tower

DTW = ((d.Twin + 273.15) - Tw(1)) / N;
DELTA = 0.005;
d.a = false;

```

```

% Runge-Kutta 4th order to resolve the ODEs system of Cooling-Tower
for n = 1:N
if d.a==false
%normal cycle
j(n + 1, 1) = DTW * f(w(n), ima(n), Tw(n), d);
k(n + 1, 1) = DTW * g(w(n), ima(n), Tw(n), d);
l(n + 1, 1) = DTW * h(w(n), ima(n), Tw(n), d);

j(n + 1, 2) = DTW * f(w(n) + (j(n + 1, 1)) / 2, ima(n) + (k(n + 1, 1)) / 2, Tw(n) + DTW / 2, d);
k(n + 1, 2) = DTW * g(w(n) + (j(n + 1, 1)) / 2, ima(n) + (k(n + 1, 1)) / 2, Tw(n) + DTW / 2, d);
l(n + 1, 2) = DTW * h(w(n) + (j(n + 1, 1)) / 2, ima(n) + (k(n + 1, 1)) / 2, Tw(n) + DTW / 2, d);

j(n + 1, 3) = DTW * f(w(n) + (j(n + 1, 2)) / 2, ima(n) + (k(n + 1, 2)) / 2, Tw(n) + DTW / 2, d);
k(n + 1, 3) = DTW * g(w(n) + (j(n + 1, 2)) / 2, ima(n) + (k(n + 1, 2)) / 2, Tw(n) + DTW / 2, d);
l(n + 1, 3) = DTW * h(w(n) + (j(n + 1, 2)) / 2, ima(n) + (k(n + 1, 2)) / 2, Tw(n) + DTW / 2, d);

j(n + 1, 4) = DTW * f(w(n) + j(n + 1, 3), ima(n) + k(n + 1, 3), Tw(n) + DTW, d);
k(n + 1, 4) = DTW * g(w(n) + j(n + 1, 3), ima(n) + k(n + 1, 3), Tw(n) + DTW, d);
l(n + 1, 4) = DTW * h(w(n) + j(n + 1, 3), ima(n) + k(n + 1, 3), Tw(n) + DTW, d);

w(n + 1) = w(n) + (j(n + 1, 1) + 2 * j(n + 1, 2) + 2 * j(n + 1, 3) + j(n + 1, 4)) / 6;
ima(n + 1) = ima(n) + (k(n + 1, 1) + 2 * k(n + 1, 2) + 2 * k(n + 1, 3) + k(n + 1, 4)) / 6;
Mep(n + 1) = Mep(n) + (l(n + 1, 1) + 2 * l(n + 1, 2) + 2 * l(n + 1, 3) + l(n + 1, 4)) / 6;

% Calculate air temperature [K]
Tw(n + 1) = Tw(n) + DTW;
Tdb(n+1) = dry(w(n+1), Tw(n+1), ima(n+1), d);
[~, ~, ~, ~, ~, wet] = Psychrometricsnew('Tdb', (Tdb(n+1)-273.15), 'w', w(n+1));
Twb(n+1) = wet + 273.15;
[~, ~, ~, ~, ~, iss(n + 1)] = checkss(w(n + 1), Tdb(n + 1), d);
imact = checkima(w(n + 1), Tdb(n + 1), d);
ERRima = abs((imact - iss(n + 1)) / (imact + iss(n + 1)));
end

if n > 1 && Twb(n) > Tdb(n) && d.a == false && ERRima > DELTA
[~, ~, ~, ~, ~, iss(n)] = checkss(w(n), Tdb(n), d);
X = ['Aria sovrassatura, ciclo n= ', num2str(n)];
disp(X);
d.a = true;
%Supersaturated equations
j(n + 1, 1) = DTW * fss(w(n), iss(n), Tw(n), Tdb(n), d);
k(n + 1, 1) = DTW * gss(w(n), iss(n), Tw(n), Tdb(n), d);
l(n + 1, 1) = DTW * hss(w(n), iss(n), Tw(n), Tdb(n), d);

j(n + 1, 2) = DTW * fss(w(n) + (j(n + 1, 1)) / 2, iss(n) + (k(n + 1, 1)) / 2, Tw(n) + DTW / 2, Tdb(n), d);
k(n + 1, 2) = DTW * gss(w(n) + (j(n + 1, 1)) / 2, iss(n) + (k(n + 1, 1)) / 2, Tw(n) + DTW / 2, Tdb(n), d);
l(n + 1, 2) = DTW * hss(w(n) + (j(n + 1, 1)) / 2, iss(n) + (k(n + 1, 1)) / 2, Tw(n) + DTW / 2, Tdb(n), d);

j(n + 1, 3) = DTW * fss(w(n) + (j(n + 1, 2)) / 2, iss(n) + (k(n + 1, 2)) / 2, Tw(n) + DTW / 2, Tdb(n), d);
k(n + 1, 3) = DTW * gss(w(n) + (j(n + 1, 2)) / 2, iss(n) + (k(n + 1, 2)) / 2, Tw(n) + DTW / 2, Tdb(n), d);
l(n + 1, 3) = DTW * hss(w(n) + (j(n + 1, 2)) / 2, iss(n) + (k(n + 1, 2)) / 2, Tw(n) + DTW / 2, Tdb(n), d);

j(n + 1, 4) = DTW * fss(w(n) + j(n + 1, 3), iss(n) + k(n + 1, 3), Tw(n) + DTW, Tdb(n), d);

```

```

k(n + 1, 4) = DTW * gss(w(n) + j(n + 1, 3), iss(n) + k(n + 1, 3), Tw(n) + DTW, Tdb(n), d);
l(n + 1, 4) = DTW * hss(w(n) + j(n + 1, 3), iss(n) + k(n + 1, 3), Tw(n) + DTW, Tdb(n), d);

w(n + 1) = w(n) + (j(n + 1, 1) + 2 * j(n + 1, 2) + 2 * j(n + 1, 3) + j(n + 1, 4)) / 6;
ima(n + 1) = iss(n) + (k(n + 1, 1) + 2 * k(n + 1, 2) + 2 * k(n + 1, 3) + k(n + 1, 4)) / 6;
Mep(n + 1) = Mep(n) + (l(n + 1, 1) + 2 * l(n + 1, 2) + 2 * l(n + 1, 3) + l(n + 1, 4)) / 6;

% Calculate air temperature [K]
Tw(n + 1) = Tw(n) + DTW;
% Tdb(n+1) = dry(w(n+1), Tw(n+1), ima(n+1), d);
[~, ~, ~, ~, ~, wet] = Psychrometricsnew('h', ima(n+1), 'w', w(n+1));
Twb(n+1) = wet + 273.15;
Tdb(n+1) = Twb(n+1);

else if d.a==true;
j(n + 1, 1) = DTW * fss(w(n), ima(n), Tw(n), Tdb(n), d);
k(n + 1, 1) = DTW * gss(w(n), ima(n), Tw(n), Tdb(n), d);
l(n + 1, 1) = DTW * hss(w(n), ima(n), Tw(n), Tdb(n), d);

j(n + 1, 2) = DTW * fss(w(n) + (j(n + 1, 1)) / 2, ima(n) + (k(n + 1, 1)) / 2, Tw(n) + DTW / 2, Tdb(n), d);
k(n + 1, 2) = DTW * gss(w(n) + (j(n + 1, 1)) / 2, ima(n) + (k(n + 1, 1)) / 2, Tw(n) + DTW / 2, Tdb(n), d);
l(n + 1, 2) = DTW * hss(w(n) + (j(n + 1, 1)) / 2, ima(n) + (k(n + 1, 1)) / 2, Tw(n) + DTW / 2, Tdb(n), d);

j(n + 1, 3) = DTW * fss(w(n) + (j(n + 1, 2)) / 2, ima(n) + (k(n + 1, 2)) / 2, Tw(n) + DTW / 2, Tdb(n), d);
k(n + 1, 3) = DTW * gss(w(n) + (j(n + 1, 2)) / 2, ima(n) + (k(n + 1, 2)) / 2, Tw(n) + DTW / 2, Tdb(n), d);
l(n + 1, 3) = DTW * hss(w(n) + (j(n + 1, 2)) / 2, ima(n) + (k(n + 1, 2)) / 2, Tw(n) + DTW / 2, Tdb(n), d);

j(n + 1, 4) = DTW * fss(w(n) + j(n + 1, 3), ima(n) + k(n + 1, 3), Tw(n) + DTW, Tdb(n), d);
k(n + 1, 4) = DTW * gss(w(n) + j(n + 1, 3), ima(n) + k(n + 1, 3), Tw(n) + DTW, Tdb(n), d);
l(n + 1, 4) = DTW * hss(w(n) + j(n + 1, 3), ima(n) + k(n + 1, 3), Tw(n) + DTW, Tdb(n), d);

w(n + 1) = w(n) + (j(n + 1, 1) + 2 * j(n + 1, 2) + 2 * j(n + 1, 3) + j(n + 1, 4)) / 6;
ima(n + 1) = ima(n) + (k(n + 1, 1) + 2 * k(n + 1, 2) + 2 * k(n + 1, 3) + k(n + 1, 4)) / 6;
Mep(n + 1) = Mep(n) + (l(n + 1, 1) + 2 * l(n + 1, 2) + 2 * l(n + 1, 3) + l(n + 1, 4)) / 6;

% Calculate air temperature [K]
Tw(n + 1) = Tw(n) + DTW;
[~, ~, ~, ~, ~, wet] = Psychrometricsnew('h', ima(n+1), 'w', w(n+1));
Twb(n+1) = wet + 273.15;
Tdb(n+1) = Twb(n+1);
end
end
%Water/Air ratio flow rate
water(n + 1) = water(n) + d.madry * (w(n + 1) - w(n));

end

end

```

Saturated air script

$f(w, i_{ma}, T_w)$

Riferimento ad Eq.

```
function dwdTw = f(w, ima, Tw, d)

[cpa, cpv, cpw] = heatcap(Tw);

% Computation of pressure of water vapor evaluated at Tw
z = 10.79586 * (1 - 273.15 / Tw) + 5.02808 * log10(273.15 / Tw) ...
+1.50474e-4 * (1 - (10 ^ (-8.29692 * (Tw / 273.15)) - 1)) ...
+4.2873e-4 * (10 ^ (4.76955 * (1 - 273.15 / Tw)) - 1) ...
+ 2.786118312;

psatw = 10 ^ z;

% Calculate the humidity mass ratio at the gas-phase side at water temperature
wsw = (0.6250 * psatw) / (d.P - 1.005 * psatw);

% Enthalpy of water vapor at the bulk water temperature Tw [J/kg]
iv = d.ifgwo + cpv * (Tw - 273.15);

% Enthalpy of air-water vapor mixture [J/kg dry air K]
imasw = cpa * (Tw - 273.15) + iv * wsw;

%Water/Air ratio flow rate
mwma = (d.mw / d.madry) * (1 - (d.madry / d.mw) * (d.wend - w));
% Lewis factor
Lef = 0.865 ^ (0.667) * (((wsw + 0.622) / (w + 0.622)) - 1) / (log((wsw + 0.622) / (w + 0.622)));

dwdTw = (cpw * mwma * (wsw - w)) / (imasw - ima + (Lef - 1) * (imasw - ima - (wsw - w) * iv) - (wsw - w) * cpw * Tw);
end
```

$g(w, i_{ma}, T_w)$

Riferimento ad Eq.

```
function dimadTw = g(w, ima, Tw, d)

[cpa, cpv, cpw] = heatcap(Tw);

% Computation of pressure of water vapor evaluated at Tw
z = 10.79586 * (1 - 273.15 / Tw) + 5.02808 * log10(273.15 / Tw) ...
+1.50474e-4 * (1 - (10 ^ (-8.29692 * (Tw / 273.15)) - 1)) ...
+4.2873e-4 * (10 ^ (4.76955 * (1 - 273.15 / Tw)) - 1) ...
+ 2.786118312;
```

```

psatw = 10 ^ z;

% Calculate the humidity mass ratio at the gas-phase side at water temperature
wsw = (0.6250 * psatw) / (d.P - 1.005 * psatw);

% Enthalpy of water vapor at the bulk water temperature Tw [J/kg]
iv = d.ifgwo + cpv * (Tw - 273.15);

% Enthlpy of air-water vapor mixture [J/kg dry air K]
imasw = cpa * (Tw - 273.15) + iv * wsw;

%Water/Air ratio flow rate
mwma = (d.mw / d.madry) * (1 - (d.madry / d.mw) * (d.wend - w));

% Lewis factor
Lef = 0.865 ^ (0.667) * (((wsw + 0.622) / (w + 0.622)) - 1) / (log((wsw + 0.622) / (w + 0.622)));

dimadTw = mwma * cpw * (1 + ((wsw - w) * cpw * Tw) / (imasw - ima + (Lef - 1) * (imasw - ima - (wsw - w) * iv) - (wsw - w) * cpw * Tw));

end

```

$h(w, i_{ma}, T_w)$

Riferimento ad Eq.

```

function dMepdT_w = h(w, ima, Tw, d)

[cpa, cpv, cpw] = heatcap(Tw);

% Computation of pressure of water vapor evaluated at Tw
z = 10.79586 * (1 - 273.15 / Tw) + 5.02808 * log10(273.15 / Tw) ...
+1.50474e-4 * (1 - (10 ^ (-8.29692 * (Tw / 273.15)) - 1)) ...
+4.2873e-4 * (10 ^ (4.76955 * (1 - 273.15 / Tw)) - 1) ...
+ 2.786118312;

psatw = 10 ^ z;

% Calculate the humidity mass ratio at the gas-phase side at water temperature
wsw = (0.6250 * psatw) / (d.P - 1.005 * psatw);

% Enthalpy of water vapor at the bulk water temperature Tw [J/kg]
iv = d.ifgwo + cpv * (Tw - 273.15);

% Enthlpy of air-water vapor mixture [J/kg dry air K]
imasw = cpa * (Tw - 273.15) + iv * wsw;

% Lewis factor
Lef = 0.865 ^ (0.667) * (((wsw + 0.622) / (w + 0.622)) - 1) / (log((wsw + 0.622) / (w + 0.622)));

```



```
dMepdTw = cpw / (imasw - ima + (Lef - 1) * (imasw - ima - (wsw - w) * iv) - (wsw - w) * cpw * Tw);
end
```

Supersaturated air script

$fss(w, i_{ss}, T_w)$

Riferimento ad Eq.

```
function dwdTw = fss(w, iss, Tw, Ta, d)

if d.a == false
[psatw, wsa, cpa, cpv, cpw, ~] = checkss(w, Ta, d);
else
% Computation of pressure of water vapor evaluated at Tdb
z = 10.79586 * (1 - 273.15 / Tw) + 5.02808 * log10(273.15 / Tw) ...
+1.50474e-4 * (1 - (10 ^ (-8.29692 * (Tw / 273.15)) - 1)) ...
+4.2873e-4 * (10 ^ (4.76955 * (1 - 273.15 / Tw)) - 1) ...
+ 2.786118312;

psatw = 10 ^ z;

% Computation of humidity ratio for saturated air
wsa = ((2501.6 - 2.3263 * (Ta - 273.15)) / (2501.6 + 1.8577 * (Ta - 273.15) - 4.184 * (Ta - 273.15))) * ((0.62509 * psatw) / (d.P - 1.005 * psatw));

[cpa, cpv, cpw] = heatcap(Tw);
end

% Calculate the humidity mass ratio at the gas-phase side at water temperature
wsw = (0.6250 * psatw) / (d.P - 1.005 * psatw);

% Enthalpy of water vapor at the bulk water temperature Tw [J/kg]
iv = d.ifgwo + cpv * (Tw - 273.15);

% Enthlpy of air-water vapor mixture [J/kg dry air K]
imasw = cpa * (Tw - 273.15) + iv * wsw;

%Water/Air ratio flow rate
mwma = (d.mw / d.madry) * (1 - (d.madry / d.mw) * (d.wend - w));

% Lewis factor
Lef = 0.865 ^ (0.667) * (((wsw + 0.622) / (wsa + 0.622)) - 1) / (log((wsw + 0.622) / (wsa + 0.622)));

dwdTw = (cpw * mwma * (wsw - wsa)) / (imasw - iss + (Lef - 1) * ((imasw - iss - (wsw - wsa) * iv) + (w - wsa) * cpw * Tw) - (w - wsw) * cpw * Tw);
end
```

gss(w,i_{ss},T_w)

Riferimento ad Eq.

```

function dimadTw = gss(w, iss, Tw, Ta, d)

if d.a == false
[psatw, wsa, cpa, cpv, cpw, ~] = checkss(w, Ta, d);
else
% Computation of pressure of water vapor evaluated at Tdb
z = 10.79586 * (1 - 273.15 / Tw) + 5.02808 * log10(273.15 / Tw) ...
+1.50474e-4 * (1 - (10 ^ (-8.29692 * (Tw / 273.15)) - 1)) ...
+4.2873e-4 * (10 ^ (4.76955 * (1 - 273.15 / Tw)) - 1) ...
+ 2.786118312;

psatw = 10 ^ z;

% Computation of humidity ratio for saturated air
wsa = ((2501.6 - 2.3263 * (Ta - 273.15)) / (2501.6 + 1.8577 * (Ta - 273.15) - 4.184 * (Ta - 273.15))) * ((0.62509 * psatw) / (d.P - 1.005 * psatw));

[cpa, cpv, cpw] = heatcap(Tw);
end

% Calculate the humidity mass ratio at the gas-phase side at water temperature
wsw = (0.6250 * psatw) / (d.P - 1.005 * psatw);

% Enthalpy of water vapor at the bulk water temperature Tw [J/kg]
iv = d.ifgw0 + cpv * (Tw - 273.15);

% Enthalpy of air-water vapor mixture [J/kg dry air K]
imasw = cpa * (Tw - 273.15) + iv * wsw;

%Water/Air ratio flow rate
mwma = (d.mw / d.madry) * (1 - (d.madry / d.mw) * (d.wend - w));

% Lewis factor
Lef = 0.865 ^ (0.667) * (((wsw + 0.622) / (wsa + 0.622)) - 1) / (log((wsw + 0.622) / (wsa + 0.622)));

dimadTw = mwma * cpw * (1+((wsw-wsa)*cpw*Tw) / (imasw-iss+(Lef-1) * ((imasw-iss-(wsw-wsa)*iv) + (w-wsa)*cpv*Tw) - (wsw-w) * cpw*Tw));
end

```

hss(w,i_{ss},T_w)

Riferimento ad Eq.

```

function dMepdT = hss(w, iss, Tw, Ta, d)

if d.a == false
[psatw, wsa, cpa, cpv, cpw, ~] = checkss(w, Ta, d);
else

```

```

% Computation of pressure of water vapor evaluated at Tdb
z = 10.79586 * (1 - 273.15 / Tw) + 5.02808 * log10(273.15 / Tw) ...
+1.50474e-4 * (1 - (10 ^ (-8.29692 * (Tw / 273.15)) - 1)) ...
+4.2873e-4 * (10 ^ (4.76955 * (1 - 273.15 / Tw)) - 1) ...
+ 2.786118312;

psatw = 10 ^ z;

% Computation of humidity ratio for saturated air
wsa = ((2501.6 - 2.3263 * (Ta - 273.15)) / (2501.6 + 1.8577 * (Ta - 273.15) - 4.184 * (Ta - 273.15))) * ((0.62509 * psatw) / (d.P - 1.005 * psatw));

[cpa, cpv, cpw] = heatcap(Tw);
end

% Calculate the humidity mass ratio at the gas-phase side at water temperature
wsw = (0.6250 * psatw) / (d.P - 1.005 * psatw);

% Enthalpy of water vapor at the bulk water temperature Tw [J/kg]
iv = d.ifgwo + cpv * (Tw - 273.15);

% Enthalpy of air-water vapor mixture [J/kg dry air K]
imasw = cpa * (Tw - 273.15) + iv * wsw;

% Lewis factor
Lef = 0.865 ^ (0.667) * (((wsw + 0.622) / (wsa + 0.622)) - 1) / (log((wsw + 0.622) / (wsa + 0.622)));

dMepdT = cpw / (imasw - iss + (Lef - 1) * ((imasw - iss - (wsw - wsa) * iv) + (w - wsa) * cpv * Tw) - (wsw - wsa) * cpw * Tw);
end

```

Check air saturation levels

```

function [pv_wb, wsa, cpa, cpv, cpw, iss] = checkss(w, Ta, d)

% Computation of pressure of water vapor evaluated at Tdb
z = 10.79586 * (1 - 273.15 / Ta) + 5.02808 * log10(273.15 / Ta) ...
+1.50474e-4 * (1 - (10 ^ (-8.29692 * (Ta / 273.15)) - 1)) ...
+4.2873e-4 * (10 ^ (4.76955 * (1 - 273.15 / Ta)) - 1) ...
+ 2.786118312;

pv_wb = 10 ^ z;

% Computation of humidity ratio for saturated air
wsa = ((2501.6 - 2.3263 * (Ta - 273.15)) / (2501.6 + 1.8577 * (Ta - 273.15) - 4.184 * (Ta - 273.15))) * ((0.62509 * pv_wb) / (d.P - 1.005 * pv_wb));

[cpa, cpv, cpw] = heatcap(Ta);

iss = cpa * (Ta - 273.15) + wsa * (d.ifgwo + cpv * (Ta - 273.15)) + (w - wsa) * cpw * (Ta - 273.15);
end

```

Check air Enthalpy

```
function ima = checkima(w, Ta, d)

[cpa, cpv, ~, ] = heatcap(Ta);
ima = cpa * (Ta - 273.15) + w * (d.ifgwo + cpv * (Ta - 273.15));
end
```

Dry Air temperature calculation

```
function Tair = dry(w, Tw, ima, d)
[cpa, cpv, ~] = heatcap(Tw);

% Specific heat of the air-water vapor mixture for unsaturated air [J/kgK]
cpma = cpa + w * cpv;

% Computation of pressure of water vapor evaluated at Tw
z = 10.79586 * (1 - 273.15 / Tw) + 5.02808 * log10(273.15 / Tw) ...
+1.50474e-4 * (1 - (10 ^ (-8.29692 * (Tw / 273.15)) - 1)) ...
+4.2873e-4 * (10 ^ (4.76955 * (1 - 273.15 / Tw)) - 1) ...
+ 2.786118312;

psatw = 10 ^ z;

% Calculate the humidity mass ratio at the gas-phase side at water temperature
wsw = (0.6250 * psatw) / (d.P - 1.005 * psatw);

% Enthalpy of water vapor at the bulk water temperature Tw [J/kg]
iv = d.ifgwo + cpv * (Tw - 273.15);

% Enthlpy of air-water vapor mixture [J/kg dry air K]
imasw = cpa * (Tw - 273.15) + iv * wsw;

Tair = Tw - (((imasw - ima) - (wsw - w) * iv) / cpma);
end
```

Heat capacity computation

```
function [cpa, cpv, cpw] = heatcap(Temp)

T = (Temp + 273.15) / 2;
cpa = 1.045356e3 -3.161783e-1 * T +7.083814e-4 * T ^ 2 -2.705209e-7 * T ^ 3;
% Specific heat of saturated water vapor [J/kgK]
cpv = 1.3605e3 + 2.31334 * T -2.46784e-10 * T ^ 5 +5.91332e-13 * T ^ 6;
% Specific heat of water [J/kgK]
cpw = 8.15599e3 - 2.80627 * 10 * T +5.11283e-2 * T ^ 2 -2.17582e-13 * T ^ 6;

end
```

Loop Simulation

```

close all
clear
clc

%% Input data test
data = readcell("tabella_dati.xlsx");

d = struct(); % Imput data della torre da validare

d.Tairin = round(cell2mat(data(2:end,3))); % °C
d.Tairindry = round(cell2mat(data(2:end,2))); % °C
d.Pair = cell2mat(data(2:end,5))*100; % Pa
d.Twout = 27.77; % °C
d.Twin = 50; % °C
d.mw = 12500; % kg/s
N = 5; % Number of steps of RK method

%% Loop
for f=1:length(d.Tairin)

% Model function calling
[Tdb, Twb, Tw, ima, w, Mep,water,d] = modellosupersaturato(d.Tairindry(f), d.Tairin(f),d.Pair(f), N, d);
pTdb(f,:) = Tdb(1:end-1);
pTwb(f,:) = Twb;
pTw(f,:) = Tw;
pima(f,:) = ima;
pw(f,:) = w(1:end-1);
pMep(f,:) = Mep;
pwater(f,:) = water;
% Create a table with the data
dataTable=array2table([(Tdb(1:end-1)' -273.15), (Twb'-273.15), (Tw' -273.15), ...
    ima(1:end-1)', w(1:end-1)', Mep'],'VariableNames',{'Tdb','Twb','Tw','ima','w','Mep'});

tabella = sprintf('data_iteration_%d.xlsx', f);
writetable(dataTable, tabella);

% Errore di convergenza
ERRima= abs((ima(end) - ima(end -1)) / (ima(end) + ima(end -1)));

%% Computation of parameter

% Convergence check
ERRima= abs((ima(end) - ima(end -1)) / (ima(end) + ima(end -1)));

%Water flow rate evaporated
mwevap = d.madry * (w(end - 1) - w(1));
mwevap_ct = d.madry * (w(end) - w(1));

%Heat calculation
sensible_heat_transfer = d.madry * (ima(end-1) - ima(1));

```

```

cooling_power_evap = mwevap * d.ifgwo;
cooling_power_total = cooling_power_evap + sensible_heat_transfer ;

%% Create the plot

% Optimization for Tdb
x = 0:length(Tdb) - 2;
coefficients = polyfit(x, Tdb(1:N+1), 2);
x_interp = linspace(min(x), max(x), 100);
Tdb_interp = polyval(coefficients, x_interp);

% Optimization for Twb
x4 = 0:length(Twb) -1;
coefficients4 = polyfit(x4, Twb, 2);
x4_interp = linspace(min(x), max(x), 100);
Twb_interp = polyval(coefficients4, x4_interp);

% Optimization for ima
x2 = 0:length(ima) -2;
coefficients2 = polyfit(x2, ima(1:N+1), 2);
x2_interp = linspace(min(x2), max(x2), 100);
ima_interp = polyval(coefficients2, x2_interp);

% Optimization for w
x3 = 0:length(w)-2;
coefficients3 = polyfit(x3, w(1:N+1), 2);
x3_interp = linspace(min(x3), max(x3), 100);
w_interp = polyval(coefficients3, x3_interp);

% Optimization for Mep
x5 = 0:length(Mep) -1;
coefficients5 = polyfit(x5, Mep, 2);
x5_interp = linspace(min(x), max(x), 100);
Mep_interp = polyval(coefficients5, x5_interp);

figure(f);
hold on;
plot(0:N, Tw-273.15, 'LineWidth', 2); % Plot Tw
plot(x_interp, Tdb_interp-273.15, 'LineWidth', 2); % Plot Tdb
plot(x4_interp, Twb_interp-273.15, 'LineWidth', 2);
hold off;
xlabel('Level of Spray zone');
ylabel('Temperature [K]');
legend('Tw', 'Tdb', 'Twb');
title('Variation of Tw and Tdb over iterations');
filename = sprintf('Tw_Tdb_Twb_%d.png', f);
saveas(gcf, filename);
close(gcf);

figure(f+1);
hold on;

```

```

plot(0:N, w(1:N+1), 'LineWidth', 2); % Plot w
hold off;
xlabel('Level of Spray zone');
ylabel('[kg/kg dry]');
title('Humidity mass ratio');
filename = sprintf('Humidity_mass_ratio_%d.png', f);
saveas(gcf, filename);
close(gcf);

figure(f+2);
hold on;
plot(0:N, ima(1:N+1), 'LineWidth', 2); % Plot ima
plot(x2_interp, ima_interp, 'LineWidth', 2);
hold off;
xlabel('Level of Spray zone');
ylabel('Enthalpy J/kg dry air');
legend('ima');
filename = sprintf('Enthalpy_of_Spray_zone_%d.png', f);
saveas(gcf, filename);
close(gcf);

figure(f+3);
hold on;
plot(0:N, water, 'LineWidth', 2); % Plot mw
hold off;
xlabel('Level of Spray zone');
ylabel('[kg/s]');
legend('mw');
title('Water flow rate');
filename = sprintf('Water_flow_rate_%d.png', f);
saveas(gcf, filename);
close(gcf);

end

axhandle=psychplotting(1,40,1,40);
figure(1)
hold on
for a=1:f
plot(axhandle,pTdb(a,:)-273.15,pw(a,:)*1000,'LineWidth',1.5);
end
hold off
saveas(gcf, 'PsychroChart.png');

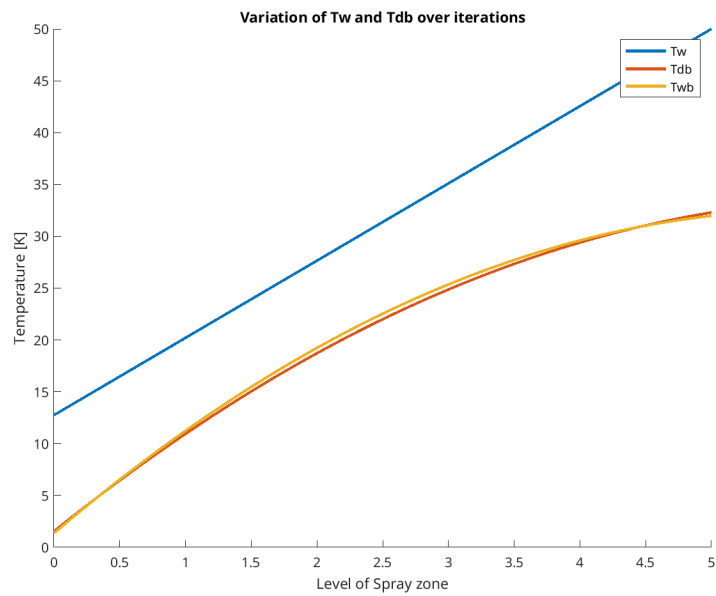
figure(2)
hold on
for b=1:f
plot(0:N,pTw(b,:)-273.15);
end
hold off
saveas(gcf, 'Watercomparison.png');

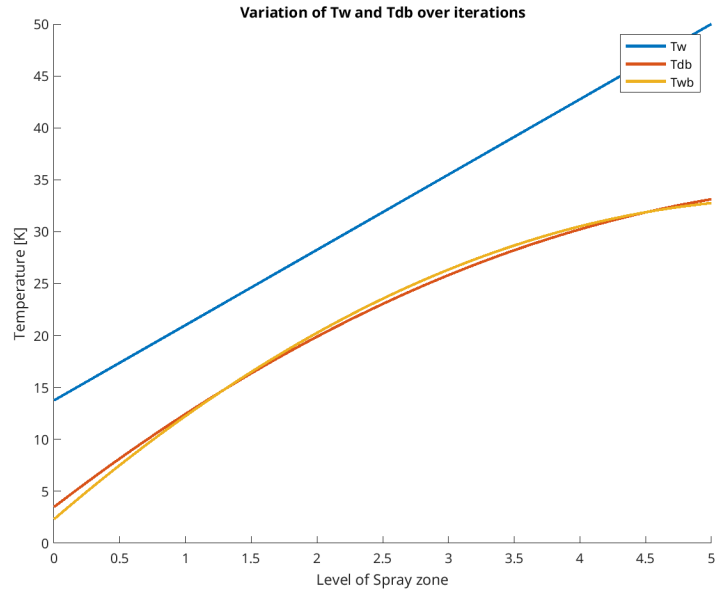
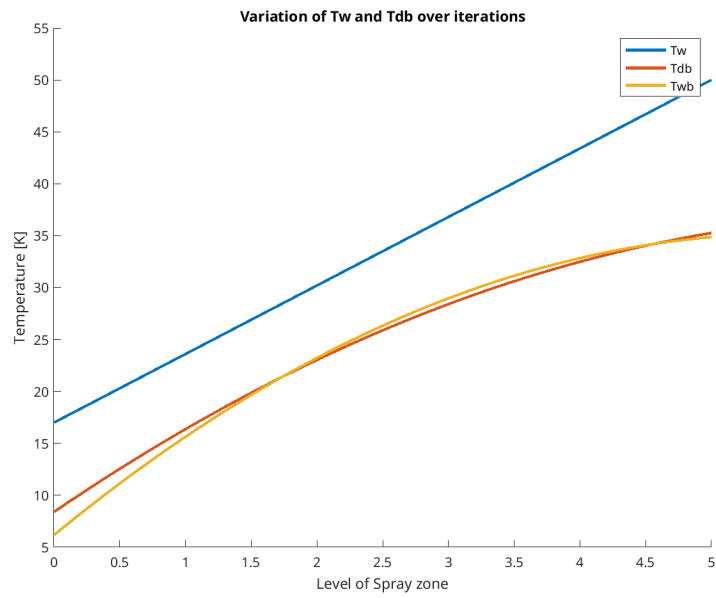
```


Appendix A

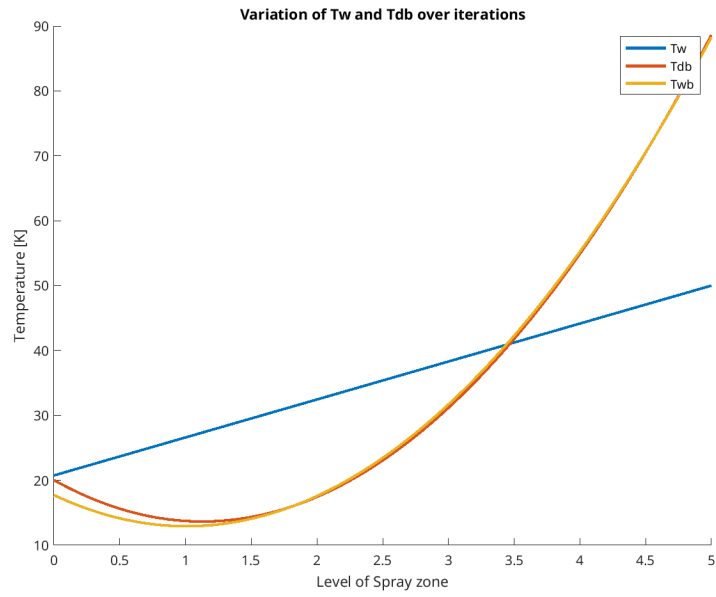
Appendix B - Plot collection

January

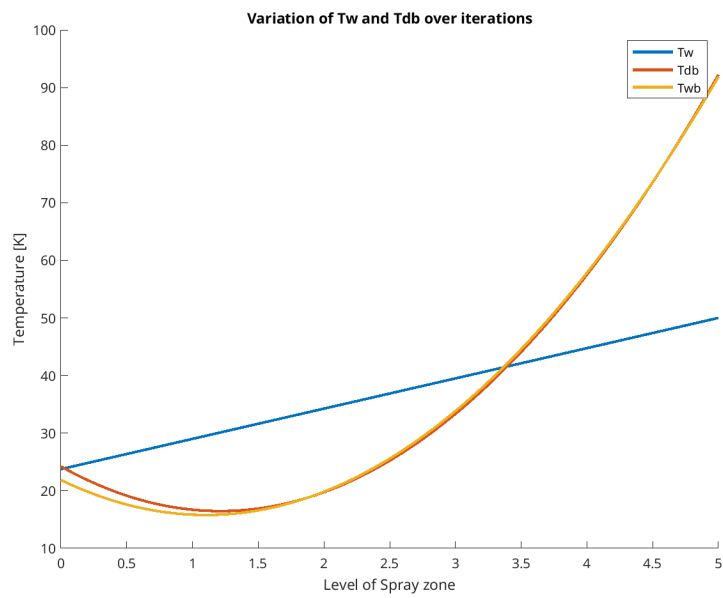


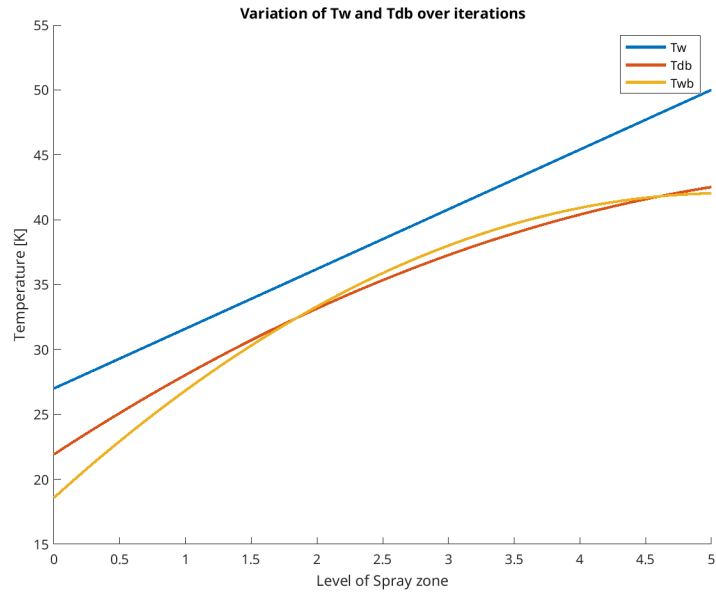
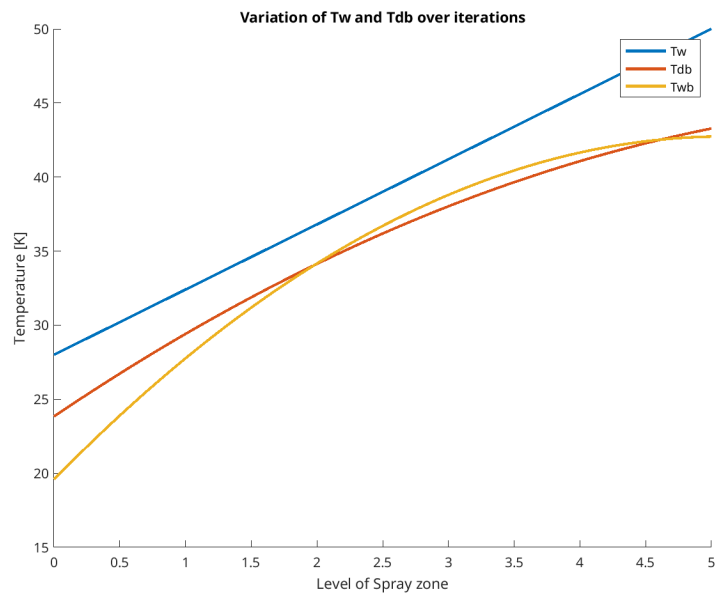
February**March**

April

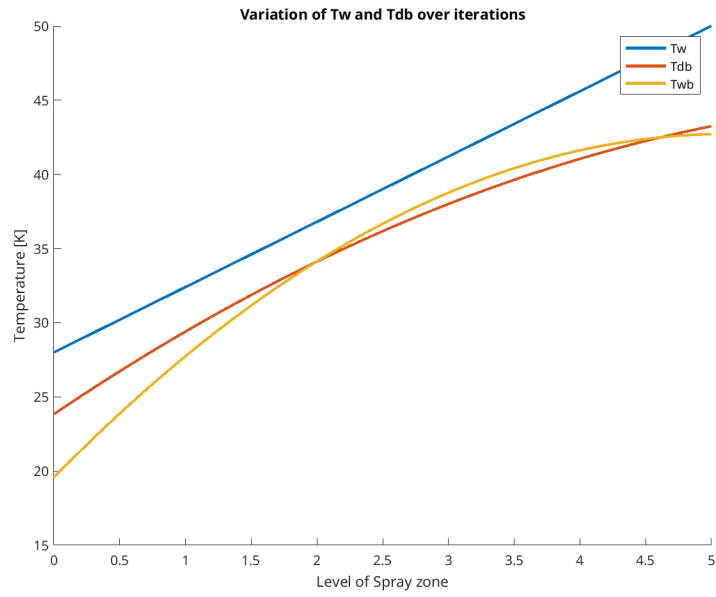


May

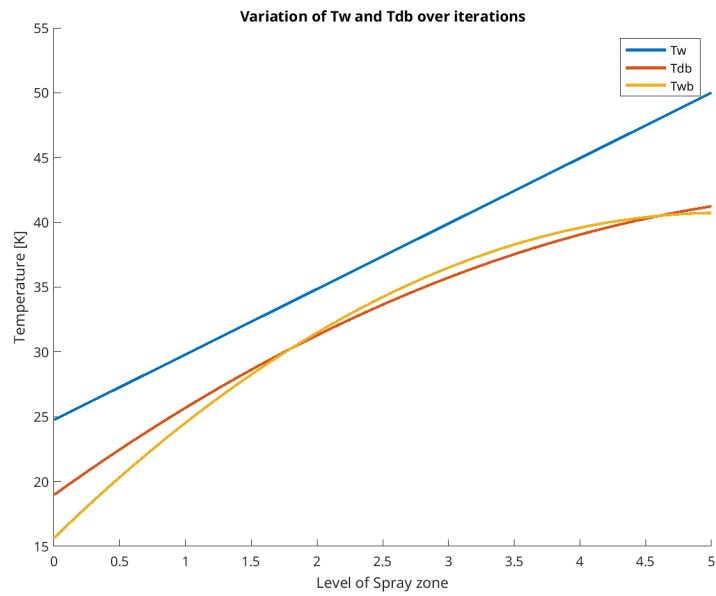


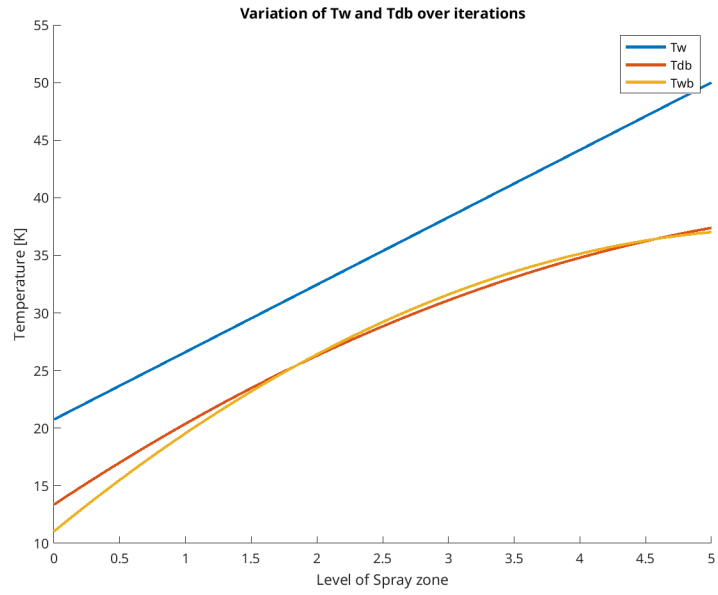
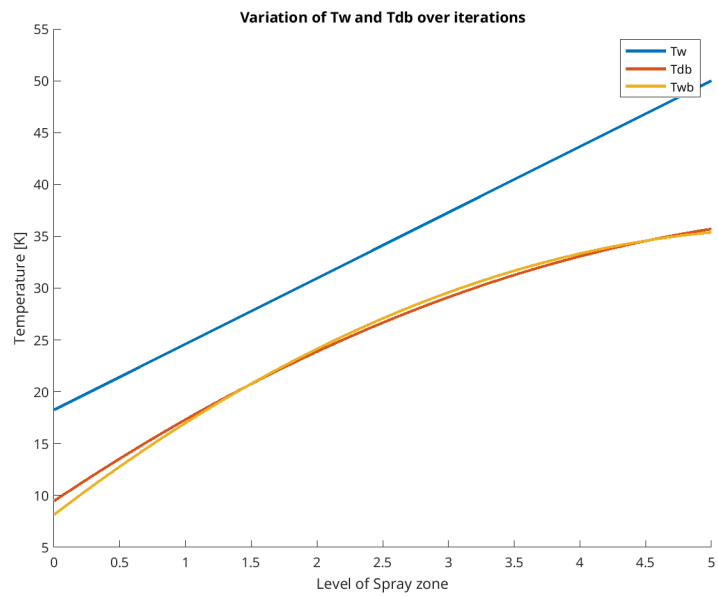
June**July**

August



September



October**November**

December

